eman ta zabal zazu
Universidad del País Vasco
Euskal Herriko Unibertsitatea

STUDY AND DEVELOPMENT OF NEW BIODEGRADABLE POLYMERIC MATERIALS CARRYING BIOACTIVE DRUGS

Oroitz Sánchez Aguinagalde

PhD Thesis

2023

Thesis (co)supervisors: Prof. Emilio Meaurio Arrate and Dr. Ainhoa Lejardi Meavebasterrechea

Doctorate Program: Engineering of Materials and Sustainable Processes

Group in Science and Engineering of Polymeric Biomaterials (Zibio Group)

Department of Mining-Metallurgy Engineering and Materials Science

Faculty of Engineering of Bilbao

University of the Basque Country (UPV/EHU)

And Polymat

ACKNOWLEDGEMENTS

First of all, I would like to thank the department of Mining-Metallurgy Engineering and Materials Science and Polymat for making the development of this thesis possible. Thank you Jose Ramon Sarasua, for believing in me from the beginning and giving me the chance of being a member of his group, and for the wise advices. Ainhoa Lejardi, for being my guide and my biggest help since I started the master until now. Emilio Meaurio, for so patiently teaching me what I needed and more, and for helping with my lack of experience or knowledge. I could not ask for better directors. And above all, thanks to the three of you for showing so much understanding and empathy with the problems I have had to face in the road.

Thanks to the ZIBIO group, especially to Ester Zuza, Jone Muñoz and Aitor Larrañaga, for giving me the confidence to consult anything with them, for their teachings, and of course, for the laughs during lunch times. Thanks to Xabier Larrañaga, for always being eager to help, always with a smile. Thanks to Carmen Mijangos and Rebeca Hernández, for your collaboration in chapter 2, and to Aitor Larrañaga, Yurena Polo and Eva Sánchez for teaching me so much about biology, and for your great contribution in chapter 3. Of course, thanks to Iulia Caraseva, Carlos Bello, Yurena Polo and Ulyana Semenenko for, in addition to being co-workers, having become very important people to me. Thanks to you the hours in the laboratory have been easier, and those outside the laboratory much more beautiful. You are the best treasure I got here.

I would like to thank all the classmates and roommates I have had since I started college, in Arrasate, Bogotá, Barcelona and Bilbo. As well as academic degrees, I accumulate so many unforgettable moments and friends for life from these years. I would also like to make an especial mention to all the inspiring teachers I have known since I was a kid, as they are the ones who make education so valuable. I would not like to forget about Maribi, who motivated me to continue studying when I did not know what to do, and made me thing about getting a PhD.

There are no words to express how thankful I feel to my parents. For the education, values and all the love they have given to me. For working so hard so I could have everything I needed and more, and for always being there for me. Thank you ama, for

awakening my passion for reading by teaching me to read with stories since I was a very little girl. Thank you aita, for repeating that I am capable of doing more than I think every time I have “went onto the field giving the game up for lost”. In this moment I think about my grandfather “aitxitxe” and my grandmother “amama”, who left us when I had just started my thesis. I also remember osaba Felix, always interested in my development, I know that he is very proud even if he is not with us anymore. To continue with family, thank you Mitxu, for being the best furry roommate one could ask for. I know you love me too, even if my legs are full of scratches. And thank you Molko, for making our lives better with your particular personality, and for showing us that the love we can have for an animal has no limits. I know you will always be by our side.

Of course, so many thanks to KUWATER. Thanks for being the best friends I could ask for. There is no need for mentioning each one of you, you know who I am talking about. Thanks for tolerating my bad days and my silliness, and for being able to always make me smile. As bad as a week can be, I know that weekend will arrive and I will leave my problems aside thanks to you. There are more friends apart from the *kuadrila*, but I would like to especially thank Ingartze, for always believing in me, and for being one of those beautiful coincidences that happen in life. I would not like to forget Marta, Haykel, Carlos, Sara, Vicente, Asya… I can feel you close to me, even if you are far away!

Finally, thank you Carlos. Thank you for being there since the first time we met more than six years ago. As a friend or as a partner, for sharing the best moments with me, and for being my greatest support during the worst ones. Thank you for still loving me despite all my mistakes.

AGRADECIMIENTOS

Para empezar, me gustaría agradecer al departamento de Ingeniería Minero-Metalúrgica y Ciencia de los Materiales y Polymat, por hacer posible el desarrollo de esta tesis. A Jose Ramon Sarasua, por creer en mí desde el principio y darme la oportunidad de ser un miembro más de su grupo, y por los grandes consejos que me ha dado. A Ainhoa Lejardi, por ser mi guía y mi mayor ayuda desde que empecé el máster hasta ahora. A Emilio Meaurio, por enseñarme tanto con gran paciencia, y por ayudarme con mis carencias. No podría pedir mejores directores. Y sobre todo, gracias a los tres por mostrar tanta comprensión y empatía con los problemas que me han surgido por el camino.

Muchas gracias al grupo ZIBIO, sobre todo a Ester Zuza, Jone Muñoz y Aitor Larrañaga, por darme la confianza de consultar cualquier cosa con ellos, por sus enseñanzas y, por supuesto, por las risas en las comidas. Gracias Xabier Larrañaga, por estar siempre dispuesto a echar una mano, siempre con una sonrisa. Muchas gracias a Carmen Mijangos y a Rebeca Hernández por la colaboración en el capítulo 2. También a Aitor Larrañaga, Yurena Polo y Eva Sánchez por su gran aportación en el capítulo 3. Cómo no, a Iulia Caraseva, Carlos Bello, Yurena Polo y Ulyana Semenenko por, además de ser compañeros de trabajo, haberos convertido en personas muy importantes para mí. Gracias a vosotros las horas de laboratorio se han hecho más fáciles, y las de fuera del laboratorio mucho más bonitas. Vosotros sois el mayor tesoro que me llevaré de aquí.

Quiero agradecer a todos los compañeros de clase y piso que he tenido desde que empecé en la universidad, tanto en Arrasate como en Bogotá, Barcelona o Bilbo. Además de obtener títulos académicos, he podido acumular momentos inolvidables y amigos para toda la vida. También me gustaría tener en cuenta a todos los profesores inspiradores que he tenido desde que era una niña, ya que ellos son los que hacen que la educación sea tan valiosa. Y no quisiera olvidar a Maribi, quien me motivó para seguir estudiando cuando no sabía qué hacer, y fue la causante de que me planteara hacer un doctorado.

No sé si hay suficientes palabras para poder expresar lo agradecida que me siento a mis padres. Por la educación, valores y el amor que siempre me han dado. Por lo que se han esforzado para que pudiera tener todo lo que he necesitado y más, y por estar siempre

ahí. Gracias ama, por despertar mi pasión por la lectura enseñándome a leer con cuentos desde que era muy pequeña. Gracias aita, por repetirme que soy capaz de hacer más de lo que creo cada vez que he “salido al campo dando el partido por perdido”. En estos momentos recuerdo a mi abuelo “aitxitxe” y a mi abuela “amama”, quienes nos dejaron cuando acababa de empezar la tesis. También a osaba Félix, siempre interesado en mi desarrollo, sé que estará orgulloso aunque ya no esté entre nosotros. Siguiendo con la familia, gracias Mitxu, por ser el mejor compañero de piso peludo que se puede tener. Sé que tú también me quieres, aunque tenga las piernas llenas de heridas. Y muchísimas gracias Molko, por mejorar nuestras vidas con tu forma de ser tan especial, y por enseñarnos que el amor que se puede tener a un animal no tiene límites. Sé que siempre estarás a nuestro lado.

Cómo no, muchas gracias KUWATER. Gracias por ser las mejores amigas que una podría pedir. No hace falta nombrar a todas, vosotras ya sabéis a quién me refiero. Gracias por aguantar mis enfados y tonterías, y por ser capaces de sacarme siempre una sonrisa. Por muy mala que sea una semana, sé que al llegar el fin de semana dejaré las penas de lado gracias a vosotras. Hay más amigos aparte de la *kuadrila*, pero entre estos me gustaría agradecer especialmente a Ingartze, por creer siempre en mí, y por ser una de esas bonitas casualidades que ocurren en la vida. No querría olvidar a Marta, Haykel, Carlos, Sara, Vicente, Asya… ¡Os siento cerca aunque estéis lejos!

Para terminar, gracias Carlos. Gracias por estar ahí desde que nos conocimos hace algo más de 6 años. Como amigo o como pareja, por compartir conmigo los mejores momentos, y por ser mi mayor apoyo en los peores. Gracias por seguir queriéndome a pesar de todos mis errores.

ESKER ONAK

Hasteko, eskerrak eman nahi dizkiot Meatzaritzako Ingeniaritza eta Materialen Zientzia departamentuari eta Polymat-eri, tesi honen garapena posible egiteagatik. Jose Ramon Sarasuari, hasieratik nigan sinistu eta bere taldeko parte izateko aukera emateagatik, eta emandako aholku handiengatik. Ainhoa Lejardiri, masterra hasi nuenetik orain arte nire gida eta laguntza nagusia izateagatik. Emilio Meauriori, pazientzia handiz hainbeste erakusteagatik, eta nire gabeziekin laguntzeagatik. Ezingo nituzke zuzendari hobeak eskatu. Eta batez ere, eskerrik asko hiruroi, bidean zehar izan ditudan arazoen aurrean ulerpen eta enpatia handia erakustearren.

Eskerrik asko ZIBIO taldeari, batez ere Ester Zuza, Jone Muñoz eta Aitor Larrañagari, edozer kontsultatzeko konfidantza emateagatik, zuen irakaspenengatik eta nola ez, jatorduetako barreengatik. Eskerrik asko Xabier Larrañaga, beti irribarre batekin laguntzeko prest egoteagatik. Eskerrik asko Carmen Mijangos eta Rebeca Hernández, 2. kapituluko elkarlanagatik, eta Aitor Larrañaga, Yurena Polo eta Eva Sánchez 3. kapituluko ekarpen handiagatik. Nola ez, Iulia Caraseva, Carlos Bello, Yurena Polo eta Ulyana Semenenkori, lankideak izateaz gain, nire bizitzako hain pertsona garrantzitsuak bihurtzearren. Zuei esker laborategiko orduak askoz errezagoak izan dira, eta laborategiz kanpokoak askoz politagoak. Zuek zarete hemendik eramango dudan altxorrik handiena.

Unibertsitatean hasi nintzenetik izan ditudan klasekide eta pisukide guztiak eskertu nahi nituzte, bai Arrasate, Bogotá, Bartzelona eta Bilbokoak. Titulu akademikoak lortzeaz gain, momentu ahaztezinak eta bizi osorako lagunak bildu ditut. Kontuan izan nahi nituzke txikitatik izan ditudan irakasle inspiratzaile guztiak, zuek zarete irakaskuntza hain baliotsua egiten dutenak. Eta ez nuke Maribi ahaztu nahi, zer egin ez nekienean ikasten jarraitzeko motibatu ninduena, eta doktoretza bat egitea planteatzera eraman ninduena.

Ez dakit hitz nahikoa dagoen nire gurasoenganako sentitzen dudan esker ona azaltzeko. Betidanik eman didaten hezkuntza, balore eta maitasunagatik. Behar nuena eta gehiago izan ahal izateko egin duten esfortzuagatik, eta beti hor egoteagatik. Eskerrik asko ama, nigan irakurtzeko grina piztearren, oso txikia nintzenetik ipuinekin irakurtzen irakastean. Eskerrik asko aita, “zelaira partidua jotzat emanda atera” naizen bakoitzean uste dudana

baino gehiago egin dezakedala errepikatzearren. Momentu honetan gogoan ditut aitona “aitxitxe” eta amona “amama”, tesia hasi berri nuenean utzi gintuztenak. Baita osaba Felix ere, beti nire garapenean hain interesatua, badakit harro zaudela naiz eta ez egon gure artean jada. Familiarekin jarraituz, eskerrik asko Mitxu, izan daitekeen pisukide iletsu onena izateagatik. Naiz eta hankak zauriz josita izan, badakit maite nauzula zuk ere. Eta eskerrik asko Molko, zure izaera bereziarekin gure bizitzak hobetzeagatik, eta animalia batenganako sentitu daitekeen maitasuna mugagabea dela erakusteagatik. Badakit beti gure ondoan egongo zarela.

Nola ez, eskerrik asko KUWATER. Eskerrik asko eskatu daitezkeen lagunik onenak izateagatik. Ez dago denak izendatu beharrik, zuek badakizute nortzuk zareten. Eskerrik asko nire umore txar eta tontokeriak jasatearren, eta beti irribarre bat ateratzeko gai izatearren. Naiz eta aste txar bat izan, badakit asteburua iristean zuei esker penak alde batera utziko ditudala. Kuadrilaz aparte badaude lagun gehiago, baina hauen artean bereziki eskertu nahi nuke Ingartze, beti nigan sinisteagatik, eta bizitzan gertatzen diren kasualitate ederretako bat izateagatik. Ahaztu gabe, eskerrik asko Marta, Haykel, Carlos, Sara, Vicente, Asya… Naiz eta urrun egon, hurbil sentitzen zaituztet!

Amaitzeko, eskerrik asko Carlos. Eskerrik asko orain dela 6 urte pasa ezagutu ginenetik hor egoteagatik. Lagun edo bikote bezala, momenturik onenak nirekin partekatzearren, eta txarrenetan nire euskarri nagusia izatearren. Eskerrik asko egin ditudan akats guztien gainetik ni maitatzeagatik.

ABSTRACT

Due to the abuse and misuse of antibiotics by our society, there are more and more pathogens that present high resistance to antimicrobial agents. This causes a drop in the effectiveness of the antibiotics we have today. This, added to the low success in the search for new antibiotics, results in a higher incidence of fatal infections that could be avoided. With a view to the future, seeing that these infections can become a cause of death even greater than cancer in a few decades, it is necessary to develop new systems with which to deal with increasingly strong microorganisms.

The strategies that are gaining prominence are mostly those based on combining drugs with different biodegradable polymers that are applicable to the human body, in the form of hydrogels, surfaces or coatings, or nanosystems such as nanoparticles or nanocapsules, among others. In addition, apart from applying already existing antibiotics in lower concentration through other systems, the use of other active agents is being studied. On the one hand, compounds derived from plants, which have shown antimicrobial and antioxidant capacities in nature, in addition to having been used as remedies in traditional Chinese or Andean medicine, for example. Although some scepticism has been shown regarding them, based on studying them, more beneficial properties for health have been attributed to them, and they can be great allies of medicine. On the other hand, metal oxides and metal nanoparticles, also used since ancient times, show properties capable of eliminating bacteria, or even interrupting the formation of biofilms resistant to antibiotics. However, there are more doubts regarding this type of compound, since its toxicity and environmental damage that may be caused by the continuous use of these systems cannot be fully dismissed (Chapter 1).

In this thesis, different systems with polymers and drugs with antimicrobial properties have been searched, wanting to take advantage of the different beneficial properties that they could present in addition to their function against bacterial infections. Divided into two chapters, on the one hand, a hydrogel system based on chitosan (CS) and poly (vinyl alcohol) (PVA) has been studied, and on the other, two polymer/drug mixture systems, paying special attention to improving their solubility and stability over time, being able to reduce the amounts of drug applied and improving its efficiency.

Hydrogels are polymeric materials with a three-dimensional structure capable of trapping large amounts of water. In this case, its base is chitosan (CS), an antimicrobial biopolymer studied for its wide variety of beneficial properties for medical applications, combined with poly (vinyl alcohol) (PVA), also highly regarded for applications such as wound dressing or the manufacture of nanoparticles. In these hydrogels, the three-dimensional structure is formed from physical interactions without the need for crosslinking agents, in addition to being thermosensitive with a transition temperature of 37°C, which gives them the property of being injectable. Despite the advantages of this combination, their mechanical properties are insufficient to withstand loads that can occur in the human body, so it has been decided to reinforce them with inorganic particles of bioactive glass. The resulting hydrogels have been experimentally analyzed by scanning electron microscopy (SEM), X-ray diffraction (XRD), swelling, rheology, and drug release tests. Thus, it has been verified that the mechanical properties have been improved, in addition to increasing its bioactivity with the formation of hydroxyapatite within the gel, thus being able to improve the formation or regeneration of new bone after a break. All this, without affecting the drug release kinetics of the hydrogel, that is, without limiting its initial advantages (Chapter 2).

Regarding polymer/drug blends, the main objective has been to find miscible blends in order to maintain crystalline drugs in an amorphous state, thus forming amorphous solid dispersions (ASD). After having carried out both theoretical and experimental selection, the selected systems have been poly (ε-caprolactone)/xanthohumol (PCL/XH) and poly (ε-caprolactone)/mycophenolic acid (PCL/MPA). In both cases, the first thing to do was to study the miscibility between polymer and drug by analyzing the glass transition temperature (T_g) of different compositions, looking for a unique intermediate T_g between those of the polymer and the drug, to then estimate the Flory-Huggins interaction parameter for each blend by studying the melting point depression of the drug. Both tests have been favorable to confirm the miscibility between polymer and drug in both cases. In addition, new interactions between the two components have been observed by Fourier transform infrared spectroscopy (FTIR) for both blends (Chapter 3).

After the initial confirmation, in the PCL/XH blends it has gone further using X-ray diffraction analysis and obtaining Atomic force microscopy (AFM) images of different compositions to be able to observe the variations of the crystalline morphology with the composition. In addition, it has been possible to study how the mechanical behavior under tensile forces of the blends changes depending on the % of xanthohumol added, carrying out tensile tests. Regarding the PCL/MPA blends, the work has focused more on the study of their *in vitro* properties. On the one hand, the drug release measurements showed that these blends can release a minimum o of 70% of the drug in three days. On the other hand, through *in vitro* cellular assays, it was confirmed that in this way MPA continues to be active against cancer cells, without actually affecting healthy cells (Chapter 3).

In summary, in this work it has been possible to study different strategies to deal with the large problem resulting from the resistance of bacteria to the most commonly used antibiotics, applying them in different systems that could be very useful for other types of pathologies. It is important to highlight that although only three different systems have been studied here, there are an infinite number of combinations between polymers, drugs and reinforcements, which highlights the need to broaden our sights with respect to the use of other types of active agents and forms of application to which we are habitually accustomed.

RESUMEN

Debido al abuso y mal uso de los antibióticos por parte de nuestra sociedad, los patógenos que presentan una gran resistencia ante agentes antimicrobianos son cada vez más. Esto causa una caída de la efectividad de los antibióticos con los que contamos hoy en día. Esto, sumado al bajo éxito en la búsqueda de nuevos antibióticos, resulta en una mayor incidencia de infecciones mortales que podrían ser evitadas. Con vistas a futuro, viendo que estas infecciones se pueden convertir en una causa de muerte mayor incluso que el cáncer en unas pocas décadas, resulta necesario el desarrollo de nuevos sistemas con los que hacer frente a microorganismos cada vez más fuertes.

Las estrategias que están obteniendo un gran protagonismo son en mayor parte las basadas en combinar fármacos con diferentes polímeros biodegradables aplicables al cuerpo humano, tanto en forma de hidrogeles, superficies o recubrimientos, o nanosistemas tales como nanopartículas o nanocápsulas, entre otros. Además, aparte de aplicar antibióticos ya existentes en menor concentración mediante otros sistemas, se estudia el uso de otros agentes activos. Por una parte, compuestos derivados de plantas, los cuales han mostrado capacidades antimicrobianas y antioxidantes en la naturaleza, además de haber sido utilizados como remedios en medicina tradicional china o andina, por ejemplo. Aunque se haya mostrado cierto escepticismo respecto a ellos, a base de estudiarlos se les han podido atribuir más propiedades beneficiosas para la salud, pudiendo ser unos grandes aliados de la medicina. Por otra parte, los óxidos de metal y nanopartículas metálicas, también utilizadas desde tiempos antiguos, muestran propiedades capaces de eliminar las bacterias, e incluso interrumpir la formación de biofilms resistentes a los antibióticos. No obstante, existen más dudas respecto a este tipo de compuestos, ya que no se puede descartar del todo su toxicidad y los daños ambientales que puedan causar el uso continuo de estos sistemas. (Capítulo 1)

En esta tesis, se han buscado diferentes sistemas con polímeros y fármacos con propiedades antimicrobianas, queriendo sacar partido a las diferentes propiedades beneficiosas que podrían presentar aparte de su función contra las infecciones bacterianas. Divididos en dos capítulos, por una parte, se ha estudiado un sistema de hidrogel basado en quitosano (CS) y poli (vinil alcohol) (PVA) y por otra, dos sistemas de

mezclas polímero/fármaco poniendo especial atención en mejorar su solubilidad y estabilidad en el tiempo, pudiendo reducir las cantidades de fármaco aplicados mejorando su eficiencia.

Por su parte, los hidrogeles son materiales poliméricos con una estructura tridimensional capaces de atrapar grandes cantidades de agua. En este caso su base es el quitosano (CS), un biopolímero antimicrobiano estudiado por su gran variedad de propiedades beneficiosas para aplicaciones médicas, combinado con poli (vinyl alcohol) (PVA), también muy considerado para aplicaciones como apósitos de heridas o fabricación de nanopartículas. En estos hidrogeles la red tridimensional se forma a partir de interacciones físicas sin necesidad de agentes entrecruzantes, además de ser termosensibles con una temperatura de transición de 37°C, lo que les da la propiedad de ser inyectables. A pesar de las ventajas de esta combinación, sus propiedades mecánicas son insuficientes para soportar cargas que se pueden dar en el cuerpo humano, por lo que se ha optado por reforzarlos con partículas inorgánicas de vidrio bioactivo. Los hidrogeles resultantes han sido analizados experimentalmente mediante microscopía de barrido electrónico (SEM), difracción de rayos-X (XRD), pruebas de hinchamiento, reología y liberación de fármaco. Así, se ha comprobado que las propiedades mecánicas han sido mejoradas, además de aumentar su bioactividad con la formación de hidroxiapatita dentro del gel, pudiendo así mejorar la formación o regeneración de nuevo hueso tras una rotura. Todo esto, sin afectar a la cinética de liberación de fármaco del hidrogel, es decir, sin limitar sus ventajas iniciales (Capítulo 2).

En cuanto a las mezclas polímero/fármaco, el mayor objetivo ha sido el de buscar mezclas miscibles para poder mantener los fármacos cristalinos en estado amorfo, formando así dispersiones sólidas amorfas (ASD). Tras haber realizado una criba tanto teórica como experimental, los sistemas seleccionados han sido poli (ε-caprolactona)/xanthohumol (PCL/XH) y poli (ε-caprolactona)/ácido micofenólico (PCL/MPA). En ambos casos lo primero ha sido estudiar la miscibilidad entre polímero y fármaco analizando la temperatura de transición vítrea (T_g) de diferentes composiciones, buscando una T_g única intermedia entre aquellas del polímero y del fármaco, para después buscar el parámetro de interacción de Flory-Huggins para cada mezcla mediante el estudio de la depresión del punto de fusión del fármaco. Ambas

pruebas han sido favorables para confirmar la miscibilidad entre polímero y fármaco en los dos casos. Además, se han podido observar nuevas interacciones entre los dos componentes mediante espectroscopía infrarroja por transformada de Fourier (FTIR) para ambas mezclas (Capítulo 3).

Tras la confirmación inicial, en las mezclas PCL/XH se ha querido ir más allá utilizando análisis de difracción de rayos-X y obteniendo imágenes AFM (Microscopía de Fuerza Atómica) de diferentes composiciones para poder observar las variaciones de la morfología cristalina con la composición. Además, se ha podido estudiar cómo cambia el comportamiento mecánico a tracción de las mezclas dependiendo del % de xanthohumol añadido, realizando pruebas de tracción. En cuanto a las mezclas PCL/MPA, el trabajo se ha enfocado más al estudio de sus propiedades *in vitro.* Por una parte, las mediciones de liberación de fármaco mostraron que estas mezclas pueden llegar a liberar un mínimo del 70% de fármaco en tres días. Por otra parte, mediante ensayos celulares *in vitro*, se confirmó que de esta forma el MPA sigue siendo activo contra células cancerígenas, sin llegar a afectar a células sanas (Capítulo 3).

En resumen, en este trabajo se han podido estudiar diferentes estrategias para hacer frente al problema de grandes dimensiones que resulta la resistencia de las bacterias a los antibióticos más comúnmente utilizados, aplicándolos en diferentes sistemas que podrían ser de gran utilidad para otros tipos de patologías. Es importante destacar que aunque aquí se hayan estudiado solamente tres sistemas diferentes, existe una infinidad de combinaciones entre polímeros, fármacos y refuerzos, lo que destaca la necesidad de ampliar las miras con respecto a la utilización de otro tipo de agentes activos y las formas de aplicación a los que estamos habitualmente acostumbrados.

LABURPENA

Gizarte honek antibiotikoei ematen dien erabilera txarraren ondorioz, agente antimikrobianoekiko erresistentzia altua erakusten duten patogenoak bakoitzean gehiago dira. Arazo hau dela eta, gaur egun erabiltzen ditugun antibiotikoetan eraginkortasun galera handia ikusi daiteke. Gainera, antibiotiko berriak bilatzean egon den arrakasta baxua kontuan izanda, sahiestu daitezkeen infekzio hilgarrien intzidentzia geroz eta handiagoa da. Etorkizunera begira, hamarkada batzuetan infekzio hauek minbizia baino heriotza-kausa handiagoa bihurtu daitezkeela ikusita, beharrezkoa da bakoitzean indartsuagoak diren mikroorganismoei aurre egiteko sistema berriak garatzea.

Gorputzean aplikatu daitezkeen polímero biodegradakor eta farmako ezberdinen arteko nahasketetan oinarritutako estrategiak protagonismo handia hartzen ari dira, hidrogel, azalera edo estaldura, edo nanopartikula eta nanokapsula formako nanosistemak, besteak beste. Gainera, beste sistema batzuen bidez dagoeneko existitzen diren antibiotikoak kontzentrazio txikiagoetan aplikatzeaz gain, beste agente aktibo batzuen erabilera ere ikertzen da. Alde batetik, landare jatorriko konposatuak, naturan ahalmen antimikrobianoak eta antioxidanteak izateaz gain, medikuntza txinatar edo andinoan oso erabiliak izan direnak. Nahiz eta hauenganako nahiko eszeptizismo egon, gehiago ikertu ondoren osasunarentzako onuragarriak diren propietate gehiago aurkitu zaizkie, medikuntzaren aliatu handiak izateko aukerak erakutsiz. Beste alde batetik, metalen oxido eta nanopartikula metalikoak, hauek ere antzinako garaietatik erabiliak, bakteriak eliminatzeko edo eta antibiotikoei erresistenteak diren biofilmen formazioa etetzeko gai dira. Hala ere, zalantza asko daude konposatu hauen inguruan, ezinezkoa baita hauen toxizitatea eta beraien erabilerak ingurumenean eragin ditzakeen kalteak baztertzea (1. Kapitulua).

Tesi honetan, propietate antimikrobianoak dituzten polimero/farmako sistema ezberdinak bilatu dira, infekzio bakterianoen aurkako eraginaz gain beste propietate onuragarri batzuk izateko gai izan daitezkeenak. Bi kapitulutan banatuta, alde batetik kitosano (CS) eta poli (binil alkohol)ean (PVA) oinarritutako hidrogelak aztertu dira, eta beste alde batetik, bi polimero/farmako nahaste sistema ezberdin, hauen solubilitatea

eta denboran zehar izango duen egonkortasuna hobetu nahian, farmako gutxiago erabiliz bere efizientzia hobetuz.

Hidrogelak ur kantitate handia xurgatzeko gai diren material polimerikoak dira, hiru dimentsioko egitura batez osatuak. Kasu honetan bere oinarria kitosanoa (CS) da, aplikazio medikuetarako propietate egokiak izateagatik asko ikertzen den biopolimero antimikrobiano bat, poli (binil alkohola)rekin (PVA) konbinatuta, hau ere oso erabilia izanik zaurientzako apositu edo nanopartikulen fabrikazioan. Hidrogel hauetan hiru dimentsioko sarea elkar-ekintza fisikoei esker eratzen da, inongo erretikulazio-osagairik erabili gabe. Gainera, termosentikorrak dira 37°Cko trantsizio tenperaturarekin, honi esker injektagarriak izanik. Naiz eta konbinazio honek abantaila asko izan, bere propietate mekanikoak ez dira nahikoa gorputzean jasan daitezkeen kargei aurre egiteko. Honegatik, beira bioaktibozko partikula inorganikoak errefortzu modura erabiltzea erabaki da. Hidrogel erresultanteak ekorketa elektronikoko mikroskopia (SEM), X-izpien difrakzioa (XRD), puzte proba, erreologia eta farmakoen liberazioa erabiliz aztertu dira esperimentalki. Horrela, propietate mekanikoak hobetu direla eta hidrogelaren barruko hidroxiapatitaren formazioarekin hezurren formazio edo regenerazioa hobetu daitekeela ikusi da. Guzti hau, farmakoaren liberazio zinetikan eraginik izan gabe, hau da, bere hasierako abantailak mugatu gabe (2. Kapitulua).

Polimero/farmako nahasteei dagokionez, helburu nagusia sistema nahasgarriak aurkitzea izan da, farmako kristalinoak egoera amorfoan mantendu ahal izateko, dispertsio solido amorfoak (ASD) eratuz. Hasierako hautaketa teoriko eta esperimental baten ondoren bi sistema aukeratu dira: poli (ε-kaprolaktona)/xanthohumol (PCL/XH) eta poli (ε-kaprolaktona)/azido mikofenolikoa (PCL/MPA). Kasu bietan lehen pausoa polimero eta farmakoaren arteko nahasgarritasuna aztertzea izan da. Lehenengo konposizio desberdinen beira trantsizio temperatura (T_g) aztertu da, polimero eta farmakoaren T_g bien arteko erdiko T_g bakarra bilatuz, ondoren nahaste bakoitzaren Flory-Huggins interakzio parametroa kalkulatzeko, farmakoaren urtze tenperaturaren depresioa aztertuz. Proba biak aldekoak izan dira nahasgarritasuna baieztatzeko sistema bietan. Gainera, Fourier transformatuaren espektroskopia infragorria (FTIR) erabiliz nahaste bietan konposatu bien arteko interakzioak ikusi dira (3. Kapitulua).

Lehen baieztapenaren ondoren, PCL/XH sisteman nahasgarritasun hau gehiago aztertu nahi izan da. Horretarako X-izpien difrakzioa eta indar atomikoen mikroskopia (AFM) erabili dira, konposizioaren arabera eman daitezkeen kristalinitatearen aldaketa morfologikoak ikusteko. Gainera, gehitutako xanthohumol portzentaiaren arabera nahasteen trakzioarekiko portaera mekanikoa nola aldatzen den ikusi ahal izan da, trakzio saiakuntzak eginez. PCL/MPA nahasketei dagokienez, lana gehiago bideratu da bere *in vitro* propietateetara. Alde batetik, farmako liberazioen neurketekin nahasketa hauetan hiru egunetan gutxienez farmakoaren %70a askatu daitekeela ikusi da. Beste alde batetik, zelulekin egindako *in vitro* saiakerei esker, MPAk minbizi zelulen aurka erabilgarria izaten jarraitzen duela ikusi da, zelula osasuntsuei kalterik eragin gabe (3. Kapitulua).

Laburbilduz, lan honetan bakteriek gehien erabilitako antibiotikoenganako garatu duten erresistentziak suposatzen duen arazo handiari aurre egiteko estrategia desberdinak aztertu dira, beste patologia mota batzuentzat ere erabilgarriak izan daitezkeen sistemetan aplikatuz. Hemen bakarrik hiru sistema ezberdin aztertu dira, baina garrantzitsua da polimero, farmako eta errefortzuen artean konbinazio infinituak sortu daitezkeela azpimarratzea. Hau kontuan izanda, beharrezkoa da erabiltzera ohituta gauden aplikazio mota eta farmakoez gain, beste sistema eta agente aktiboen erabilerari aukera ematea.

CONTENIDO

CHAPTER 1. INTRODUCTION. NEW POLYMER-BASED STRATEGIES TO COMBAT ANTIMICROBIAL RESISTANCE: A REVIEW

ABSTRACT

The rise in antimicrobial resistance (AMR) pathogens is growing, while the efficacy of traditional use of antibiotics is declining. This translates into a major health problem, with a catastrophic future view. To cope with this situation, the use of different types of antibacterial agents is studied, being able to increase their effectiveness with polymers. This review shows new approaches to strategies to avoid bacterial infections, making use of agents such as classic antibiotics, plant-derived compounds or metallic nanoparticles, combining them with polymers in the form of nanosystems such as particles, surfaces or coatings, or hydrogels. The use of these new systems, mainly incorporated in implantable devices or in contact with the human body such as prostheses, catheters or wound healing patches, may present a future with a lower risk of infections, avoiding becoming a cause of death greater than cancer.

1.1. INTRODUCTION

Bacterial infections have become a huge risk for the well-being of hospitalized patients, especially for the ones who undergo surgical procedures or invasive medical devices. Urinary tract infections being the most common, there are more dangerous infections as ventilator-associated pneumonia or catheter-associated bloodstream infection [1], [2].The concern about these infections has grown as different pathogens have become extremely resistant to antimicrobial agents [3], [4]. The misuse and abuse of antibiotics is the main responsible of this situation, which is increased due to the ease to travel and the exchange of goods all around the world. In addition, in the recent years there has not been much progress in the development of new antibiotics [5], [6].

The principal consequence of the antimicrobial resistance (AMR) is the human suffering and lost, followed by a high economical cost. Patients that are affected by these pathogens with AMR have more probabilities of spending longer times in hospital and higher mortality rates than those infected with more susceptible bacterial strains [7], [8].

Among these dangerous bacteria, ESKAPE pathogens (*Enterococcus faecium, Staphylococcus aureus, Klebsiella pneumoniae, Acinetobacter baumanii, Pseudomonas aeruginosa* and *Enterobacter species*) are the major cause of nosocomial infections [9].

Over time, ESKAPE bugs have become such resistant and virulent bacteria, that they have been considered critical and a high priority by the World Health Organization. It is evident that this priority is mainly due to the high mortality caused by these pathogens, but there is still more: understanding the functioning of these bugs, any type of bacteria could be faced, since their resistance, pathogenesis and transmission mechanisms would be known [10], [11]. As for resistance mechanisms, different processes can be found: enzymatic inactivation, changes in cell permeability, modification of drug targets or the formation of biofilms, among others [12].

Biofilms are responsible for a large part of infections caused by medical devices, and may be the cause of between 65-70% of them [13]. These biofilms are the result of a process by which harmful microorganisms and their subproducts adhere to the surfaces, creating a layer. The formation of these biofilms is a complicated process that involves many steps, in addition to forming different structures depending on the species and the environment that surrounds them [14]. Still, four main phases that can be seen in Figure 1.1. can be distinguished: (i) reversible attachment, (ii) irreversible attachment, (iii) development and (iv) maturation and dispersion [13], [15].

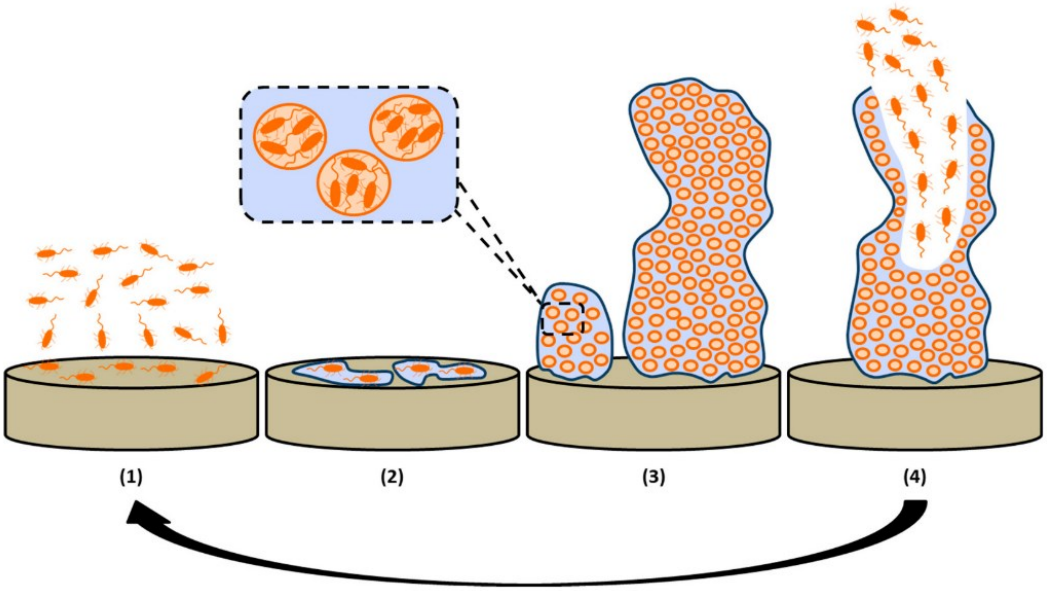

Figure 1. 1. Main stages of biofilm formation: 1) reversible attachment, 2) irreversible attachment, 3) biofilm development and 4) maturation and dispersion [13]

To form the biofilm, the microorganisms begin to settle on the surface using their flagella, forming a reversible attachment. The forces that bind them to the surface are

weak, making them still relatively easy to remove. Changes in bacteria population density cause the production of signalling molecules, called autoinducers. Thanks to these autoinducers, bacteria can detect bacterial density through quorum sensing (QS) ability. Upon reaching the density threshold, an alteration in gene expression is caused, taking way to irreversible attachment [16], [17].

After a change in RNA transcription, secretion of EPM starts, an extracellular polymeric matrix composed by polysaccharides, proteins and nucleic acids, which will give structural support to the biofilm [18]. At the same time, the individual bacteria will form small aggregates in the form of microcolonies, which will be encapsulated in the matrix. These microcolonies will be dispersed between water channels, which will provide the bacteria with the necessary nutrients [19], [20]. In addition, EPM will protect them from antimicrobial agents, making them more resistant.

At this point, planktonic bacteria have become a community of sessile bacteria, developing the biofilm. During biofilm maturation, some of the bacterial microcolonies find difficulties obtaining nutrients, due to their position far from the water channels. This threatens their survival; therefore, they develop mechanisms such as dispersion [21], in which the bacteria detach from the biofilm, in order to nourish themselves and find another place to start to form another biofilm, thus closing the circle.

This way of organizing allows bacteria to adapt better to any environment. Thus, they can resist any unfavourable condition or any attack they receive, such as treatment with antimicrobial agents, much easier. They are considerably stronger than their planktonic equivalents, which is a major problem in medical applications.

As mentioned before, due to the antimicrobial resistance that these pathogens have acquired over the last decades, classic antibiotic treatments are ceasing to work. Furthermore, there has not been much progress in the development of new antibiotics, and even if there were, we would probably face the same problem of tolerance by bacteria after some years [22].

For this reason it is necessary to search for new alternatives, working in an interdisciplinary way. One of the options is to optimize the use of current antibiotics. As much of the blame for acquired resistance lies with overuse of these compounds,

increasing their effectiveness in smaller amounts would be a big step forward. Applying antibiotics in a localized way, with a controlled release, would help to reduce the necessary concentrations to act satisfactorily. Furthermore, by improving the solubility of these drugs, large amounts of antibiotics could be prevented from being lost by our organisms, and thus prevent bacteria from mutating to deal with these compounds. Many of the systems that are being studied to achieve these objectives consist of polymeric systems, either nanoparticles or nanocapsules, hydrogels, coatings or amorphous solid dispersions, among others. This review collects different techniques developed during the last years, divided into three main groups: (i) polymeric nanosystems, (ii) antimicrobial surfaces and coatings and (iii) chitosan-based hydrogels.

However, before talking about systems, it must be said that antibiotics are not the only antimicrobial compounds. Apart from improving the bioavailability of antibiotics, another solution may be to opt for other antibacterial agents. For this reason, before polymeric systems, different antimicrobial options will be presented, also divided into three groups: (i) antibiotics, (ii) metal oxides and metal nanoparticles and (iii) plant-derived compounds.

1.2. ANTIBACTERIAL COMPOUNDS

Antibacterial compounds are antimicrobial agents that are capable of preventing or eliminating infections caused by bacteria, either by inhibiting or slowing their formation of development (bacteriostatic) or by killing them (bactericides). It is clear that in modern medicine the best known and used antibacterials are antibiotics, which will be discussed later. However, its effectiveness is decreasing, so it is time to look at other types of compounds. For example, metals have been used as antibacterials since ancient times, until penicillin was discovered by Sir Alexander Fleming in 1928 [23]. From sutures to treatments for leprosy of tuberculosis, different metals such as silver or copper have shown great value for medical applications [24]. Furthermore, humans have benefited from the healing properties of plants since prehistoric times. However, although there are a large number of plant-derived drugs on the market, they are not used as antibacterials, even if there is evidence that they work as such [25].

1.2.1. Antibiotics

According to Webster's Third International Dictionary (1981), an antibiotic is defined as "a substance produced by a microorganism and in dilute solution having the capacity to inhibit the growth of or kill another microorganism". These small molecules can be of natural origin, synthetic or semi-synthetic, and depending on the type, they act against gram-negative bacteria, gram-positive bacteria, or both. It must be said that small molecules produced by microorganisms are not automatically antibiotics, since to act as such, concentrations that are not probable in nature are required, and this is achieved in laboratories [26].

Antibiotics, in addition to bactericides of bacteriostatics, can be classified according to their mechanisms of action. These are complex processes caused by the physical interaction between the drug and its target, which triggers harmful changes for the bacteria. Fluoroquinolones cause an inhibition of DNA synthesis, which causes bacteriostasis, leading to cell death. Semi-synthetic antibiotics of the ripamycin class also kill bacteria, inhibiting RNA synthesis, impariring the metabolism of prokaryotic nucleic acids. β-lactams and glycopeptides cause cell lysis, since they inhibit the synthesis of cell walls, causing a change in shape and size, and therefore celular stress. Finally, there are other families of antibiotics that inhibit protein synthesis, by suppressing the two ribonucleoprotein subunits that constitute the ribosome (50S and 30S). On the one hand, macrolides, lincosamides, amphenicols, oxazolidinones and streptogramins inhibit the 50S ribosome, while aminocyclitols and tetracyclines act on 30S [27].

Almost all of the antibiotics shown in Table 1.1. fight bacteria that are resistant to them. For this reason, new antibiotics are needed [28]. However, nowadays almost all infections can be cured with existing drugs, so researching new antibiotics is not profitable. There will come a time when we cannot fight different pathogens with current antibiotics, so it is necessary to investigate other systems to apply these same antibacterial drugs more effectively.

Table 1. 1. List of antibiotics according to their killing mechanisms.

Killing mechanism	Drug	Species range	
DNA SYNTHESIS INHIBITIOR	*Fluoroquinolones*		
	Ciprofloxacin	GP/GN	[29]
	Levofloxacin	GP/GN/An	[30]
	Moxifloxacin	GP/GN/An	[31], [32]
	Gatifloxacin	GP/GN/An	[32]
RNA SYNTHESIS INHIBITORS	*Rifamicyns*		
	Rifampicin	GP/GN	[33]
CELL WALL SYNTHESIS INHIBITORS	B-Lactams		
	Penicillins		
	Penicillin G	GP/GN/An	[34]
	Oxacillin	GP	[35]
	Dicloxacillin	GP	[36]
	Ampicillin	GP/GN/An	[37]
	Amoxicillin	GP/GN/An	[38]
	Carbenicillin	GN	[39]
	Mezlocillin	GP/GN/An	[40]
	Cephalosphorins		
	Cefazolin	GP/GN	[41]
	Cefaclor	GP/GN	[42]
	Cefepime	GP/GN	[43]
	Carbapenems		
	Ertapenem	GP/GN/An	[44]
	Imipenem	GP/GN/An	[45]
	Meropenem	GP/GN/An	[46]
	Glicopeptides		
	Vancomycin	GP/An	[47]
PROTEIN SYNTHESIS INHIBITORS	50S		
	Macrolides		
	Erithromycin	GP/GN	[48]
	Azithromycin	GP	[48]
	Clarithromycin	GP/GN	[48]
	Amphenicols		
	Chloramphenicol	GP/GN	[49]
	Lincosamides		
	Clindamicyn	GP/An	[49], [50]
	Lincomycin	GP/An	[50]
	Streptogramins		
	Pristinamycin	GP	[51]

Quinupristin	GP/GN/An	[52]
30S		
Tetracyclines		
Tetracycline	GP/GN	[53], [54]
Doxycicline	GP/GN	[53], [54]
Aminoglycosides		
Streptomycin	GP/GN	[55]
Neomycin	GP/GN	[56], [57]
Hygromycin B	GP/GN	[57]
Gentamicin	GP/GN	[58]
Verdamicin	GP/GN	[59]

It is important when working on antibiotics for the future, to be able to increase bioavailability and optimize localized release so that there is no unnecessary antibiotic left that can affect other parts of the body (as occurs with the "good bacteria" in the digestive system, causing antibiotic-associated diarrhea). In addition, it would be necessary to take into account what freedom of use the patient would have over the treatment. As has been mentioned, the irresponsibility of the users themselves is one of the great causes of bacterial resistance. Therefore, systems that only doctors can apply should be developed, systems over which the patient has no responsibility or power of management, so that the professional can control that the drug is not misused.

1.2.2. Metal oxides and metal nanoparticles

As mentioned before, metals have been used as antibacterial since ancient times. Today they are still used in medicine, being able to interrupt the formation of antibiotic resistant biofilms. Nowadays, the use of these metals in the form of nanoparticles is being studied, since by having a smaller size and a greater surface to volume ratio, the bactericidal effect is not only due to the release of metal ions, but also the interaction of nanoparticles with microbial membranes, thus causing greater cell death [60].

There are metals such as Cu, Ag of Hg that can cause the death of most bacteria, without the need to use large concentrations [24]. Regarding the passive antimicrobial mechanisms of these elements, it is difficult to classify them individually. Due to this problem, Cheeseman et al. proposed three different categories (Figure 1.2.): (i) physical

interactions, (ii) ion leaching/dissolution, and (iii) production of reactive oxygen species (ROS) [61].

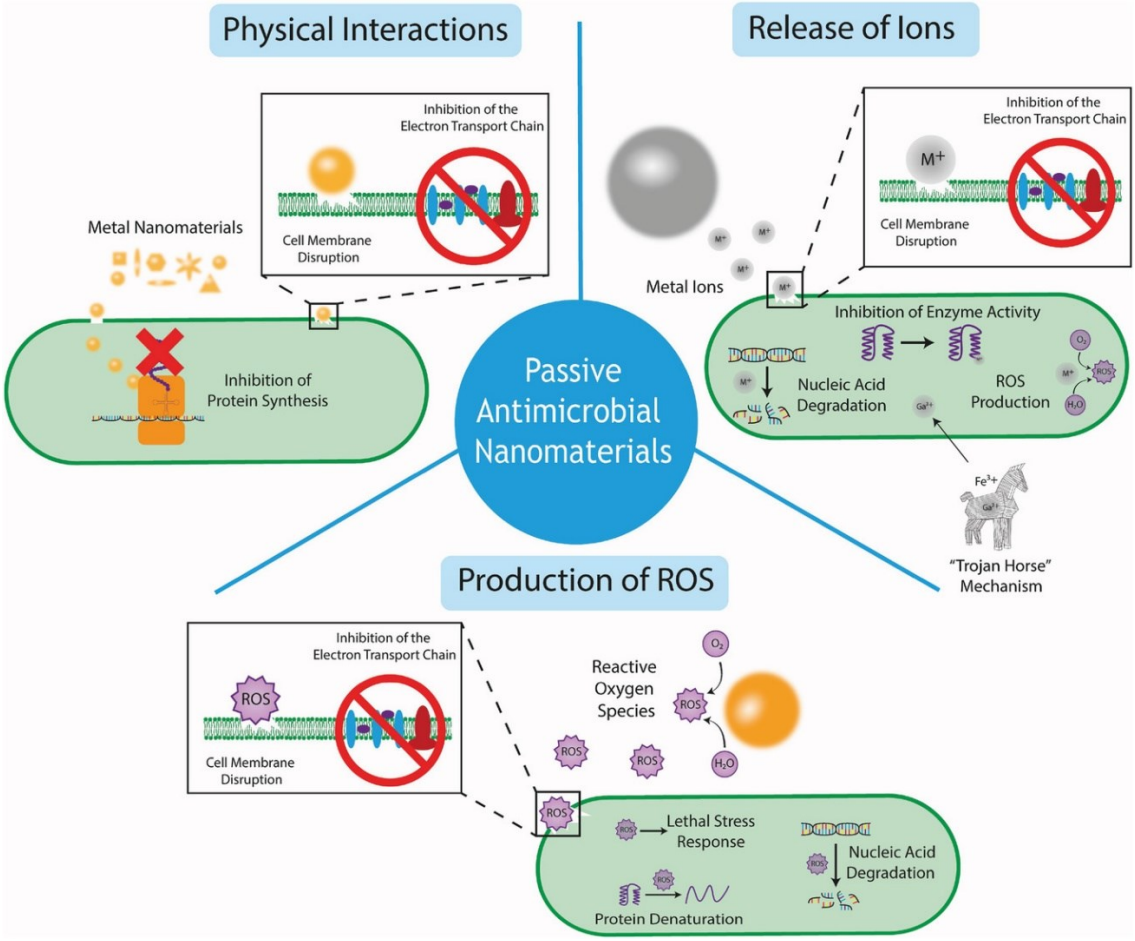

Figure 1. 2. Diagram representing the range of passive antimicrobial mechanisms of metal nanomaterials: physical interactions, realease of ions and production of ROS [61].

In this section, commonly used metal oxides and metal nanoparticles are mentioned, as well as a brief explanation of their antimicrobial mechanisms.

Silver

Despite being inert in the metallic state, ionized silver is highly reactive, being able to inhibit the replication of bacteria, and cause cell death [62]. Silver nanoparticles are effective against bacteria such as *Escherichia coli, Staphylococcus aureus, Staphylococcus epidermis, Bacillus subtilis, Klebsiella mobilis, Klebsiella pneumonia* or *Leucconostoc mesentedamientos*. Of course, the different species of bacteria, which can be gram-positive or gram-negative, show differences in their membrane structures, with the antimicrobial effect of the Ag particles being different in each case [63]

Although contradictions are found, the most commonly proposed mechanisms of toxicity are three. On the one hand, uptake of free silver ions followed by disruption of ATP production and DNA replication. On the other hand, the excess production of free radicals caused by the reactions with oxygen catalyzed by the nanoparticles. Lastly, direct damage to cell membranes, due to the penetration of silver nanoparticles into the cell. This is believed to be due to the interaction caused by the electrostatic attraction of negatively charged cell membranes, and positively charged nanoparticles [64]. However, a study by Sondi and Salopek-Sondi [65] caused confusion by noting that negatively charged silver particles were also bactericidal. It seems that even with a negative charge, they can cause structural changes and cell death by interacting in some way with the membranes of bacteria, having observed the formation of "pits" on their surfaces.

It is worth mentioning that some recent studies such as those performed by Khan et al. and Chand et al. have managed to biosynthesize silver nanoparticles from the bacterial strain *Bacillus sp.* (MB353) and *Acacia catechu* extract, respectively [66], [67]. By using these methods, a more economical and environmentally friendly synthesis is achieved.

Zinc oxide

Zinc oxide in nanoparticle form is part of the group of elements with antibacterial effects. It is non-toxic to human cells, since it is an essential inorganic element[68].

These nanoparticles are toxic to a wide spectrum of bacteria, both Gram-positive and Gram-negative. But the bactericidal mechanisms are still not entirely clear, since there are different causes such as cell death due to the generation of intracellular ROS, damage to cell walls caused by the adhesion of nanoparticles to the cell membrane or due to the release of Zn^{2+} ions, or even by the internalization of nanoparticles [69], [70]. The fact that different mechanisms arise could be owing to the possibility of changes in the physicochemical properties of the nanoparticles and of the dissolved zinc due to the medium in which they are found [71].

The advantages shown by zinc oxide nanoparticles are various, but it has been appreciated that both their production and application can be ecologically problematic. For this reason, some studies have resorted to the biosynthesis of these nanoparticles - which have been found to have greater biocidal activity when compared to chemical

ZnO - such as Gunalan et al., biosynthesizing them using plants such as *Aloe vera* [72] or Naseer et al. who have done the same using extracts of the medicinal plants *Cassia fistula* and *Melia azedarach* [73].

Copper

With more than thirty types of copper-containing proteins, this metal is an essential element for the survival of most living organisms [74]. In fact, for humans, a copper deficiency can cause diseases such as anaemia, neutropenia and bone abnormalities [75].

Copper has attracted attention due to its accessibility. It is an element with a lower cost than gold or silver, despite sharing its antibacterial properties. Copper or copper oxide nanoparticles have the capacity to deal with both Gram-negative and Gram-positive bacterial strains, their activity being dependent on the particle size. However, it is not known with certainty if the antibacterial effectiveness depends on the nanoparticles, or on the Cu^{2+} ions that it releases [76].

As with silver and zinc, the chemical process to obtain the nanoparticles is an environmental problem. But in this case, another limitation of copper must be added, which is its rapid oxidation when exposed to air. Therefore, it has also been proposed to use plant extract in a green synthesis to stabilize the nanoparticles [77]. For example, Asghar et al. concluded that copper nanoparticles could be synthesized using extracts of leaves o *E. camaldulensis, A. indica, M. koenigii, A. marina, R. rubiginosa* or *D. stramonium* [78].

Others

Apart from those previously discussed, more metals with antibacterial properties in the form of nanoparticles have been proposed, such as titanium oxide (TiO_2), gold (Au), silica (SiO_2), or magnesium oxide (MgO), among others [79]–[82].

In addition to having several possible elements, the antimicrobial activity of each one of them depends on factors such as physicochemical characteristics or morphology [83]. Therefore, there is a wide range of possibilities in the use of metallic nanoparticles.

Although metal particles offer many interesting options, it is often mentioned that their production can be harmful to the environment. This damage could be assumed if it were for some specific cases, but if we reached a point where the use of this type of particles was normalized, it could become unacceptable. As a solution, it is proposed to synthesize these particles from natural extracts, which will be discussed in the next part. However, if the absolute efficacy of these plant extracts were to be demonstrated, the question arises whether it would not make more sense to cover everything possible with them and use the metallic particles for very specific applications.

1.2.3. Plant-derived compounds

Throughout history, the healing capacity of plants has been trusted, in the form of infusions, plasters or even as a part of the diet. This type of remedy can be found in any culture, with traditional Chinese or Andean medicine as important examples. However, there has always been certain scepticism towards the use of these plants, since they have also been linked to magic during history. But leaving this aside, science has been investigating how these natural compounds act. Their antioxidant and antimicrobial properties have been studies above all, given the possibility of being one of the solutions to the acquired resistance of bacteria against antibiotics [25], [84].

Currently, research goes beyond knowing the beneficial properties of plants. Studies have become more specific, determining which plants or which active principles of these plants can attack specific microorganisms, in order to isolate them and apply them directly, either alone or with antibiotics, in order to increase their potency. The aromatic substances synthesized by plants can be divided into various groups such as alkaloids, terpenoids, essential oils, lectins… but those that show the greatest chemical activity are phenolic substances (Figure 1.3.), acting mainly against Gram-negative bacteria.

Phenolics and polyphenols

Polyphenols are secondary metabolites produced by plants, whose molecular structures are characterized by having one or more phenolic rings. They have several beneficial properties for the human body, such as antioxidant, anti-inflammatory, anti-cancer or antimicrobial properties, among others. More than 8000 phenolic substances are known, which range from simple molecules (e.g., phenolic acids) to highly polymerized

compounds (e.g., tannins). Due to this great variety, polyphenols are divided into two main groups based on their chemical structures: flavonoids and non-flavonoids [85], [86].

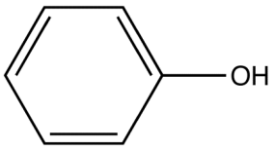

Figure 1. 3. Simple phenol structure.

Flavonoids

Flavonoids are compounds that can be found in plants, such as vegetables, fruits, flowers… even in tea and honey. They are formed from the aromatic amino acids phenylalanine and tyrosine and have three rings (C_6-C_3-C_6), called A, B and C, with a total of 15 carbon atoms. There are several subfamilies of flavonoids, and each type differs in the level of oxidation and the substitution pattern of the C ring (Figure 1.4.). These families of flavonoids include flavones, isoflavones, flavon-3-ols (or catechins), among others, depending on the level of oxidation on the mentioned ring. On the other hand, the substitution patterns of rings A and B are those that define the compounds individually [87], [88].

Several research groups have studied the *in vitro* activity of flavonoids obtained from plant extracts that have been used in history [89]–[96], and synergistic effects have even been observed between flavonoids and other antibacterial agents, dealing with resistant strains of bacteria [97]–[102]. The antibacterial mechanisms that these flavonoids may have are diverse, including inhibition of nucleic acid synthesis, inhibition of energy metabolism, or inhibition of cytoplasmic membrane function [103].

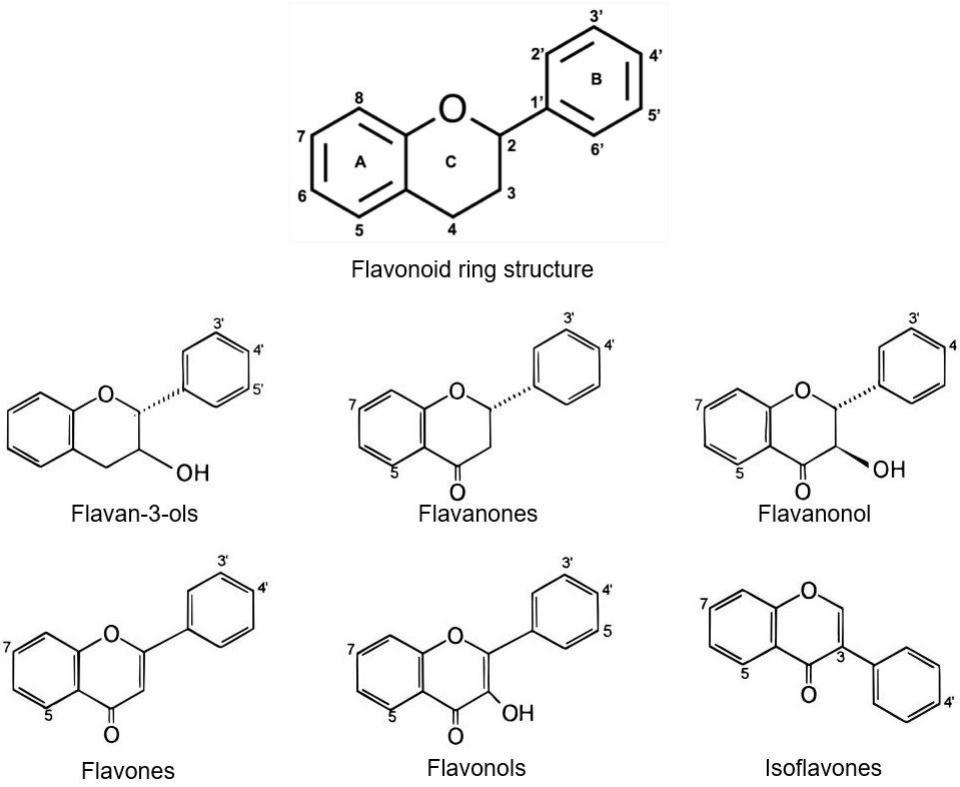

Figure 1. 4. Structures of flavonoids.

Non-flavonoids

As mentioned before, there is another group formed by non-flavonoid metabolites. In this case, the basic structure of these compounds is a single aromatic ring. Although non-flavonoids show less effectiveness against bacteria than flavonoids, they are worth taking into account, since some of these compounds (i.e. gallic, caffeic and ferulic acids) have been found to be more effective than certain antibiotics (i.e. gentamicin, streptomycin) against both Gram-positive and Gram-negative bacteria [86].

Different subgroups are also divided among non-flavonoid metabolites. The most widespread and known are phenolic acids, which consist of simple molecules with a carboxylic acid group. These are divided into two subgroups: hydroxycinnamic acids (C_6-C_3), the most common being *p*-hydroxybenzoic, protocatechuic, vanillic and syringic acid, and hydroxybenzoic acids (C_6-C_1), such as ferulic, *p*-coumaric, caffeic, or sinapic acid. Phenolic acids are capable of altering the physicochemical properties on the surfaces of bacteria, and their mechanisms of action can range from destabilizing the cytoplasmic

membrane of the bacteria, to altering microbial metabolism directly. Caffeic acid is considered one of the most important compounds [104]–[108].

The second group is formed by stilbenes, characterized by having two aromatic rings joined by an ethylene moiety. They can be found in two different diastereoisomeric forms, the E-stilbenes (*trans* configuration), which are the most common, and the Z-stilbenes (*cis* configuration) [109]. Furthermore, they can be present in monomeric or oligomeric form, resveratrol being one of the most representative monomers, in addition to forming the largest oligomeric groups, being able to polymerize between 2 and 8 units [110]. Resveratrol became well known when it was associated with the benefits of moderate consumption of red wine, the so-called "French paradox" [111], [112]. Since then, it is one of the most studied natural products [113], including its antibacterial properties [114]–[116].

Despite its benefits, one of the biggest barriers that this type of compound can encounter is the scepticism that has been created around it. This opinion is partly justified, since many pseudosciences have been based on the power of plants to sell miracle cures. These types of products claim to be able to help you be happier, lose weight or cure diseases such as cancer, arthritis and even Alzheimer's, among many other illnesses. However, it must be born in mind that what is used in scientific studies are the active agents of these plants, not the plant itself. Therefore, it is necessary to publicize the benefits of these compounds, to make proper use of the resources that nature offers us, and stop relating them to pseudoscience or scams.

1.3. POLYMER BASED STRATEGIES

As mentioned before, one of the main problems of antibiotics has been their excessive use. Apart from the abuse on our part, the high amounts used for the treatments have helped to create this resistance of the bacteria. Although other options are now open with plant-derived compounds, we still ignore if we could have the same problem in the future. Therefore, it is important to work on an approach aimed at reducing the dose of administered drug, improving its bioavailability, with more efficient treatments [117].

With this objective, the use of both synthetic and natural polymers presents a wide range of possibilities. On the one hand, some polymers are known to be capable of

acting as antimicrobial agents on their own [118]. On the other hand, polymeric systems can be created combined with bioactive substances, thus being able to improve the performance of these compounds, improving, for example, their solubility, controlled release or localized application, among other properties [119].

These systems can be both to prevent bacterial infections from the initial stages, and to act as biocides once the bacteria have adhered. For both approaches, different strategies based on polymeric materials can be designed, such as drug-loaded nanosystems, hydrogels, or modified surfaces. In the next section some of the options that have been studied recently are exposed.

1.3.1. Polymeric nanosystems

Most nanosystems consist of means of transporting antibacterial agents, so that they are released in the right place and at the right time. These systems, such as nanoparticles, polymersomes, nanocapsules or nanogels, among others, prevent the drug from being lost in the cleaning system of the body, being able to maintain therapeutic concentrations without having to introduce an excessive amount. Furthermore, it facilitates the arrival of the antibacterial agent to the area in need, being able to improve penetration through different tissue barriers [117]. In Figure 1.5., some antibacterial polymeric systems are shown, including antibiotic-containing polymeric nanosystems and intrinsic antibacterial polymer nanosystems.

Some polymers, as mentioned above, have antibacterial properties without the need to add any active molecules. For example, Barman et al. describe self-assembled polyurethane capsules capable of acting against Gram-negative bacteria. In this study they observed the antibacterial capacities of amphiphilically segmented polyurethanes, PU-1 and PU-2, in which primary or secondary amino groups, respectively, had been placed in a flexible hydrophobic PU scaffold. A PU-3 was also synthesized without any amino group, and it was observed that the latter was not effective against Gram-negative bacteria (in this case *E. coli*), while those that contained amino groups were. It should be added that none of the three caused any effect against Gram-positive bacteria (*S.aureus*) [120].

Belbekhouche et al. also studied the antibacterial capacity of other polymers, in this case polysaccharides such as chitosan or alginate. Chitosan will be given greater prominence later in this same review, as it shows many interesting properties for medical applications. In this case, nanocapsules were manufactured using de LbL (Layer-by-Layer) technique onto gold nanoparticles as a sacrificial matrix. Briefly, on this gold nanoparticles, the polycation (chitosan) was applied until they were completely covered, to after add a layer of polyanion (alginate), thus forming a single bilayer: $(\text{chitosan/alginate})_n$, where *n* is the number of bilayers applied. After forming the particles with the desired number of layers, the gold template was dissolved, in order to create empty capsules. The antibacterial activity of these capsules of different amounts of bilayers was studied in both Gram-positive (*S.aureus*) and Gram-negative (*E.coli*) bacteria. In addition, they also performed the same studies without having eliminated the gold template, that is, in the form of rigid particles. Results showed a similar effect in both strains: the more layers, the more bacterial growth inhibition, in addition to having a greater inhibitory effect in the form of flexible capsules, and not as rigid particles [121].

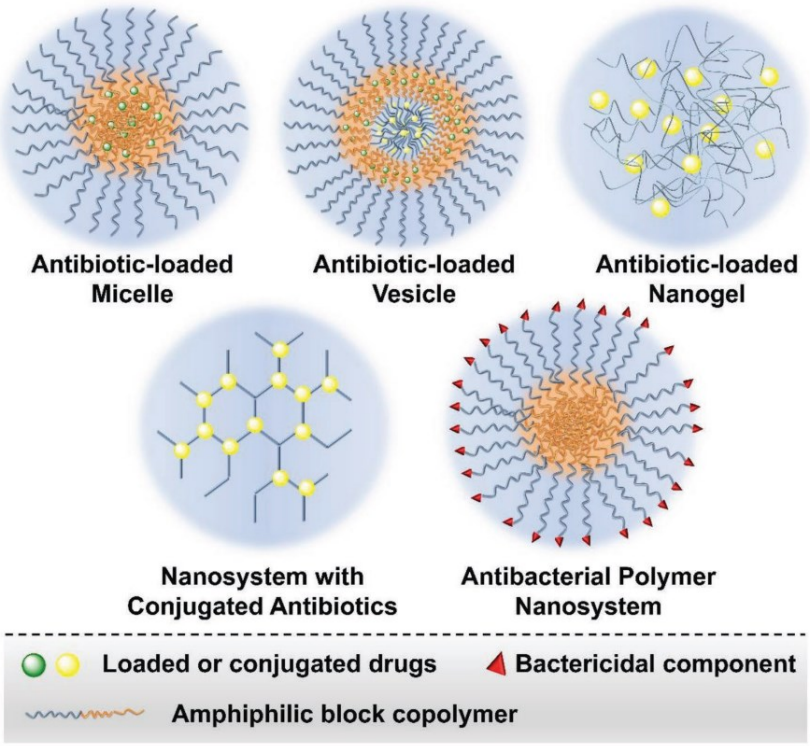

Figure 1. 5. Biodegradable antibacterial polymeric nanosystems in the forms of micelles, vesicles, nanogels, hyperbranched nanoclusters, and antibacterial polymer nanoparticles. Green dots represent the hydrophobic antibiotics, while the yellow dots represent hydrophilic ones.

However, as mentioned at the beginning of this section, the main objective of these nanosystems is to transport all kinds of drugs or active agents. Focusing on polymeric nanoparticles and nanocapsules, several examples of these combined systems can be seen, making use of natural or synthetic polymers, of varied active agents such as antibiotics, essential oils or even metals such as calcium or zinc. The use of the latter can be observed in the work of Toledano-Osorio et al. [122] , where nanoparticles (NP) whose main components are 2-hydroxyethyl methacrylate, ethylene glycol dimethacrylate and methacylic acid were tested with three types of antibacterial agents: the antibiotic doxycycline (DOX), and the metals (Ca) and zinc (Zn). Against bacteria such as *P. gingivalis*, *S. mutans* and *L. lactis*, calcium or zinc loaded NPs were found to be more effective than unloaded NPs. However, the ones that showed to be the most effective were those loaded with doxycycline. It is worth mentioning that the bacteria *S. gordonii* and *S. sobrinus* were the least susceptible to nanoparticles.

Ong et al. [123] opted for the use of more natural components. The chitosan-propolis nanoparticles (CPNP) that were tested against *S. epidermidis* were prepared using Malaysian propolis, a natural product obtained from beehives. A significant decrease in bacteria in the biofilm could be seen due to the effect of CPNP, with a reduction of up to 90%. It should be noted that in addition to eliminating bacteria in the formed biofilm, these nanoparticles showed the ability to inhibit the creation or growth of new biofilm. These CPNPs are a good example of the possibility of synergy that exists when combining different polymers and natural compounds with antibiotics. In this case, this phenomenon could be observed with antibiotics such as rifampicin, ciprofloxacin, vancomycin and doxycycline, being able to reduce the antibiotic dose by at least 4-fold.

Another case in which a synergistic effect between a polymeric system and a drug can be suggested is that of starch nanocapsules (NC) loaded with fluoxetine (FLX). In this work by dos Santos et al. [124], NCs of crosslinked polymer shell with a hydrophylic core were obtained, with regular spherical structures and high drug loading capacity, using an interfacial polyaddition reaction. When applying these FLX-loaded NCs on resistant *S. aureus*, the required MIC values were found to be much lower than free-FLX.

Continuing with nanocapsules, combining a natural essential oil with natural and synthetic polymers da Silva et al. [125] have tested chitosan (CS) and poly(ε-

caprolactone) (PCL) nanocapsules (NC) loaded with tea tree oil (TTO) for the treatment of topical acne. PCL nanocapsules did not show any activity against *C. acnes*, and these NCs loaded with TTO maintained the same MIC values as those obtained for free-TTO. In contrast, when chitosan was added, a significant increase in activity against *C. acnes* was seen, with a x4 reduction in MIC.

The antibacterial help of chitosan has also been observed in the work of Anversa et al. [126]. In this case, they encapsulated the antibiotic clarithromycin (CLARI) in PLGA nanocapsules, being able to reduce the number of intracellular *S. aureus* in vitro by 1000 compared to the same dose of CLARI. By coating the particles with chitosan, it could be seen that the effect was even greater, due to the intracellular absorption caused by the cationic surface.

These kinds of systems have also been proposed for veterinary medicine, as is the case in the work of Araújo et al [127]. Poly (ε-caprolactone) nanocapsules were loaded with the veterinary antibiotic cloxacillin benzathine, to confront bovine intramammary infections, such as *S. aureus* caused mastitis. This research resulted in a complete elimination of the pathogen after treatment, without any clinical signs of toxicity.

The option of using polymeric nanosystems presents a great advantage when it comes to its application. Due to their size, they have the chance of being injected, which could make it possible to direct them directly to the needed area without the need to use any invasive technique. In addition, especially in the case of nanocapsules, they can present a wide range of options. Once the capsules have been developed, they could be loaded with different active compounds, those that are needed at any given case. Due to these advantages, today they are one of the most attractive options for localized applications, with a wide variety of possible combinations.

1.3.2. Antimicrobial surfaces and coatings

The development of antibacterial surfaces is an advance that can reduce the use of antibiotics and even eliminate it. These surfaces, used mainly in implantable devices, but also in external devices in contact with the body such as contact lenses, catheters or wound patches, can prevent a large number of infections. They can attack the bacteria that cover the biofilm, but ideally they can avoid the formation of said biofilm,

preventing any type of infection. The key to achieving this goal is in the interactions between cells and the surface, and these variations depend on factors such as the architecture of the surface, the surface energy of the material, or the chemical composition [128], [129]. There are polymers that by themselves, due to their type of surface, are antibiofouling and resist the adhesion of bacteria, such as zwitterionic polymers or polymers incorporating oligosaccharide moieties [130]. But this section will focus on polymeric matrices loaded with antimicrobial substances.

In these systems the loads can be distributed in different ways. There are systems that focus antimicrobial substances to the surface, so that there is more direct contact with the surrounding environment. However, this type of coating can be harmful. If the release is too rapid, too much drug may be released before the bacteria arrive, leaving insufficient quantity to deal with them [131]. This could increase the resistance of the bacteria, as the system would not be able to kill them. On the other hand, it must be taken into account that most devices that need this kind of antimicrobial materials have to withstand different mechanical loads during their application, which could damage their surfaces and lose antibacterial effect [132]. Obviously there are systems that work well with their charge distributed on the surface, as is the case of Giraud et al., where they incorporate carbon nanomaterials (CNM) on the surface of the polymeric matrix. In this work, it has been seen that CNMs are more effective when they are on the surface, since they damage cell membranes through electrostatic interactions, so that the particles found inside are practically useless [133]. Another system with this characteristic can be seen in the work of Aničić et al., in which they compare three polymers (poly-lactide-co-glycolide (PLGA), poly-lactide (PLA) and polycaprolactone (PCL)) loaded with nano-textured MgO microrods. The objective was to combine the antibacterial and regenerative properties of MgO with a polymer that would allow to keep the surface of the microrods accessible to interact with the cells, with PLGA being the most effective [134].

Focusing on the bulk manufactured composites, a wide variety of mixtures can be found, in which loaded substance performs the antibacterial function. This function is usually biocidal, and can be through release killing or contact killing. In release killing, antimicrobial particles act when released, and can even prevent bacteria from adhering

to the surface, causing an antifouling behaviour. On the contrary, if they act by contact killing, the bacteria are damaged once they have reached the material. These different mechanisms are shown in Figure 1.6. These fillers can be of various types, from natural clay minerals [135] to essential oils, and even combinations of various types [136].

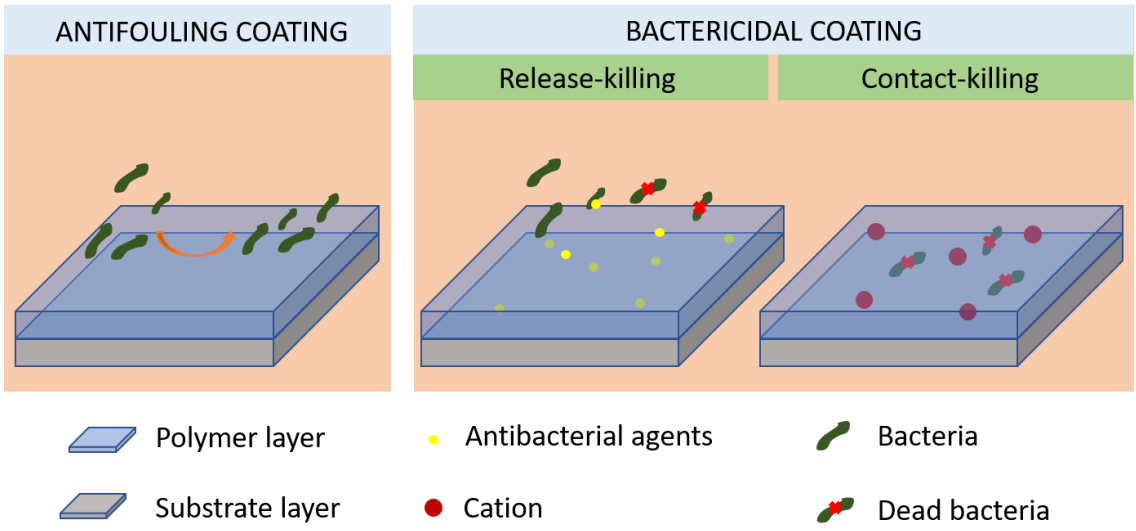

Figure 1. 6. Different types of antibacterial coatings.

Metallic nanofillers are widely used in these types of materials. One metal that stands out above all is silver, both as a single charge, and in combination with other types of active molecules [132], [136], [138]. It is known to work as an antimicrobial, but the effects it may have regarding toxicity are not entirely clear [138]. In this kind of fillers, in which electrostatic interactions act, the shape and dimensions of the particles are highly influential. A good example is the work by Stamenović et al., where they study two nanocomposites of polyaniline/polyvinylpyrrolidone loaded with silver nanoparticles (AgNPs). The difference between the two systems lies in the morphological characteristics of the nanoparticles, being spherical in one, and triangular in the other. Research results show significant antimicrobial activity for both systems, although the matrix containing the triangular nanoparticles shows higher activity. They may be due to the highly reactive crystallographic planes on the surface of the particles providing higher surface energy [138].

Leaving aside metallic particles, polymeric matrix compounds can be formed with loads of active molecules such as antibiotics or plant-derived compounds. In these cases, the biggest problem resides in the fact that most of these compounds used nowadays are in

crystalline form, reducing their solubility and bioavailability. In addition to causing problems in the release of the compound, it can create weaknesses in the mechanical properties, due to the heterogeneity of its composition and the separation of phases. To solve this problem, one of the strategies is to form amorphous solid dispersions (ASD), where the amorphous polymers create a structure that inhibits the crystallization of the active molecules. Drugs can interact with polymer chains, reducing their mobility and keeping them amorphous, thus creating a homogeneous and miscible mixture [139]. To form these blends, it is necessary to confirm the miscibility and interactions between the polymer and the drug [139], [140].

The release of the antimicrobial compound can also be a problem. It is common for surfaces to have a burst release before the arrival of bacteria, losing its effect. To avoid this burst, coatings that respond to external stimuli are being designed, such as the one designed by Albright et al. In their work, they have created a coating using the layer-by-layer technique with a poly (methacrylic acid) hydrogel loaded with antibiotic (gentamicin or polymyxin B), sensitive to pH changes. As the adhesion of bacteria produces localized changes in pH, these coatings respond with the release of the drug to this adhesion. Thus, the drug acts at the necessary time and location [131].

These systems seem to be the most likely option in the short-medium term, although their applications are limited to surfaces. Even so, the advantages they present could represent a great advance. On the one hand, by applying it to medical devices such as catheters or intravenous lines, a large number of nosocomial infections could be prevented, thus avoiding a significant number of unnecessary deaths. Using them as prosthesis coatings, many rejections and surgeries derived from them would also be avoided, saving a lot of money and, above all, discomfort and pain for the patients. On the other hand, through their use as skin patches, they are very useful for treating burns, wounds or even skin cancer. Although their use is more limited for internal injuries, the possibilities they present can save many lives.

1.3.3. Chitosan based hydrogels

During this review, chitosan has been mentioned several times. This is because it is a widely used material for biomedical applications, due to its favourable properties. Chitosan is obtained from the deacetylation of chitin, which can be found in the shells of

crustaceans. It is a hydrophilic and cationic polymer, one of the most abundant polysaccharides in nature. Its structure contains abundant hydroxyl (-OH) and amino ($-NH_2$) groups, which facilitate its crosslinking with crosslinking agents. Its properties include biodegradability and biocompatibility, as well as being able to imitate the extracellular matrix by forming hydrogels. It has antibacterial properties, being positively charged, it can bind to negatively charged bacteria and kill them. Several mechanisms by which chitosan can act as an antibacterial agent are studied, as summarized by Guarnieri et al. in their work [142]. On the one hand, chitosan can change the osmotic balance of the cell wall, thus altering its amount of calcium. Another of the proposed mechanisms is the blockade that positively charged chitosan can produce in the synthesis of RNA and proteins. The action in Gram-positive and Gram-negative bacteria is also different, since in the former chitosan affects the anionic structures of the surface, while in the latter it interacts directly with the negative charges of the cell wall. The way in which chitosan affects bacteria can vary depending on their physical characteristics, and among them, the molecular weight is considered the one that probably affects the most. Even so, this correlation is not entirely clear [143].

Chitosan is used mainly for the formation of hydrogels. Hydrogels are three-dimensional polymeric structures, formed by interconnected flexible polymeric chains. Their main characteristics are the porous structures they form, and their ability to absorb and trap large amounts of water. Due to these characteristics, hydrogels are ideal for drug delivery or tissue engineering applications. In the case of chitosan-based hydrogels, reviewing different studies it can be seen that their application focuses mainly on wound healing [144]–[149], since they can provide a suitable environment for debridement and healing. However, although it has many positive properties, its mechanical stability and strength are not sufficient for most applications, so it is strengthened with other polymers or nanoparticles, among others [150].

Hydrogels can be classified in several ways, but one of the main ones is the differentiation between chemical and physical hydrogels. This depends on the types of bonds that are formed during the manufacturing process. On the one hand, physical hydrogels are formed by weak bonds, such as hydrogen bonds or ionic interactions, and are reversible. This type of gels has advantages such as greater water absorption,

greater possibility of drug loading, or injectability. They degrade easily, and have much lower resistance than chemical hydrogels. Chemical hydrogels are formed by covalent bonds, these being permanent, and much more resistant. The biggest problem with this type of hydrogels is that crosslinking agents or catalysts are often used to achieve these covalent bonds, and these could affect their environment, drugs or proteins, and be toxic. To avoid these negative effects, the alternative is to study physical hydrogels with improved mechanical properties, or to obtain hydrogels with covalent bonds without any crosslinker.

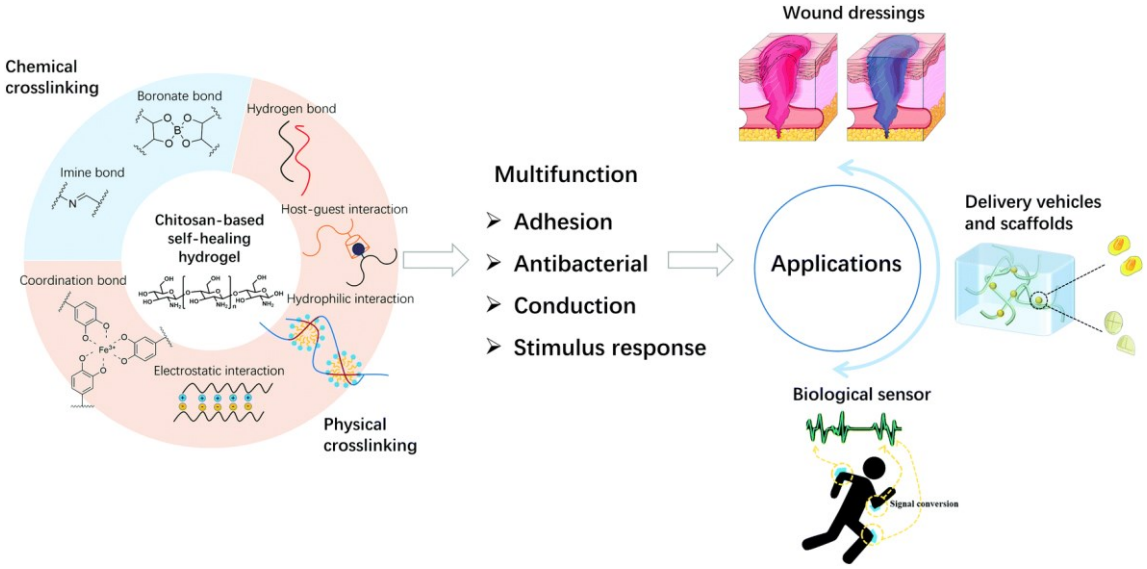

Figure 1. 7. Chitosan-based self-healing hydrogels: self-healing mechanisms, functions and applications [151].

Ling et al. manufactured hydrogels based on L-arginine conjugated chitosan (CA), benzaldehyde group functionalized poly(ethylene glycol) (CHO-PEG-CHO), and polydopamine nanoparticles (pDA-NPs), named as CA-pDA. These hydrogels were prepared using dynamic Schiff-base based crosslinking [148]. Shiff's base reactions have received great attention in the manufacture of hydrogels, since it is possible to perform them without using any catalyst, and it is possible to form in-situ forming hydrogels. A Schiff's base is obtained when amines of hydrazides react with electrophilic carbon atoms of aldehydes or ketones, however, aldehyde-containing molecules can affect the molecules of the extracellular matrix tissues by reacting with amino groups [152].

One of the crosslinking agents used to form chitosan hydrogels is glutaraldehyde. This compound is seriously toxic, so Hoang Thi et al. decided to reduce the amount used and

replace it with the bioactive compound *aloe barbadensis Mille*r (aloe vera). They managed to manufacture chitosan/*aloe barbadensis Miller*-glutaraldehyde hydrogels (CS/AV-GDA) with 4-fold lower glutaraldehyde concentration, and without causing changes in the characteristics of the hydrogel. Thus, these hydrogels with less than 1% glutaraldehyde as a crosslinker did not show any type of cytotoxicity. In addition, the mechanical and physicochemical properties were maintained or even improved, and were shown to be effective for antibacterial, vascular, or angiogenesis treatments [153].

As previously discussed, physical hydrogels have the advantage of injectability. This is also possible with chemicals, but they have the risk of dissolving after injection, due to their slow gelation kinetics [152]. In the case of physical hydrogels, this gelation occurs in-situ under certain environmental conditions, such as pH, light or temperature. Chitosan-based hydrogels are very useful for temperature-based transformation, that is, to form thermosensitive hydrogels, because their gelling temperature is around 35°C, very close to body temperature [145], [154], [155]. Although the formation of these hydrogels is considered in-situ, there may be cases in which this transformation takes longer due to different causes, such as different pH. One of the ways to ensure that this does not happen is by using near-infrared light (NIR) as a "trigger switch". Liu et al. manufactured synergistic chitosan-based thermosensitive hydrogels, formed by chitosan and *β*-sodium glycerophosphate, with mesoporous polydopamine nanoparticles (MPDA NPs) combined with the antibacterial agent ciprofloxacin (Cip) and human epidermal growth factor (h-EGF) (h-EGF-CS/ *β*-GP-MPDA@Cip). These hydrogels had the ability to change phase rapidly and release drug under near-infrared light (NIR). Using this strategy, they not only managed to form the gel and release the drug, but the high temperatures caused bacterial lysis, creating a synergistic effect between chemotherapy and photothermal therapy (PTT), with low invasiveness and high tissue penetration capacity [146].

The injectability and in-situ formation is what most differentiates this strategy from the others, since it allows the material to conform to the necessary tissues and spaces without the need for invasive techniques. In addition to the antibacterial activity of chitosan itself, these hydrogels can be loaded with different drugs of active agents, thus being able to apply them for many therapies. However, it has some limitations, such as

aforementioned mechanical properties. Although they can be modified, and achieve sufficient resistance to be applied to soft tissues, it is not sufficient for hard tissues such as bone tissue, or to be applied to joints. This is largely due to the difficulty of achieving homogeneous dispersions of water-insoluble particles such as ceramics. In addition, the release kinetics of each designed hydrogel must also be taken into account, since changing the mechanical properties also modifies the swelling capacity, the initial burst or the release time.

1.4. CONCLUSIONS

Due to the looming problem of antimicrobial resistant pathogens, it is of great importance to continue researching, and above all, implementing new antibacterial systems. Different options have been discussed in this review, both for antibacterial agents and for polymeric systems. As for antibacterial agents, we can still count on some antibiotics, although their use must be reduced and modified so that they do not completely lose their effect, and to prevent bacteria from continuing to increase their resistance to them. One option to reduce its use is the help of other types of compounds, such as metal oxides or metal nanoparticles. They are effective against different types of bacteria, but their toxicity is not entirely discarded and their production can be harmful to the environment, so their use should not be abused. Compounds derived from plants are also getting attention, which can be very beneficial, but there is still much to investigate about them, in addition to having to gain the acceptance of a large part of society. On the other hand, it is known that the oral administration of drugs is inefficient in many cases, since the bioavailability of the active compound can be affected, in addition to directing the active compound to unnecessary places, affecting other systems of our bodies. This is where the new strategies with polymeric systems take part, since they allow adapting the form of application of each treatment to the different needs that might arise. Polymeric nanosytems, in the form of capsules, particles or nanogels among others, allow drugs to penetrate all types of tissues due to their small size. Antibacterial surfaces and coatings could reduce or even eliminate nosocomial infections through their application in catheters or intravenous lines, avoiding a large number of unnecessary deaths. Lastly, hydrogels, in this case those made of chitosan, facilitate in-situ injection and formation, as well as being able to

control drug release by means of external stimuli. However, it is necessary to mention that the existence of these advances does not mean that we have to do without antibiotics altogether. With correct use and through appropriate strategies, it is possible to increase the effectiveness of antibiotics and reduce the amount used, always also relying on individual responsibility. The strategies mentioned in this review, among many others, can be of great help in the future, but there is still much to investigate and test, so we cannot relax thinking that we already have a solution. It may take a few years for the common use of these techniques to become a reality; until then, it is up to us to act carefully and fight bacteria as efficiently as possible.

1.5. REFERENCES

[1] D. J. Weber and W. A. Rutala, "Understanding and Preventing Transmission of Healthcare-Associated Pathogens Due to the Contaminated Hospital Environment," *Infection Control & Hospital Epidemiology*, vol. 34, no. 5, pp. 449–452, 2013, doi: 10.1086/670223.

[2] A. Y. Peleg and D. C. Hooper, "Hospital-Acquired Infections Due to Gram-Negative Bacteria," *The New England Journal of Medicine*, vol. 362, pp. 1804–1813, 2010.

[3] R. Greenhalgh, N. C. Dempsey-Hibbert, and K. A. Whitehead, "Antimicrobial strategies to reduce polymer biomaterial infections and their economic implications and considerations," *International Biodeterioration and Biodegradation*, vol. 136, no. October 2018, pp. 1–14, 2019, doi: 10.1016/j.ibiod.2018.10.005.

[4] D. I. Andersson and B. R. Levin, "The biological cost of antibiotic resistance," *Current Opinion in Microbiology*, vol. 2, no. 5. Current Biology Ltd, pp. 489–493, Oct. 01, 1999. doi: 10.1016/S1369-5274(99)00005-3.

[5] M. Sundqvist, "Reversibility of antibiotic resistance," *Upsala Journal of Medical Sciences*, vol. 119, no. 2, pp. 142–148, May 2014, doi: 10.3109/03009734.2014.903323.

[6] T. P. M. Editors, "Antimicrobial Resistance: Is the World UNprepared?," *PLOS Medicine*, vol. 13, no. 9, p. e1002130, Sep. 2016, doi: 10.1371/journal.pmed.1002130.

[7] Review on Antimicrobial Resistance, "Antimicrobial Resistance: Tackling a crisis for the health and wealth of nations," 2014.

[8] G. L. French, "The continuing crisis in antibiotic resistance," *International Journal of Antimicrobial Agents*, vol. 36, no. SUPPL. 3, pp. S3–S7, Nov. 2010, doi: 10.1016/S0924-8579(10)70003-0.

[9] H. W. Boucher *et al.*, "Bad Bugs, No Drugs: No ESKAPE! An Update from the Infectious Diseases Society of America," *Clinical Infectious Diseases*, vol. 48, no. 1, pp. 1–12, Jan. 2009, doi: 10.1086/595011.

[10] N. F. Kamaruzzaman *et al.*, "Antimicrobial polymers: The potential replacement of existing antibiotics?," *International Journal of Molecular Sciences*, vol. 20, no. 11, 2019, doi: 10.3390/ijms20112747.

[11] L. B. Rice, "Federal Funding for the Study of Antimicrobial Resistance in Nosocomial Pathogens: No ESKAPE," *The Journal of Infectious Diseases*, vol. 197, no. 8, pp. 1079–1081, Apr. 2008, doi: 10.1086/533452.

[12] S. Santajit and N. Indrawattana, "Mechanisms of Antimicrobial Resistance in ESKAPE Pathogens," 2016, doi: 10.1155/2016/2475067.

[13] J. A. del Olmo, L. Ruiz-Rubio, L. Pérez-Alvarez, V. Sáez-Martínez, and J. L. Vilas-Vilela, "Antibacterial coatings for improving the performance of biomaterials," *Coatings*, vol. 10, no. 2, 2020, doi: 10.3390/coatings10020139.

[14] T. Tolker-Nielsen, "Biofilm Development," *Microbiology Spectrum*, vol. 3, no. 2, Apr. 2015, doi: 10.1128/microbiolspec.mb-0001-2014.

[15] C. R. Armbruster and M. R. Parsek, "New insight into the early stages of biofilm formation," *Proceedings of the National Academy of Sciences of the United States of America*, vol. 115, no. 17. National Academy of Sciences, pp. 4317–4319, Apr. 24, 2018. doi: 10.1073/pnas.1804084115.

[16] D. G. Davies, M. R. Parsek, J. P. Pearson, B. H. Iglewski, J. W. Costerton, and E. P. Greenberg, "The involvement of cell-to-cell signals in the development of a bacterial biofilm," *Science (1979)*, vol. 280, no. 5361, pp. 295–298, Apr. 1998, doi: 10.1126/science.280.5361.295.

[17] N. C. Caiazza and G. A. O'Toole, "SadB is required for the transition from reversible to irreversible attachment during biofilm formation by Pseudomonas aeruginosa PA14," *Journal of Bacteriology*, vol. 186, no. 14, pp. 4476–4485, Jul. 2004, doi: 10.1128/JB.186.14.4476-4485.2004.

[18] A. E. Levack, E. L. Cyphert, M. P. Bostrom, C. J. Hernandez, H. A. von Recum, and A. v. Carli, "Current Options and Emerging Biomaterials for Periprosthetic Joint Infection," *Current Rheumatology Reports*, vol. 20, no. 6, 2018, doi: 10.1007/s11926-018-0742-4.

[19] S. M. Hinsa, M. Espinosa-Urgel, J. L. Ramos, and G. A. O'Toole, "Transition from reversible to irreversible attachment during biofilm formation by Pseudomonas fluorescens WCS365 requires an ABC transporter and a large secreted protein," *Molecular Microbiology*, vol. 49, no. 4, pp. 905–918, Jul. 2003, doi: 10.1046/j.1365-2958.2003.03615.x.

[20] P. Stoodley, K. Sauer, D. G. Davies, and J. W. Costerton, "Biofilms as Complex Differentiated Communities," *Annual Review of Microbiology*, vol. 56, no. 1, pp. 187–209, Oct. 2002, doi: 10.1146/annurev.micro.56.012302.160705.

[21] O. E. Petrova and K. Sauer, "Escaping the biofilm in more than one way: Desorption, detachment or dispersion," *Current Opinion in Microbiology*, vol. 30. Elsevier Ltd, pp. 67–78, Apr. 01, 2016. doi: 10.1016/j.mib.2016.01.004.

[22] C. Walsh, "Where will new antibiotics come from?," *Nature Publishing Group*, vol. 1, no. October, pp. 5–10, 2003.

[23] A. Fleming, "ON THE ANTIBACTERIAL ACTION OF CULTURES OF A PENICILLIUM, WITH SPECIAL REFERENCE TO THEIR USE IN THE ISOLATION OF B. INFLUENZ?1E," Wiley-Blackwell, 1929.

[24] J. A. Lemire, J. J. Harrison, and R. J. Turner, "Antimicrobial activity of metals: mechanisms, molecular targets and applications," *Nature Publishing Group*, vol. 11, no. 6, pp. 371–384, 2013, doi: 10.1038/nrmicro3028.

[25] M. M. Cowan, "Plant Products as Antimicrobial Agents," *Clinical Microbiology Reviews*, vol. 12, no. 4, pp. 564–582, Oct. 1999, doi: 10.1128/CMR.12.4.564.

[26] J. Davies, "Are antibiotics naturally antibiotics?," *Journal of Industrial Microbiology & Biotechnology*, vol. 33, no. 7, pp. 496–499, Jul. 2006, doi: 10.1007/s10295-006-0112-5.

[27] M. A. Kohanski, D. J. Dwyer, and J. J. Collins, "How antibiotics kill bacteria : from targets to networks," *Nature Publishing Group*, vol. 8, no. 6, pp. 423–435, 2010, doi: 10.1038/nrmicro2333.

[28] D. M. Livermore, "The need for new antibiotics," *Clinical Microbiology and Infection*, vol. 10, no. 4, pp. 1–9, Nov. 2004, doi: 10.1111/j.1465-0691.2004.1004.x.

[29] R. Davis *et al.*, "Ciprofloxacin: An Updated Review of its Pharmacology , Therapeutic Efficacy and Tolerability," *Drugs*, vol. 51, no. 6, pp. 1019–1074, 1996.

[30] R. Davis and H. M. Bryson, "Levofloxacin: A Review of its Antibacterial Activity, Pharmacokinetics and Therapeutic Efficacy," *Drugs*, vol. 47, no. 4, pp. 677–700, 1994.

[31] G. M. Keating and L. J. Scott, "Moxifloxacin: A review of its use in the management of bacterial infections," *Drugs*, vol. 64, no. 20. Springer, pp. 2347–2377, Sep. 17, 2004. doi: 10.2165/00003495-200464200-00006.

[32] C. M. Perry, J. A. B. Balfour, and H. M. Lamb, "Gatifloxacin," *Drugs*, vol. 58, no. 4, pp. 683–696, 1999.

[33] E. A. Campbell *et al.*, "Structural mechanism for rifampicin inhibition of bacterial RNA polymerase," *Cell*, vol. 104, no. 6, pp. 901–912, Mar. 2001, doi: 10.1016/S0092-8674(01)00286-0.

[34] A. J. Wright, "The Penicillins," *Mayo Clinic Proceedings*, vol. 74, pp. 290–307, 1999, doi: 10.4065/74.3.290.

[35] W. M. M. Kirby, L. S. Rosenfeld, and J. Brodie, "Oxacillin: Laboratory and Clinical Evaluation," *The Journal of the American Medical Association*, vol. 181, no. 9, pp. 739–744, 1962.

[36] S. S. Castle, "Dicloxacillin," vol. 3, no. 1, pp. 1–5, 2007.

[37] P. I. Rafailidis, E. N. Ioannidou, and M. E. Falagas, "Ampicillin/Sulbactam Current Status in Severe Bacterial Infections," 2007.

[38] H. C. Neu, "Antimicrobial Activity and Human Pharmacology of Amoxicillin," *The Journal of Infectious Diseases*, vol. 129, no. June, pp. S123–S131, 1974.

[39] E. T. Knudsen, F. C. Path, G. N. Rolinson, and R. Sutherland, "Carbenicillin *: A New Semisynthetic Penicillin Active against Pseudomonas pyocyanea," *British Medical Journal*, no. July, pp. 8–11, 1967.

[40] G. M. Eliopoulos and R. C. Moellering, "Azlocillin, Mezlocillin, and Piperacillin: New Broad-Spectrum Penicillins," *Annals of Internal Medicine*, vol. 97, pp. 755–760, 1982.

[41] K. Kariyone, H. Harada, M. Kurita, and T. Takano, "CEFAZOLIN, A NEW SEMISYNTHETIC CEPHALOSPORIN ANTIBIOTIC. I," *The jJournal of Antibiotics*, vol. 23, no. 3, pp. 131–136, 1970.

[42] H. C. Neu and K. P. Fu, "Cefaclor: in vitro spectrum of activity and beta-lactamase stability," *Antimicrobial Agents and Chemotherapy*, vol. 13, no. 4, pp. 584–588, Apr. 1978, doi: 10.1128/AAC.13.4.584.

[43] L. B. Barradell and H. M. Bryson, "Cefepime: A Review of its Antibacterial Activity , Pharmacokinetic Properties and Therapeutic Use," *Drugs*, vol. 47, no. 3, pp. 471–505, 1994.

[44] G. M. Keating and C. M. Perry, "Ertapenem: A review of its use in the treatment of bacterial infections," *Drugs*, vol. 65, no. 15. Springer, pp. 2151–2178, Sep. 17, 2005. doi: 10.2165/00003495-200565150-00013.

[45] S. P. Clissold, P. A. Todd, and D. M. Campoli-Richards, "Imipenem / Cilastatin A Review of its Antibacterial Activity , Pharmacokinetic Properties and Therapeutic Efficacy," *Drugs*, vol. 33, pp. 183–241, 1987.

[46] C. M. Baldwin, K. A. Lyseng-williamson, and S. J. Keam, "Meropenem: A Review of its Use in the Treatment of Serious Bacterial Infections," *Drugs*, vol. 68, no. 6, pp. 803–838, 2008.

[47] D. P. Levine, "Vancomycin: A History," *Clinical Infectious Diseases*, vol. 42, no. Supplement_1, pp. S5–S12, Jan. 2006, doi: 10.1086/491709.

[48] S. Alvarez-Elcoro and M. J. Enzler, "The Macrolides: Erythromycin, Clarithromycin, and Azithromycin," *Mayo Clinic Proceedings*, vol. 74, no. 6, pp. 613–634, 1999, doi: 10.4065/74.6.613.

[49] M. J. Kasten, "Clindamycin, Metronidazole, and Chloramphenicol," *Mayo Clinic Proceedings*, vol. 74, no. 8, pp. 825–833, 1999, doi: 10.4065/74.8.825.

[50] J. T. Spížek Řezanka, "Lincomycin, clindamycin and their applications," *Appl Microbiol Biotechnol*, vol. 64, pp. 455–464, 2004, doi: 10.1007/s00253-003-1545-7.

[51] M. Barber and P. M. Waterworth, "Antibacterial Activity of Lincomycin and Pristinamycin: A Comparison with Erythromycin," *British Medical Journal*, vol. 2, no. 5409, pp. 603–606, Sep. 1964, doi: 10.1136/bmj.2.5409.603.

[52] H. M. Lamb, D. P. Figgitt, and D. Faulds, "Quinupristin/dalfopristin: A review of its use in the management of serious Gram-positive infections," *Drugs*, vol. 58, no. 6. Adis International Ltd, pp. 1061–1097, Oct. 27, 1999. doi: 10.2165/00003495-199958060-00008.

[53] J. J. Hlavka and J. H. Boothe, "The Tetracyclines," in *Progress in Drug Research / Fortschritte der Arzneimittelforschung / Progrès des recherches pharmaceutiques*, Basel: Birkhäuser Basel, 1973, pp. 210–240. doi: 10.1007/978-3-0348-7084-9_5.

[54] I. Chopra and M. Roberts, "Tetracycline Antibiotics: Mode of Action, Applications, Molecular Biology, and Epidemiology of Bacterial Resistance," *Microbiology and Molecular Biology Reviews*, vol. 65, no. 2, pp. 232–260, Jun. 2001, doi: 10.1128/mmbr.65.2.232-260.2001.

[55] A. Schatz, E. Bugie, and S. A. Waksman, "Streptomycin, a Substance Exhibiting Antibiotic Activity Against Gram-Positive and Gram-Negative Bacteria," *Experimental Biology and Medicine*, vol. 55, no. 1, pp. 66–69, 1944.

[56] B. B. A. Waisbren and W. W. Spink, "A Clinical Appraisal of Neomycin," *Annals of Internal Medicine*, vol. 33, no. 5, pp. 1099–1119, 1950.

[57] M. A. Borovinskaya, S. Shoji, K. Fredrick, and J. H. D. Cate, "Structural basis for hygromycin B inhibition of protein biosynthesis," *RNA*, vol. 14, pp. 1590–1599, 2008, doi: 10.1261/rna.1076908.6.

[58] S. Yoshizawa, D. Fourmy, and J. D. Puglisi, "Structural origins of gentamicin antibiotic action," *The EMBO Journal*, vol. 17, no. 22, pp. 6437–6448, 1998.

[59] M. J. Weinstein, G. H. Wagman, J. A. Marquez, R. T. Testa, and J. A. Waitz, "Verdamicin, a new broad spectrum aminoglycoside antibiotic," *ANTIMICROB.AGENTS CHEMOTHER.*, vol. 7, no. 3, pp. 246–249, Mar. 1975, doi: 10.1128/AAC.7.3.246.

[60] J. P. Ruparelia, A. K. Chatterjee, S. P. Duttagupta, and S. Mukherji, "Strain specificity in antimicrobial activity of silver and copper nanoparticles," *Acta Biomaterialia*, vol. 4, no. 3, pp. 707–716, May 2008, doi: 10.1016/j.actbio.2007.11.006.

[61] S. Cheeseman *et al.*, "Antimicrobial Metal Nanomaterials: From Passive to Stimuli-Activated Applications," *Advanced Science*, vol. 7, no. 10, p. 1902913, May 2020, doi: 10.1002/advs.201902913.

[62] M. Rai, A. Yadav, and A. Gade, "Silver nanoparticles as a new generation of antimicrobials," *Biotechnology Advances*, vol. 27, no. 1. pp. 76–83, Jan. 2009. doi: 10.1016/j.biotechadv.2008.09.002.

[63] J. S. Kim *et al.*, "Antimicrobial effects of silver nanoparticles," *Nanomedicine: Nanotechnology, Biology, and Medicine*, vol. 3, no. 1, pp. 95–101, Mar. 2007, doi: 10.1016/j.nano.2006.12.001.

[64] C. Marambio-Jones and E. M. V. Hoek, "A review of the antibacterial effects of silver nanomaterials and potential implications for human health and the environment," *Journal of Nanoparticle Research*, vol. 12, no. 5. pp. 1531–1551, Jun. 2010. doi: 10.1007/s11051-010-9900-y.

[65] I. Sondi and B. Salopek-Sondi, "Silver nanoparticles as antimicrobial agent: A case study on E. coli as a model for Gram-negative bacteria," *Journal of Colloid and Interface Science*, vol. 275, no. 1, pp. 177–182, Jul. 2004, doi: 10.1016/j.jcis.2004.02.012.

[66] T. Khan, A. Yasmin, and H. E. Townley, "An evaluation of the activity of biologically synthesized silver nanoparticles against bacteria, fungi and mammalian cell lines," *Colloids and Surfaces B: Biointerfaces*, vol. 194, Oct. 2020, doi: 10.1016/j.colsurfb.2020.111156.

[67] K. Chand *et al.*, "Photocatalytic and antimicrobial activity of biosynthesized silver and titanium dioxide nanoparticles: A comparative study," *Journal of Molecular Liquids*, p. 113821, 2020, doi: 10.1016/j.molliq.2020.113821.

[68] N. Padmavathy and R. Vijayaraghavan, "Enhanced bioactivity of ZnO nanoparticles - An antimicrobial study," *Science and Technology of Advanced Materials*, vol. 9, no. 3, Jul. 2008, doi: 10.1088/1468-6996/9/3/035004.

[69] A. Sirelkhatim *et al.*, "Review on zinc oxide nanoparticles: Antibacterial activity and toxicity mechanism," *Nano-Micro Letters*, vol. 7, no. 3. SpringerOpen, pp. 219–242, Apr. 19, 2015. doi: 10.1007/s40820-015-0040-x.

[70] K. Qi, B. Cheng, J. Yu, and W. Ho, "Review on the improvement of the photocatalytic and antibacterial activities of ZnO," *Journal of Alloys and Compounds*, vol. 727. Elsevier Ltd, pp. 792–820, Dec. 15, 2017. doi: 10.1016/j.jallcom.2017.08.142.

[71] M. Li, L. Zhu, and D. Lin, "Toxicity of ZnO nanoparticles to escherichia Coli: Mechanism and the influence of medium components," *Environmental Science and Technology*, vol. 45, no. 5, pp. 1977–1983, Mar. 2011, doi: 10.1021/es102624t.

[72] S. Gunalan, R. Sivaraj, and V. Rajendran, "Green synthesized ZnO nanoparticles against bacterial and fungal pathogens," *Progress in Natural Science: Materials International*, vol. 22, no. 6, pp. 693–700, 2012, doi: 10.1016/j.pnsc.2012.11.015.

[73] M. Naseer, U. Aslam, B. Khalid, and B. Chen, "Green route to synthesize Zinc Oxide Nanoparticles using leaf extracts of Cassia fistula and Melia azadarach and their antibacterial potential," *Scientific Reports*, vol. 10, no. 1, Dec. 2020, doi: 10.1038/s41598-020-65949-3.

[74] G. Grass, C. Rensing, and M. Solioz, "Metallic copper as an antimicrobial surface," *Applied and Environmental Microbiology*, vol. 77, no. 5. pp. 1541–1547, Mar. 2011. doi: 10.1128/AEM.02766-10.

[75] R. Uauy, M. Olivares, and M. Gonzalez, "Essentiality of copper in humans," *Am J Clin Nutr*, vol. 67, no. February, pp. 952S–9S, 1998.

[76] A. Azam, A. S. Ahmed, M. Oves, M. S. Khan, and A. Memic, "Size-dependent antimicrobial properties of CuO nanoparticles against Gram-positive and -negative bacterial strains," *International Journal of Nanomedicine*, vol. 7, pp. 3527–3535, 2012, doi: 10.2147/IJN.S29020.

[77] M. S. Usman, M. E. el Zowalaty, K. Shameli, N. Zainuddin, M. Salama, and N. A. Ibrahim, "Synthesis, characterization, and antimicrobial properties of copper nanoparticles," *International Journal of Nanomedicine*, vol. 8, pp. 4467–4479, 2013, doi: 10.2147/IJN.S50837.

[78] M. A. Asghar and M. A. Asghar, "Green synthesized and characterized copper nanoparticles using various new plants extracts aggravate microbial cell membrane damage after interaction with lipopolysaccharide," *International Journal of Biological Macromolecules*, vol. 160, pp. 1168–1176, Oct. 2020, doi: 10.1016/j.ijbiomac.2020.05.198.

[79] K. Chand *et al.*, "Photocatalytic and antimicrobial activity of biosynthesized silver and titanium dioxide nanoparticles: A comparative study," *Journal of Molecular Liquids*, p. 113821, 2020, doi: 10.1016/j.molliq.2020.113821.

[80] Y. Cui, Y. Zhao, Y. Tian, W. Zhang, X. Lü, and X. Jiang, "The molecular mechanism of action of bactericidal gold nanoparticles on Escherichia coli," *Biomaterials*, vol. 33, no. 7, pp. 2327–2333, Mar. 2012, doi: 10.1016/j.biomaterials.2011.11.057.

[81] E. M. Hetrick, J. H. Shin, H. S. Paul, and M. H. Schoenfisch, "Anti-biofilm efficacy of nitric oxide-releasing silica nanoparticles," *Biomaterials*, vol. 30, no. 14, pp. 2782–2789, May 2009, doi: 10.1016/j.biomaterials.2009.01.052.

[82] A. Pugazhendhi, R. Prabhu, K. Muruganantham, R. Shanmuganathan, and S. Natarajan, "Anticancer, antimicrobial and photocatalytic activities of green synthesized magnesium oxide nanoparticles (MgONPs) using aqueous extract of Sargassum wightii," *Journal of Photochemistry and Photobiology B: Biology*, vol. 190, pp. 86–97, Jan. 2019, doi: 10.1016/j.jphotobiol.2018.11.014.

[83] S. M. Dizaj, F. Lotfipour, M. Barzegar-Jalali, M. H. Zarrintan, and K. Adibkia, "Antimicrobial activity of the metals and metal oxide nanoparticles," *Materials Science and Engineering C*, vol. 44. Elsevier Ltd, pp. 278–284, Nov. 01, 2014. doi: 10.1016/j.msec.2014.08.031.

[84] J. L. Ríos and M. C. Recio, "Medicinal plants and antimicrobial activity," *Journal of Ethnopharmacology*, vol. 100, no. 1–2, pp. 80–84, 2005, doi: 10.1016/j.jep.2005.04.025.

[85] L. Bravo, "Polyphenols: Chemistry, dietary sources, metabolism, and nutritional significance," *Nutrition Reviews*, vol. 56, no. 11. International Life Sciences Institute, pp. 317–333, 1998. doi: 10.1111/j.1753-4887.1998.tb01670.x.

[86] M. Daglia, "Polyphenols as antimicrobial agents," *Current Opinion in Biotechnology*, vol. 23, no. 2. pp. 174–181, Apr. 2012. doi: 10.1016/j.copbio.2011.08.007.

[87] P. G. Pietta, "Flavonoids as antioxidants," *Journal of Natural Products*, vol. 63, no. 7, pp. 1035–1042, 2000, doi: 10.1021/np9904509.

[88] I. Górniak, R. Bartoszewski, and J. Króliczewski, *Comprehensive review of antimicrobial activities of plant flavonoids*, vol. 18, no. 1. 2019. doi: 10.1007/s11101-018-9591-z.

[89] B. X. V. Quecan, J. T. C. Santos, M. L. C. Rivera, N. M. A. Hassimotto, F. A. Almeida, and U. M. Pinto, "Effect of quercetin rich onion extracts on bacterial quorum sensing," *Frontiers in Microbiology*, vol. 10, no. APR, 2019, doi: 10.3389/fmicb.2019.00867.

[90] H. Q. Li, J. Y. Xue, L. Shi, S. Y. Gui, and H. L. Zhu, "Synthesis, crystal structure and antimicrobial activity of deoxybenzoin derivatives from genistein," *European Journal of Medicinal Chemistry*, vol. 43, no. 3, pp. 662–667, Mar. 2008, doi: 10.1016/j.ejmech.2007.05.013.

[91] L. N. Zhang, P. Cao, S. H. Tan, W. Gu, L. Shi, and H. L. Zhu, "Synthesis and antimicrobial activities of 7-O-modified genistein derivatives," *European Journal of Medicinal Chemistry*, vol. 43, no. 7, pp. 1543–1551, Jul. 2008, doi: 10.1016/j.ejmech.2007.09.008.

[92] M. Cheng *et al.*, "An ointment consisting of the phage lysin LysGH15 and apigenin for decolonization of methicillin-resistant Staphylococcus aureus from skin wounds," *Viruses*, vol. 10, no. 5, May 2018, doi: 10.3390/v10050244.

[93] Y. Morimoto, T. Baba, T. Sasaki, and K. Hiramatsu, "Apigenin as an anti-quinolone-resistance antibiotic," *International Journal of Antimicrobial Agents*, vol. 46, no. 6, pp. 666–673, Dec. 2015, doi: 10.1016/j.ijantimicag.2015.09.006.

[94] R. Liu *et al.*, "Synthesis and biological evaluation of apigenin derivatives as antibacterial and antiproliferative agents," *Molecules*, vol. 18, no. 9, pp. 11496–11511, Sep. 2013, doi: 10.3390/molecules180911496.

[95] K. Bogdanova *et al.*, "Antibiofilm activity of bioactive hop compounds humulone, lupulone and xanthohumol toward susceptible and resistant staphylococci," *Research in Microbiology*, vol. 169, no. 3, pp. 127–134, Apr. 2018, doi: 10.1016/j.resmic.2017.12.005.

[96] M. Stompor and B. Zarowska, "Antimicrobial activity of xanthohumol and its selected structural analogues," *Molecules*, vol. 21, no. 5, May 2016, doi: 10.3390/molecules21050608.

[97] D. George, P. U. Maheswari, and K. M. M. S. Begum, "Synergic formulation of onion peel quercetin loaded chitosan-cellulose hydrogel with green zinc oxide nanoparticles towards controlled release, biocompatibility, antimicrobial and anticancer activity," *International Journal of Biological Macromolecules*, vol. 132, pp. 784–794, Jul. 2019, doi: 10.1016/j.ijbiomac.2019.04.008.

[98] P. S. Bustos *et al.*, "Protective effect of quercetin in gentamicin-induced oxidative stress in vitro and in vivo in blood cells. Effect on gentamicin antimicrobial activity," *Environmental Toxicology and Pharmacology*, vol. 48, pp. 253–264, Dec. 2016, doi: 10.1016/j.etap.2016.11.004.

[99] C. R. da Silva *et al.*, "Synergistic effect of the flavonoid catechin, quercetin, or epigallocatechin gallate with fluconazole induces apoptosis in Candida tropicalis resistant to fluconazole," *Antimicrobial Agents and Chemotherapy*, vol. 58, no. 3, pp. 1468–1478, Mar. 2014, doi: 10.1128/AAC.00651-13.

[100] A. K. Mittal, S. Kumar, and U. C. Banerjee, "Quercetin and gallic acid mediated synthesis of bimetallic (silver and selenium) nanoparticles and their antitumor and antimicrobial

potential," *Journal of Colloid and Interface Science*, vol. 431, pp. 194–199, Oct. 2014, doi: 10.1016/j.jcis.2014.06.030.

[101] I. L. K. Wong, K. F. Chan, Y. Zhao, T. H. Chan, and L. M. C. Chow, "Quinacrine and a novel apigenin dimer can synergistically increase the pentamidine susceptibility of the protozoan parasite Leishmania," *Journal of Antimicrobial Chemotherapy*, vol. 63, no. 6, pp. 1179–1190, 2009, doi: 10.1093/jac/dkp130.

[102] R. M. S. Pereira *et al.*, "Synthesis and characterization of a metal complex containing naringin and Cu, and its antioxidant, antimicrobial, antiinflammatory and tumor cell cytotoxicity," *Molecules*, vol. 12, no. 7, pp. 1352–1366, Jul. 2007, doi: 10.3390/12071352.

[103] T. P. T. Cushnie and A. J. Lamb, "Antimicrobial activity of flavonoids," *International Journal of Antimicrobial Agents*, vol. 26, no. 5, pp. 343–356, 2005, doi: 10.1016/j.ijantimicag.2005.09.002.

[104] N. Kumar and N. Goel, "Phenolic acids: Natural versatile molecules with promising therapeutic applications," *Biotechnology Reports*, vol. 24, p. e00370, 2019, doi: 10.1016/j.btre.2019.e00370.

[105] J. Liu, C. Du, H. T. Beaman, and M. B. B. Monroe, "Characterization of phenolic acid antimicrobial and antioxidant structure–property relationships," *Pharmaceutics*, vol. 12, no. 5, 2020, doi: 10.3390/pharmaceutics12050419.

[106] V. N. Lima *et al.*, "Antimicrobial and enhancement of the antibiotic activity by phenolic compounds: Gallic acid, caffeic acid and pyrogallol," *Microbial Pathogenesis*, vol. 99, pp. 56–61, 2016, doi: 10.1016/j.micpath.2016.08.004.

[107] J. Fu, K. Cheng, Z. ming Zhang, R. qin Fang, and H. liang Zhu, "Synthesis, structure and structure-activity relationship analysis of caffeic acid amides as potential antimicrobials," *European Journal of Medicinal Chemistry*, vol. 45, no. 6, pp. 2638–2643, Jun. 2010, doi: 10.1016/j.ejmech.2010.01.066.

[108] M. O. Araújo, H. L. Freire Pessoa, A. B. Lira, Y. P. Castillo, and D. P. de Sousa, "Synthesis, Antibacterial Evaluation, and QSAR of Caffeic Acid Derivatives," *Journal of Chemistry*, vol. 2019, 2019, doi: 10.1155/2019/3408315.

[109] P. Pecyna, J. Wargula, M. Murias, and M. Kucinska, "More than resveratrol: New insights into stilbene-based compounds," *Biomolecules*, vol. 10, no. 8. MDPI AG, pp. 1–40, Aug. 01, 2020. doi: 10.3390/biom10081111.

[110] T. Shen, X. N. Wang, and H. X. Lou, "Natural stilbenes: An overview," *Natural Product Reports*, vol. 26, no. 7, pp. 916–935, 2009, doi: 10.1039/b905960a.

[111] B. Catalgol, S. Batirel, Y. Taga, and N. K. Ozer, "Resveratrol: French paradox revisited," *Frontiers in Pharmacology*, vol. 3 JUL. 2012. doi: 10.3389/fphar.2012.00141.

[112] J. Chong, A. Poutaraud, and P. Hugueney, "Metabolism and roles of stilbenes in plants," *Plant Science*, vol. 177, no. 3. Elsevier, pp. 143–155, Sep. 01, 2009. doi: 10.1016/j.plantsci.2009.05.012.

[113] J. A. Baur and D. A. Sinclair, "Therapeutic potential of resveratrol: The in vivo evidence," *Nature Reviews Drug Discovery*, vol. 5, no. 6, pp. 493–506, 2006, doi: 10.1038/nrd2060.

[114] J. H. Lee, Y. G. Kim, S. Y. Ryu, M. H. Cho, and J. Lee, "Resveratrol oligomers inhibit biofilm formation of escherichia coli O157:H7 and pseudomonas aeruginosa," *Journal of Natural Products*, vol. 77, no. 1, pp. 168–172, 2014, doi: 10.1021/np400756g.

[115] M. Vestergaard and H. Ingmer, "Antibacterial and antifungal properties of resveratrol," *International Journal of Antimicrobial Agents*, vol. 53, no. 6. Elsevier B.V., pp. 716–723, Jun. 01, 2019. doi: 10.1016/j.ijantimicag.2019.02.015.

[116] D. Hwang and Y. H. Lim, "Resveratrol antibacterial activity against Escherichia coli is mediated by Z-ring formation inhibition via suppression of FtsZ expression," *Scientific Reports*, vol. 5, May 2015, doi: 10.1038/srep10029.

[117] X. Ding, A. Wang, W. Tong, and F. J. Xu, "Biodegradable Antibacterial Polymeric Nanosystems: A New Hope to Cope with Multidrug-Resistant Bacteria," *Small*, vol. 15, no. 20, pp. 1–29, 2019, doi: 10.1002/smll.201900999.

[118] I. Babutan, A.-D. Lucaci, and I. Botiz, "Antimicrobial Polymeric Structures Assembled on Surfaces," *Polymers 2021, Vol. 13, Page 1552*, vol. 13, no. 10, p. 1552, May 2021, doi: 10.3390/POLYM13101552.

[119] R. Yañez-Macías *et al.*, "Combinations of antimicrobial polymers with nanomaterials and bioactives to improve biocidal therapies," *Polymers (Basel)*, vol. 11, no. 11, 2019, doi: 10.3390/polym11111789.

[120] R. Barman, T. Mondal, J. Sarkar, A. Sikder, and S. Ghosh, "Self-Assembled Polyurethane Capsules with Selective Antimicrobial Activity against Gram-Negative E. coli," *ACS Biomaterials Science and Engineering*, vol. 6, no. 1, pp. 654–663, 2020, doi: 10.1021/acsbiomaterials.9b00932.

[121] S. Belbekhouche *et al.*, "Chitosan based self-assembled nanocapsules as antibacterial agent," *Colloids and Surfaces B: Biointerfaces*, vol. 181, pp. 158–165, Sep. 2019, doi: 10.1016/J.COLSURFB.2019.05.028.

[122] M. Toledano-Osorio, J. P. Babu, R. Osorio, A. L. Medina-Castillo, F. García-Godoy, and M. Toledano, "Modified polymeric nanoparticles exert in vitro antimicrobial activity against oral bacteria," *Materials*, vol. 11, no. 6, 2018, doi: 10.3390/ma11061013.

[123] T. H. Ong, E. Chitra, S. Ramamurthy, C. C. S. Ling, S. P. Ambu, and F. Davamani, "Cationic chitosan-propolis nanoparticles alter the zeta potential of S. Epidermidis, inhibit biofilm formation by modulating gene expression and exhibit synergism with antibiotics," *PLoS ONE*, vol. 14, no. 2, pp. 1–13, 2019, doi: 10.1371/journal.pone.0213079.

[124] S. B. F. dos Santos *et al.*, "Antibacterial activity of fluoxetine-loaded starch nanocapsules," *International Journal of Biological Macromolecules*, vol. 164, pp. 2813–2817, Dec. 2020, doi: 10.1016/J.IJBIOMAC.2020.08.184.

[125] N. P. da Silva *et al.*, "Improved anti-Cutibacterium acnes activity of tea tree oil-loaded chitosan-poly(ε-caprolactone) core-shell nanocapsules," *Colloids and Surfaces B: Biointerfaces*, vol. 196, p. 111371, Dec. 2020, doi: 10.1016/J.COLSURFB.2020.111371.

[126] F. Anversa Dimer *et al.*, "PLGA nanocapsules improve the delivery of clarithromycin to kill intracellular Staphylococcus aureus and Mycobacterium abscessus," *Nanomedicine: Nanotechnology, Biology and Medicine*, vol. 24, p. 102125, Feb. 2020, doi: 10.1016/J.NANO.2019.102125.

[127] R. S. Araújo *et al.*, "Cloxacillin benzathine-loaded polymeric nanocapsules: Physicochemical characterization, cell uptake, and intramammary antimicrobial effect,"

Materials Science and Engineering: C, vol. 104, p. 110006, Nov. 2019, doi: 10.1016/J.MSEC.2019.110006.

[128] A. Muñoz-Bonilla and M. Fernández-García, "Polymeric materials with antimicrobial activity," *Progress in Polymer Science (Oxford)*, vol. 37, no. 2, pp. 281–339, 2012, doi: 10.1016/j.progpolymsci.2011.08.005.

[129] K. Bazaka, M. v. Jacob, R. J. Crawford, and E. P. Ivanova, "Efficient surface modification of biomaterial to prevent biofilm formation and the attachment of microorganisms.," *Applied microbiology and biotechnology*, vol. 95, no. 2. Springer, pp. 299–311, May 18, 2012. doi: 10.1007/s00253-012-4144-7.

[130] S. Krishnan, C. J. Weinman, and C. K. Ober, "Advances in polymers for anti-biofouling surfaces," *Journal of Materials Chemistry*, vol. 18, no. 29, pp. 3405–3413, Jul. 2008, doi: 10.1039/B801491D.

[131] V. Albright *et al.*, "Self-defensive antibiotic-loaded layer-by-layer coatings: Imaging of localized bacterial acidification and pH-triggering of antibiotic release," *Acta Biomaterialia*, vol. 61, pp. 66–74, Oct. 2017, doi: 10.1016/J.ACTBIO.2017.08.012.

[132] T. Flak *et al.*, "Novel antibacterial modification of polycarbonate for increment prototyping in medicine," *Materials*, vol. 14, no. 16, 2021, doi: 10.3390/ma14164725.

[133] L. Giraud, A. Tourrette, and E. Flahaut, "Carbon nanomaterials-based polymer-matrix nanocomposites for antimicrobial applications: A review," *Carbon N Y*, vol. 182, pp. 463–483, 2021, doi: 10.1016/j.carbon.2021.06.002.

[134] N. Aničić, M. Kurtjak, S. Jeverica, D. Suvorov, and M. Vukomanović, "Antimicrobial Polymeric Composites with Embedded Nanotextured Magnesium Oxide," *Polymers 2021, Vol. 13, Page 2183*, vol. 13, no. 13, p. 2183, Jun. 2021, doi: 10.3390/POLYM13132183.

[135] S. Holešová *et al.*, "Development of Novel Thin Polycaprolactone (PCL)/Clay Nanocomposite Films with Antimicrobial Activity Promoted by the Study of Mechanical, Thermal, and Surface Properties," *Polymers 2021, Vol. 13, Page 3193*, vol. 13, no. 18, p. 3193, Sep. 2021, doi: 10.3390/POLYM13183193.

[136] N. Sallak, A. M. Moghanjoughi, M. Ataee, A. Anvar, and L. Golestan, "Antimicrobial biodegradable film based on corn starch/Satureja khuzestanica essential oil/Ag–TiO2 nanocomposites," *Nanotechnology*, vol. 32, p. 405703, 2021, doi: 10.1088/1361-6528/ac0a15.

[137] M. Fu *et al.*, "Recent advances in hydrogel-based anti-infective coatings," *Journal of Materials Science & Technology*, vol. 85, pp. 169–183, Sep. 2021, doi: 10.1016/J.JMST.2020.12.070.

[138] U. Stamenović, S. Davidović, S. Petrović, A. Leskovac, M. Stoiljković, and V. Vodnik, "Antimicrobial and biological effects of polyaniline/polyvinylpyrrolidone nanocomposites loaded with silver nanospheres/triangles," *New Journal of Chemistry*, vol. 45, no. 28, pp. 12711–12720, 2021, doi: 10.1039/d1nj02729h.

[139] E. Sanchez-Rexach, I. Martínez de Arenaza, J. R. Sarasua, and E. Meaurio, "Antimicrobial poly(ε-caprolactone)/thymol blends: Phase behavior, interactions and drug release kinetics," *European Polymer Journal*, vol. 83, no. 83, pp. 288–299, Oct. 2016, doi: 10.1016/j.eurpolymj.2016.08.029.

[140] E. Sanchez-Rexach *et al.*, "Miscibility, interactions and antimicrobial activity of poly(ε-caprolactone)/chloramphenicol blends," *European Polymer Journal*, vol. 102, no. March, pp. 30–37, 2018, doi: 10.1016/j.eurpolymj.2018.03.011.

[141] O. Sánchez-Aguinagalde, E. Meaurio, A. Lejardi, and J. R. Sarasua, "Amorphous solid dispersions in poly(ϵ-caprolactone)/xanthohumol bioactive blends: Physicochemical and mechanical characterization," *Journal of Materials Chemistry B*, vol. 9, no. 20, pp. 4219–4229, 2021, doi: 10.1039/d0tb02964e.

[142] A. Guarnieri *et al.*, "Antimicrobial properties of chitosan from different developmental stages of the bioconverter insect Hermetia illucens," *Scientific Reports 2022 12:1*, vol. 12, no. 1, pp. 1–12, May 2022, doi: 10.1038/s41598-022-12150-3.

[143] L. Y. Zheng and J. F. Zhu, "Study on antimicrobial activity of chitosan with different molecular weights," *Carbohydrate Polymers*, vol. 54, no. 4, pp. 527–530, Dec. 2003, doi: 10.1016/J.CARBPOL.2003.07.009.

[144] B. Hu *et al.*, "An intrinsically bioactive hydrogel with on-demand drug release behaviors for diabetic wound healing," *Bioactive Materials*, vol. 6, no. 12, pp. 4592–4606, Dec. 2021, doi: 10.1016/J.BIOACTMAT.2021.04.040.

[145] S. Lin *et al.*, "Chitosan-poloxamer-based thermosensitive hydrogels containing zinc gluconate/recombinant human epidermal growth factor benefit for antibacterial and wound healing," *Materials Science and Engineering: C*, vol. 130, p. 112450, Nov. 2021, doi: 10.1016/J.MSEC.2021.112450.

[146] S. Liu *et al.*, "NIR as a 'trigger switch' for rapid phase change, on-demand release, and photothermal synergistic antibacterial treatment with chitosan-based temperature-sensitive hydrogel," *International Journal of Biological Macromolecules*, vol. 191, pp. 344–358, Nov. 2021, doi: 10.1016/J.IJBIOMAC.2021.09.093.

[147] M. Lazaridou *et al.*, "Super absorbent chitosan-based hydrogel sponges as carriers for caspofungin antifungal drug," *International Journal of Pharmaceutics*, vol. 606, p. 120925, Sep. 2021, doi: 10.1016/J.IJPHARM.2021.120925.

[148] Z. Ling *et al.*, "A novel self-healing polydopamine-functionalized chitosan-arginine hydrogel with enhanced angiogenic and antibacterial activities for accelerating skin wound healing," *Chemical Engineering Journal*, vol. 420, p. 130302, Sep. 2021, doi: 10.1016/J.CEJ.2021.130302.

[149] S. Li, X. Wang, J. Zhu, Z. Wang, and L. Wang, "Synthesis and characterization of photothermal antibacterial hydrogel with enhanced mechanical properties," *New Journal of Chemistry*, vol. 45, no. 36, pp. 16804–16815, Sep. 2021, doi: 10.1039/D1NJ02529E.

[150] M. Kamaci and I. Kaya, "Preparation of biodegradable, and pH-sensitive poly(azomethine)-chitosan hydrogels for potential application of 5-fluoro uracil delivery," *European Polymer Journal*, vol. 158, p. 110680, Sep. 2021, doi: 10.1016/J.EURPOLYMJ.2021.110680.

[151] Y. Ou and M. Tian, "Advances in multifunctional chitosan-based self-healing hydrogels for biomedical applications," *Journal of Materials Chemistry B*, vol. 9, no. 38, pp. 7955–7971, Oct. 2021, doi: 10.1039/D1TB01363G.

[152] Q. V. Nguyen, D. P. Huynh, J. H. Park, and D. S. Lee, "Injectable polymeric hydrogels for the delivery of therapeutic agents: A review," *European Polymer Journal*, vol. 72, pp. 602–619, 2015, doi: 10.1016/j.eurpolymj.2015.03.016.

[153] T. T. Hoang Thi, B. D. T. Trinh, P. le Thi, D. L. Tran, K. D. Park, and D. H. Nguyen, "Self-antibacterial chitosan/Aloe barbadensis Miller hydrogels releasing nitrite for biomedical applications," *Journal of Industrial and Engineering Chemistry*, vol. 103, pp. 175–186, Nov. 2021, doi: 10.1016/J.JIEC.2021.07.029.

[154] A. Lejardi *et al.*, "Novel hydrogels of chitosan and poly(vinyl alcohol)-g-glycolic acid copolymer with enhanced rheological properties," *Carbohydrate Polymers*, vol. 103, no. 1, pp. 267–273, 2014, doi: 10.1016/j.carbpol.2013.12.040.

[155] O. Sánchez-Aguinagalde, A. Lejardi, E. Meaurio, R. Hernández, C. Mijangos, and J. R. Sarasua, "Novel hydrogels of chitosan and poly (Vinyl alcohol) reinforced with inorganic particles of bioactive glass," *Polymers (Basel)*, vol. 13, no. 5, pp. 1–15, 2021, doi: 10.3390/polym13050691.

CHAPTER 2. NOVEL HYDROGELS OF CHITOSAN AND POLY(VINYL ALCOHOL) REINFORCED WITH INORGANIC PARTICLES OF BIOACTIVE GLASS

ABSTRACT

Chitosan and poly (vinyl alcohol) hydrogels, a polymeric system that shows a broad potential in biomedical applications, were developed. Despite the advantages they present, their mechanical properties are insufficient to support the loads that appear on the body. Thus, it was proposed to reinforce these gels with inorganic glass particles, in order to improve mechanical properties and bioactivity, and see how this reinforcement affects levofloxacin drug release kinetics. Scanning Electron Microscopy (SEM), X-Ray Diffraction (XRD), swelling tests, rheology and drug release studies characterized the resulting hydrogels. The experimental results verified the bioactivity of these gels, showed an improvement of the mechanical properties, and proved that the added bioactive glass does affect the release kinetics.

2.1. INTRODUCTION

Hydrogels are polymeric materials with ability to entrap large amounts of water that maintain a three-dimensional structure formed by interconnected flexible polymer chains [1]. In particular, hydrophilic, water insoluble and elastic hydrogels are suitable for a wide range of applications, including biomedical applications [2], [3]. Due to their ability to simulate biological environments, they are receiving a great interest for tissue engineering [4], [5]. In addition, these hydrogels are appropriate for controlled drug release systems, being able to administer a drug in a constant way in the organism [6], [7]. This is possible thanks to their swelling properties, as their three-dimensional size increases with water absorption, enabling the release of the drug through the polymeric network.

This study is focused on chitosan/poly (vinyl alcohol) hydrogels. Chitosan (CS) is a semicrystalline aminopolysaccharide obtained by deacetylation of chitin. Owing to properties such as non-toxicity, antimicrobial [8], biodegradability and excellent biocompatibility, it is being widely used in biomedical and pharmaceutical fields. These applications include tissue engineering [9], drug delivery systems [10], wound healing [11], [12], nanoparticle carriers [13], or coatings for implants [14], for example.

Poly (vinyl alcohol) (PVA) is a semicrystalline synthetic polymer of vinyl acetate and vinyl alcohol. It is a suitable material for biomedical applications [15] such as wound dressings

[16] or nanoparticles fabrication [17], due to its properties. It is water soluble, non- toxic and biocompatible.

The combination of both polymers results in a hydrogel with a three-dimensional network formed through physical interactions, avoiding the use of cross-linking agents. One of the characteristics to highlight of these hydrogels is their thermosensitivity [18]. This property enables them to change from sol to gel state when it reaches the transition temperature, which is 37°C in this case, close to body temperature [19]. Thanks to this characteristic, its use as an injectable liquid which transforms into a semisolid hydrogel is possible [20], [21].

Although they have many advantages, the mechanical properties of these hydrogels are insufficient to withstand some loads that can occur in certain areas of the body, such as joints. Therefore, it is proposed to add inorganic particles of bioactive glass in order to improve these properties [22]. In addition to improving the mechanical properties, bioactive glass is a class A bioactive material, that is, osteoconductive and osteoinductive. Moreover, it does not only forms bonds with bone tissues, but it can also form chemical and biological bonds with soft tissues [23]. The formation of these bonds is based on the fact that the products of the bioactive glass solution have a direct effect on the deposition of an apatite layer on the surface of the material and on the genetic expression of the surrounding cells [24]. Consequently, there is better integration with the surrounding tissues, prolonging the period that can remain implanted without causing rejection reactions.

In the present work, chitosan and PVA hydrogels with different amounts of bioactive glass were developed, with the aim of studying their effect on the mechanical properties, bioactivity and drug release of the resulting hydrogels. These hydrogels were prepared by blending PVA with chitosan at two different concentrations followed by addition of the inorganic nanoparticles. The swelling and rheological properties were determined as a function of chitosan concentration and bioactive glass content. The bioactivity was determined through the observation of the formation of an apatite layer on the surface of gels by Scanning Electron Microscopy (SEM) and the determination of the crystalline structure as a function of time of immersion of gels in Simulated Body

Fluid (SBF) at 37°C. Finally, the release kinetics of a model drug, Levofloxacin, was determined.

2.2. EXPERIMENTAL SECTION

2.2.1. Materials

Poly (vinyl alcohol) (PVA, M_w = 13000-23000 g/mol), chitosan (CS) of low molecular weight (degree of deacetylation = 75%), sodium bicarbonate ($NaHCO_3$), phosphate buffered saline (PBS), hydrochloric acid (HCl) and Levofloxacin ($C_{18}H_{20}FN_3O_4$, M_w = 316.37 g/mol) were supplied by Sigma Aldrich and used as received. 0.5 L of Simulated Body Fluid (SBF) was prepared by dissolving 4.0145 g sodium chloride (NaCl) purchased from Panreac Química S.A.U., 0.1775 g sodium bicarbonate ($NaHCO_3$), 0.1125 g potassium chloride (KCl), 0.1155 g potassium hydrogen phosphate trihydrate ($K_2HPO_4{\cdot}3H_2O$), 0.1555 g magnesium chloride hexahydrate ($MgCl_2{\cdot}6H_2O$), 0.146 g calcium chloride ($CaCl_2$) and 0.036 g sodium sulfate (Na_2SO_4), all of them acquired from Sigma Aldrich and adjusting its pH to 7.4 using hydrochloric acid (HCl) and 3.059 g tris (hydroxymethyl aminomethane) [$(CH_2OH)_3CNH_2$] also from Panreac Química S.A.U.

Bioactive glass was purchased from Novabone and used as received, and distilled water was provided by Iberia Agua.

2.2.2. Preparation of chitosan/PVA hydrogels

Hydrogels were prepared using the method described by Tang et al [25]. A 2% (w/w) CS solution was obtained by dissolving chitosan in 0.1 M HCl, and stored in the fridge. A 0.5% (w/w) PVA aqueous solution was obtained by adding PVA to distilled water, under magnetic stirring at 80°C for one hour. To prepare the hydrogel, 0.3 ml of 1 M $NaHCO_3$ were added to 3 ml of 0.5% (w/w) PVA, and kept in an ice bath under magnetic stirring for 5 minutes. This mixture was slowly added to 3 ml of 2% (w/w) CS solution in an ice bath, and kept under magnetic stirring for 2 minutes. Then, bioactive glass was added and maintained under magnetic stirring in ice bath, until homogeneous dispersion. The gels were then formed by putting them in the oven at 37°C.

Different samples were prepared with varying concentrations of bioactive glass (0% (v/v), 0.5% (v/v) and 1.5% (v/v)) at two CS concentrations (2 and 4% (w/w)). The designation of the different samples under study is reported in Table 2.1.

Table 2. 1. Designation of all samples under study.

Sample name of the gel	*Ratio between PVA/CS in the gel*	*Concentration of PVA (% w/w) in the gel*	*Concentration of CS (% w/w) in the gel*	*Concentration of bioactive glass (% v/v) in the gel*
PVA/CS 2	50/50	0.5	2	0
PVA/CS/BG 2/0.5	50/50	0.5	2	0.5
PVA/CS/BG 2/1.5	50/50	0.5	2	1.5
PVA/CS 4	50/50	0.5	4	0
PVA/CS/BG 4/0.5	50/50	0.5	4	0.5
PVA/CS/BG 4/1.5	50/50	0.5	4	1.5

2.2.3. Swelling properties

Samples were lyophilized and immersed in distilled water (50ml) at room temperature. At various time intervals, the excess surface water was removed with filter paper, and the swollen samples were weighed. This procedure was repeated until the equilibrium swelling of the samples was reached. With the obtained data, swelling index (SI) (Eq. (2.1)) and equilibrium water content (EWC) (Eq. (2.2)) were determined, using the following equations:

$$Swelling\ ratio\ = \frac{Swollen\ weight\ of\ the\ sample}{Dry\ weight\ of\ the\ sample} \tag{2.1}$$

$$EWC\ (\%)\ = \frac{Weight\ of\ water\ in\ the\ gel}{Total\ weight\ of\ the\ hydrated\ gel} \times 100 \tag{2.2}$$

The experiment was repeated with three different samples to ensure reproducibility.

2.2.4. Rheological measurements

The rheological characterization of the hydrogels was performed in a TA Instruments AR-G2 Rheometer using a steel plate cross hatched geometry (20 mm diameter). Aqueous solutions were poured in Teflon molds (20 mm diameter) and maintained overnight at 37°C for sol-to-gel transition. A strain sweep test was carried out to determine the linear viscoelastic range. Frequency sweep experiments were performed over the frequency

range of 0.01 – 100 Hz. All experiments were carried out at 37°C and at a constant strain of 1% located within the linear viscoelastic region. The elastic modulus (G') and viscous modulus (G'') were calculated using the Rheology Advantage Data Analysis Software. The experiment was performed in triplicate for each sample.

2.2.5. Bioactivity studies

For the study of the *in vitro* bioactivity of the prepared samples, PVA/CS 2, PVA/CS/BG 2/0.5 and PVA/CS/BG 2/1.5 were immersed in SBF at 37°C and extracted at different periods (0, 7, 14 and 28 days). Then, they were washed and frozen, in order to lyophilize them and obtain dehydrated samples. In order to maintain the concentration of cations throughout the whole experiment, the SBF was renewed every 7 days [24].

The formation of an apatite layer on the surface of the hydrogel was observed through scanning electron microscopy (SEM) performed on dehydrated samples using a Hitachi S-4800, after coating them with a 15 nm gold layer in an Emitech k55x Sputter Coater at 25 mA.

An X-ray diffraction (XRD) analysis was performed to confirm the formation and crystallization of the apatite layer. A Phillips X'pert Pro diffractometer was used operating at 40 kV and at 40 mA, theta-theta configuration, with a Cu anode and a PSD detector. The scanning scope of 2θ was 10-50°, with a step size of 0.026° and step time of 148.92 s, at 25°C.

Experiments were repeated with three different samples to ensure reproducibility.

2.2.6. Drug release

For the study of the drug release from PVA/CS hydrogels, levofloxacin was employed as a model drug. Levofloxacin (5 mg/ml) was dissolved in PVA/CS solutions by magnetic stirring, and then the chitosan/PVA gels were prepared following the same procedure previously described. Gels were immersed into 100 ml of 0.1 M phosphate buffered saline (PBS), pH 7.4, at 37°C and aliquots of 0.2 ml were taken out at regular time intervals. The release of Levofloxacin was determined by UV spectrophotometry at 288 nm (Perkin Elmer Lambda 265).

The kinetics of the release from the different samples was determined by finding the best fit of the curves to different kinetic models. Four different mathematical models were considered:

Zero order: $C_t/C_\infty = k_0 t$ (2.3)

First order: $\ln(1 - C_t/C_\infty) = -k_1 t$ (2.4)

Higuchi: $C_t/C_\infty = k_h t^{1/2}$ (2.5)

Korsmeyer – Peppas: $C_t/C_\infty = k t^n$ (2.6)

where C_t is the cumulative amount of drug released at time *t,* C_∞ is the starting amount of drug, *n* is the release exponent, and k_0, k_1, k_h and *k* are the kinetic constants. Zero order kinetics represents a release process that is controlled by relaxation of polymeric chains, with a constant release rate of drug, independent of its concentration (Eq. (2.3)). On the other hand, a drug release rate that depends on its concentration is represented by first order kinetics model (Eq. (2.4)) [26]. In the case of Higuchi (Eq. (2.5)), it describes drug release as a diffusion process, square root time dependent, based in Fick's law. The last model, Korsmeyer – Peppas model (Eq. (2.6)), is useful when the release mechanism is not well known or when more than one type of release phenomena could be involved. Depending on the values obtained for the release exponent, *n*, it is possible to define whether if the release happens by Fickian diffusion, anomalous transport, Case-II transport or Super Case-II transport [27].

2.2.7. Statistical analysis

Data were subjected to one-way analysis of variant (ANOVA) with the level of significance set at $p < 0.05$.

2.3. RESULTS AND DISCUSSION

2.3.1. Gel formation

To determine gel formation after the addition of bioactive glass, an inverted vial test was employed and the representative images corresponding to samples prepared at 2% w/v CS concentration are shown in Figure 2.1. The formation of gel was verified for the

samples as the non-flowing gel maintained its position after vial inversion. Similar results were obtained for samples prepared at 4% w/v CS concentration (results not shown).

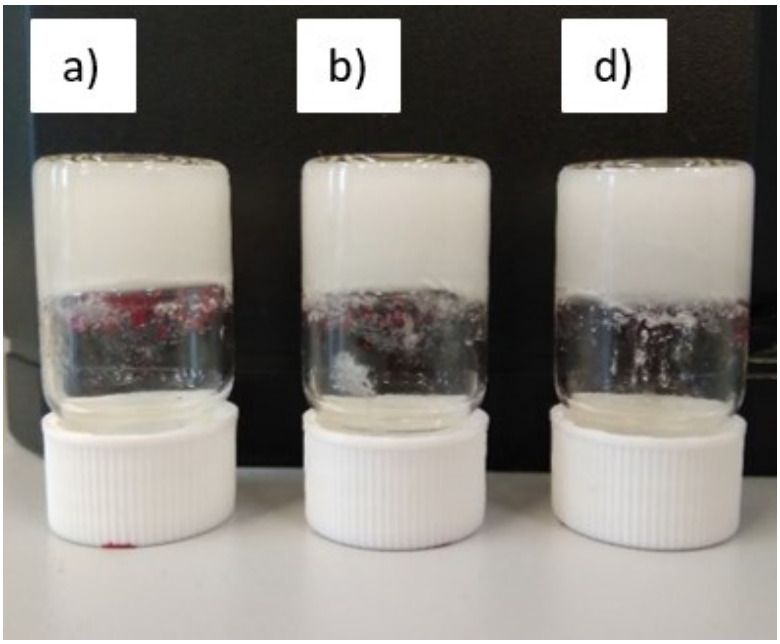

Figure 2. 1. Representative results obtained from inverted vial tests: a) PVA/CS 2, b) PVA/CS/BG 2/0.5 and c) PVA/CS/BG 2/1.5 hydrogels.

2.3.2. Effect of the chitosan concentration and bioactive glass content on the swelling and rheological properties

Figure 2.2. shows the result corresponding to swelling experiments carried out on the samples under study. As can be observed, all the samples showed a fast swelling, reaching equilibrium after 20 minutes of immersion in distilled water at room temperature, with equilibrium water contents (EWC) that exceeded 90%. The increase of chitosan concentration caused a decrease of the swelling index (SI) (Figure 2.3.), which is in agreement with the work of Tang et al. [25], as long as the PVA proportion is kept low. Regarding the effect of the bioactive glass concentration on the swelling properties of the samples under study, except for the case of PVA/CS/BG 4/0.5, a decrease of the swelling ability with the increase of bioactive glass concentration was observed (Figure 2.2.). This same effect was described in literature, and could be the result of retractile forces of the hydrogel caused by the ion release of bioactive glass particles [28], or to the lack of empty gaps after the addition of bioactive glass.

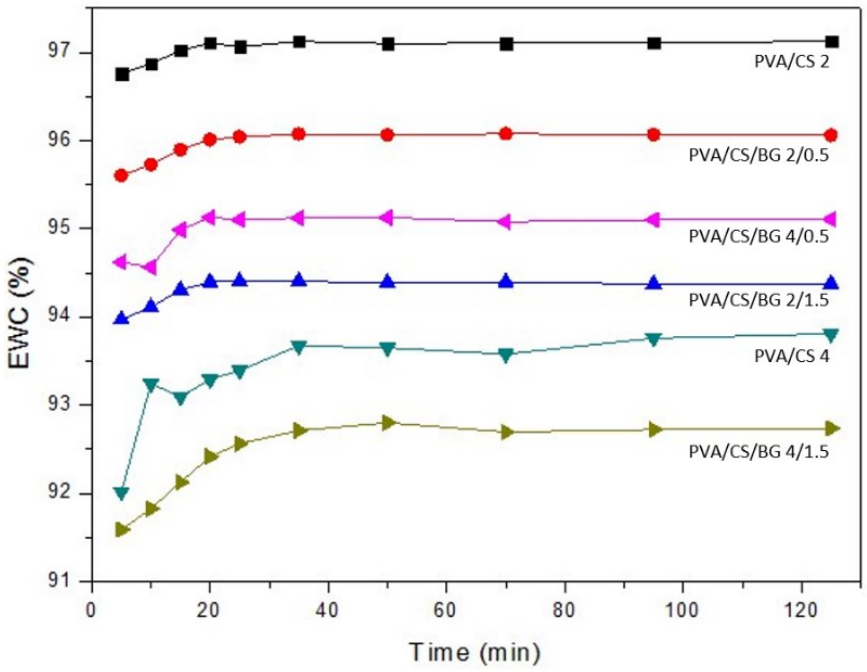

Figure 2. 2. Equilibrium Water Content (EWC) of the hydrogels immersed into 50 ml distilled water at room temperature for 2 hours.

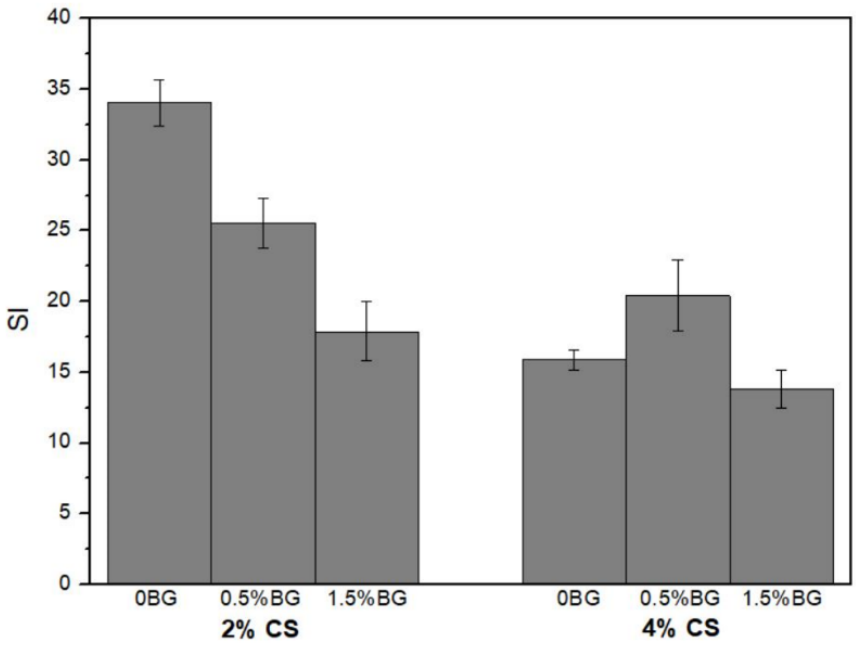

Figure 2. 3. a) Swelling Index (SI) of the hydrogels immersed into 50 ml distilled water at room temperature for 2 hours.

The effect of the incorporation of bioactive glass on PVA/CS on the rheological properties of PVA/CS hydrogels was determined by means of oscillatory shear measurements. Figure 2.4. shows representative results corresponding to frequency experiments carried out on samples PVA/CS 2 and PVA/CS/BG 2/1.5. As can be

observed both samples present gel-like behavior which is characterized by i) values of the elastic modulus higher than the corresponding to the viscous modulus (G' > G") in all the frequency range and ii) G and G´´ are independent on frequency in all the range under study.

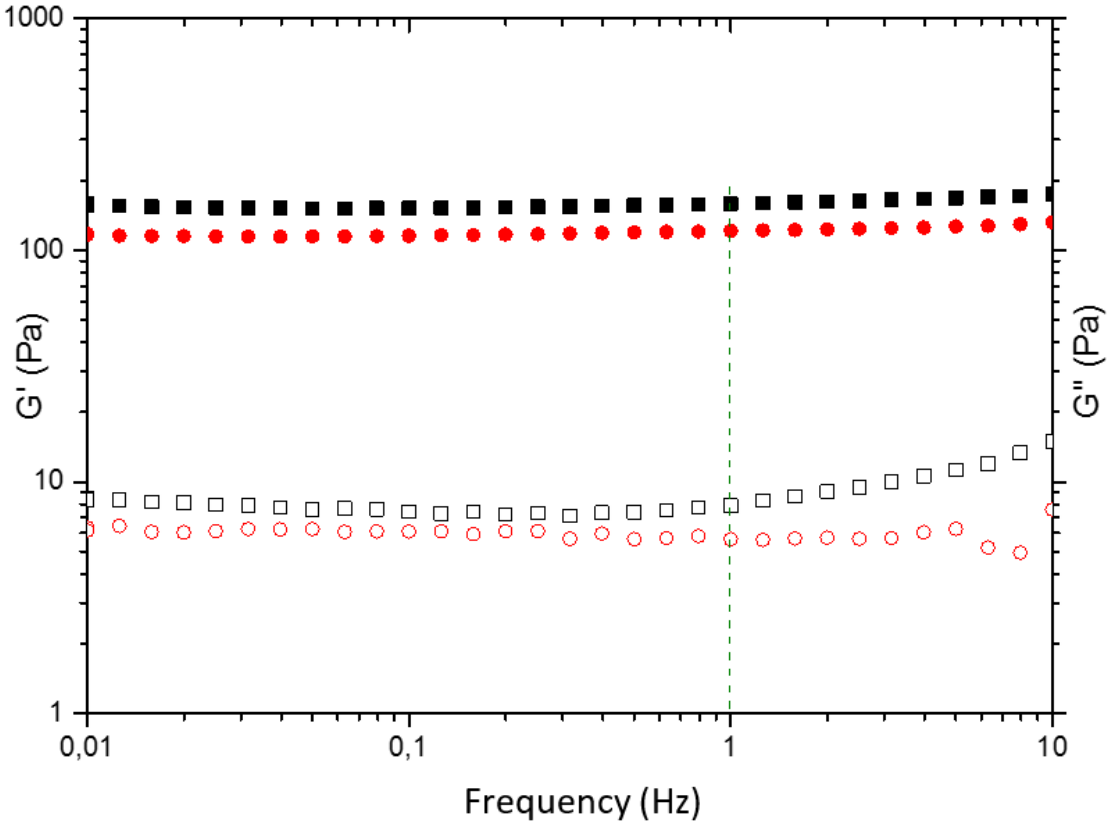

Figure 2. 4. Elastic modulus (closed symbols) and loss modulus (open symbols) as a function of frequency of PVA/CS 2 (●) and PVA/CS/BG 2/1.5 (■).

The values of the elastic modulus measured at frequency =1Hz are depicted in Figure 2.5. for samples PVA/CS and samples PVA/CS/BG. As can be observed, the increase of chitosan concentration results in an increase of the elastic moduli obtained for gels without bioactive glass, which can be related to the decrease of the swelling index (SI) [29] found for PVA/CS 4 with respect to sample PVA/CS 2 (Figure 2.3.). With the incorporation of 1.5% (w/v) bioactive glass, the elastic modulus measured for PVA/CS and PVA/CS/BG 1.5 hydrogels remains within the experimental error being 129±9 y 149±11 Pa respectively. Taken into account that the SI determined for PVA/CS/BG 1.5 greatly decreases with respect to PVA/CS, the results might indicate that the

incorporation of 1.5% bioactive glass prevent the formation of crosslinking interactions between PVA and CS leading to the loss of elastic properties of the resulting composite gel [30]. In contrast, the sample PVA/CS/BG 4/1.5 shows an increase of elastic modulus with respect to PVA/CS 4. In this case, and taking into account that the swelling index does not change with the incorporation of bioactive glass, the results obtained could be attributed to the reinforcement effect of micrometric bioactive glass particles onto the polymer matrix as previously reported for other composite gels [31], [32].

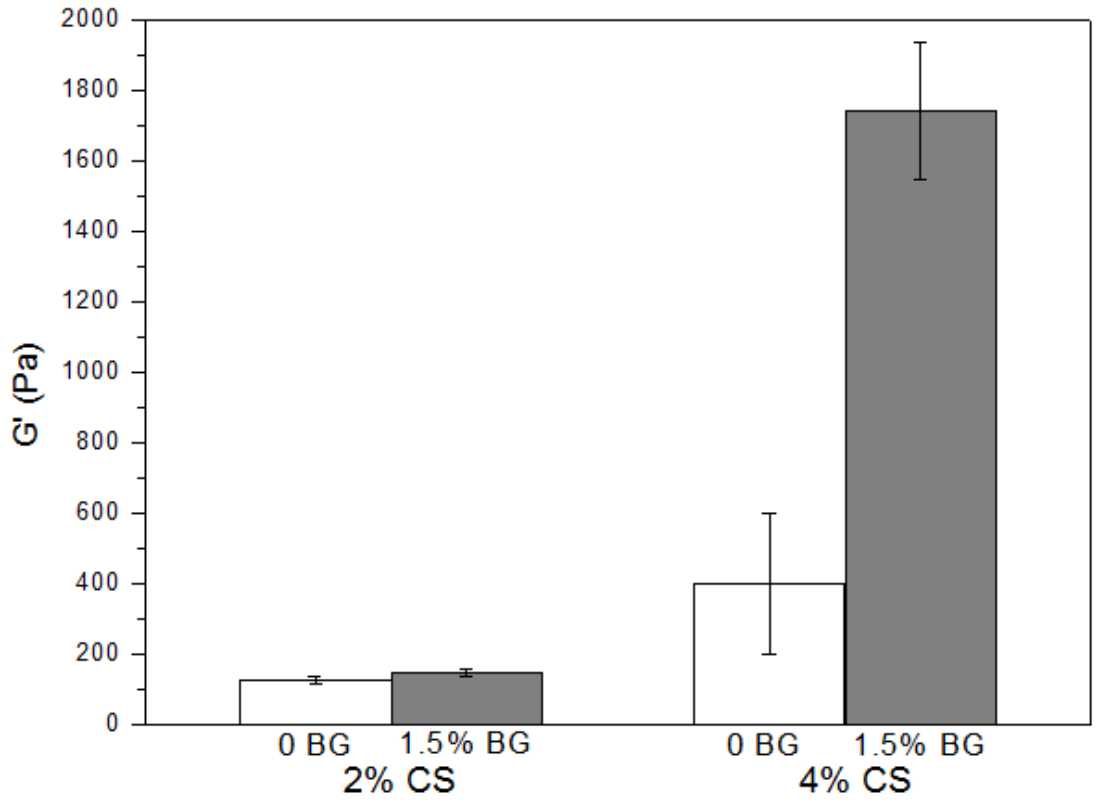

Figure 2. 5. Elastic modulus at frequency =1Hz for PVA/CS 2, PVA/CS/BG 2/1.5, PVA/CS 4 and PVA/CS/BG 4/1.5.

2.3.3. Determination of the bioactivity

When introducing the hydrogels with bioactive glass in SBF, a layer of apatite must form on the surface, creating both chemical and biological bonds with bone or soft tissue. Observing this layer, it is possible to determine if the samples under study are bioactive.

The morphology of PVA/CS 2/1.5 hydrogels after being immersed in SBF for 28 days can be observed in Figure 2.6c and d at two different magnifications (x600 and x3500). The results obtained are compared to the morphology obtained for PVA/CS (figures a and b).

The hydrogel with no BG particles shows a porous morphology typical of a hydrogel. In contrast, the surface corresponding to PVA/CS/BG 2/1.5 hydrogels shows no porosity and seems to be covered by an external layer that presents a cauliflower shape. It is thought that this layer could be the result of the formation of hydroxyapatite from the added bioactive glass, as it has been reported in other works [28], [33], [34].

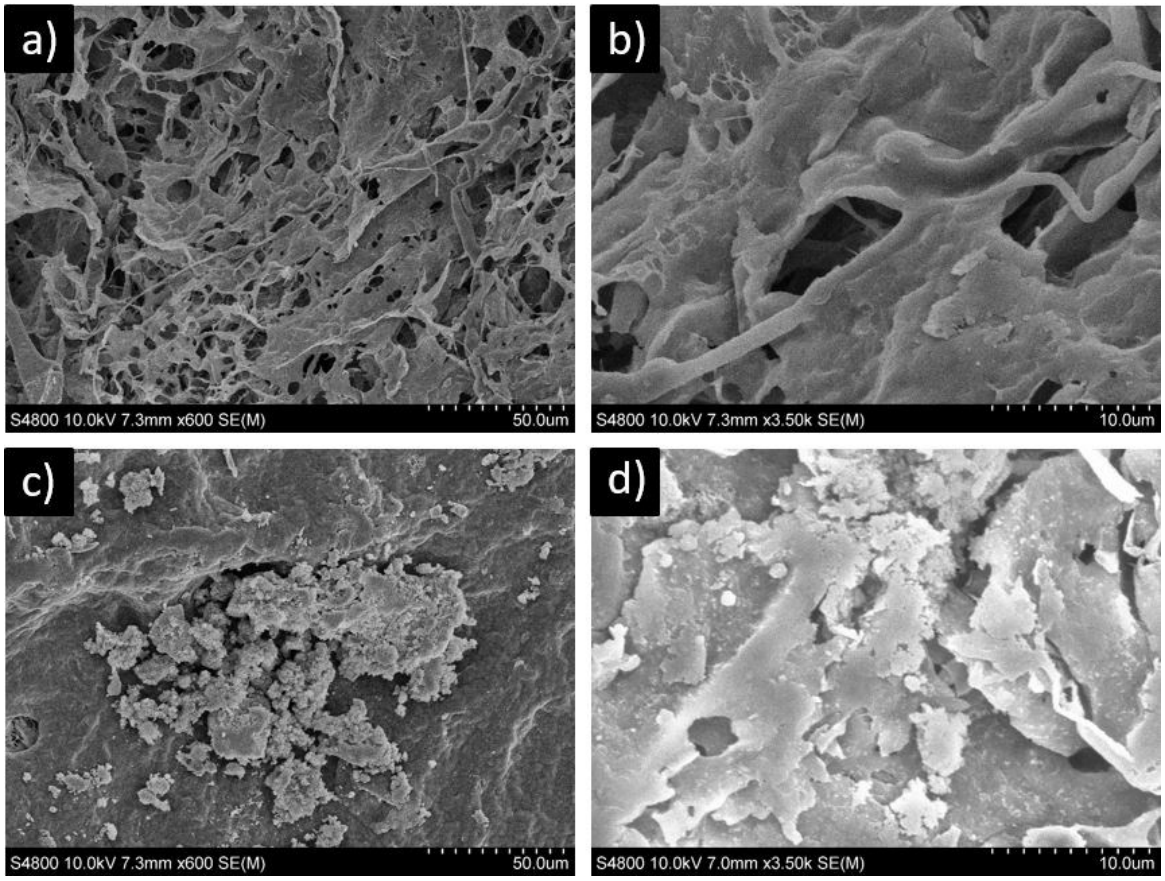

Figure 2. 6. Scanning electron micrographs of PVA/CS 2 at day 0 (a) magnification x600, b) magnification x3500) and PVA/CS/BG 2/1.5 after 28 days submerged in SBF (c) magnification x600, d) magnification x3500).

By means of X-ray crystallography (XRD), the formation of crystalline structures on hydrogels immersed in SBF for different periods of time up to one month was determined. In order to deduce whether there was hydroxyapatite formation or not, special attention was paid to the characteristic peaks of HA found at 2Θ of ~ 26° and ~ 32°. In hydrogels without any added bioactive glass (Figure 2.7a), it was possible to see that there are calcium impurities (~ 27° and ~ 32°), and no hydroxyapatite was found. Impurities could be due to insufficient washing of the gels after being immersed in SBF. With the incorporation of 0.5% (w/v) bioactive glass, hydroxyapatite appears almost from the beginning (Figure 2.7b), increasing over the course of days. This could be

ascertained because of the appearance of the diffraction peaks located at ~ 26° and ~ 32°. Although at the beginning the peak was more characteristic of calcium, it widened to become more similar to that of hydroxyapatite. Finally, hydrogels with 1.5% (w/v) concentration of bioactive glass exhibited similar results to those corresponding to hydrogels with 0.5% (w/v) BG (Figure 2.7c), showing a progressive increase of the peak located at ~ 26° and the broadening of the peak located at ~32°. The diffraction peaks observed in the experiments corresponding to hydrogels with added bioactive glass are wide which suggests that the size of the crystalline structures is small, as those that can be found in bone [33].

XRD experiments allowed confirming that the formation of hydroxyapatite is progressive over time. The reason why there was not much difference between the results found for samples with two different concentrations of bioactive glass (0.5 and 1.5% (w/v)) could be attributed to the formation of agglomerates. It is extremely difficult to achieve a homogenous dispersion with such a considerable amount of bioactive glass, losing surface due to the agglomerates. The results obtained are in agreement to those reported in literature for hydrogels [28], [33], [34] and other types of scaffolds with added bioactive glass [24].

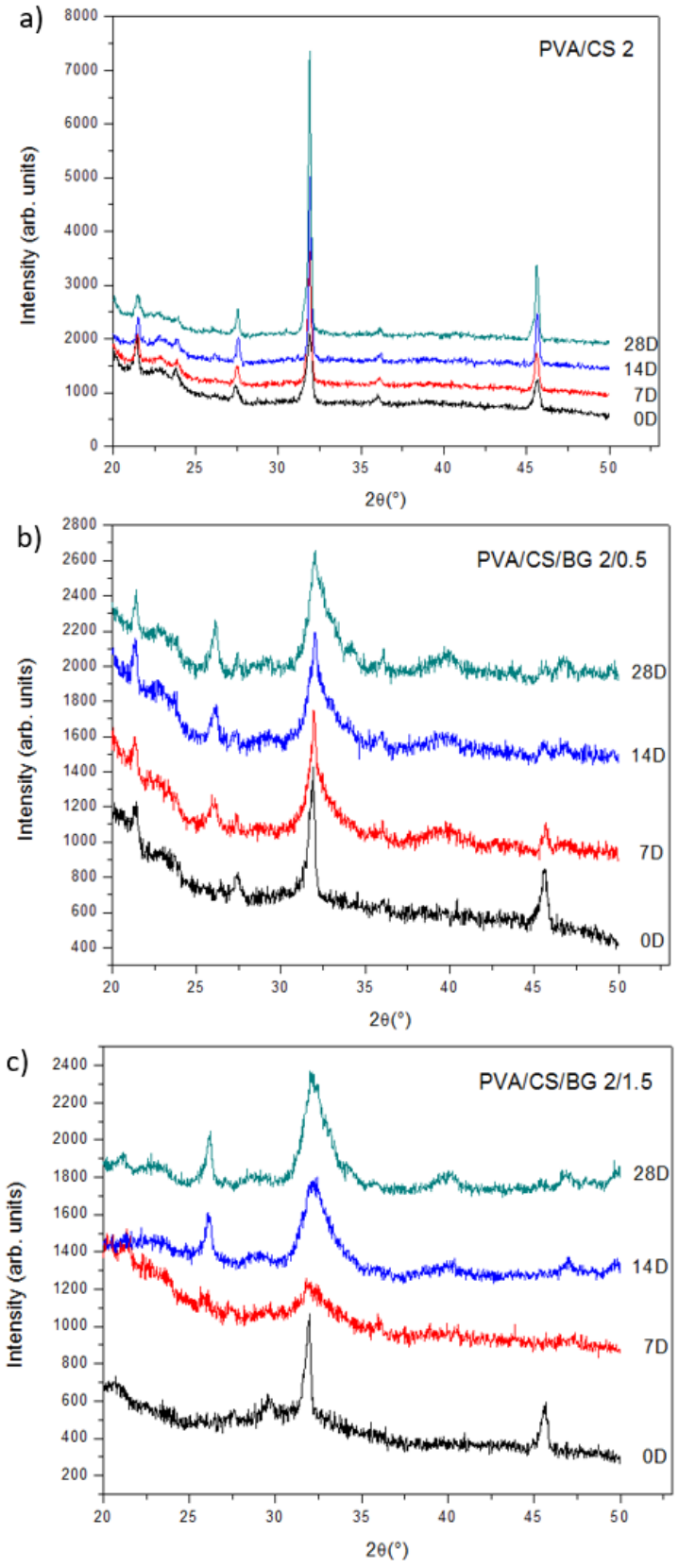

Figure 2. 7. XRD patterns of hydrogels after immersion in SBF for different times.a) PVA/CS 2 ; b) PVA/CS/BG 2/0.5 and c) PVA/CS/BG 2/1.5.

2.3.4. Study of the kinetics of release of a model drug

Drug release was tested for all the samples under study employing Levofloxacin as a model drug. For hydrogels with 2% (w/v) chitosan concentration, the release was almost complete after 5 hours regardless the concentration of bioactive glass (Figure 2.8.). In fact, no differences were observed in between the sample with no added bioactive glass and samples with 0% and 1.5% (w/v) bioactive glass which indicates that the release kinetics of Levofloxacin are not affected by the presence of BG particles. On the other hand, hydrogels with 4% (w/v) chitosan concentration showed a much faster release rate reaching an almost complete release after 2h (Figure 2.9.). It is important to note that the amount of drug release was lower with respect to that found for samples with 2% (w/v) chitosan concentration. In addition, hydrogels with added bioactive glass showed a lower amount of drug release with respect to the hydrogel with no added bioactive glass.

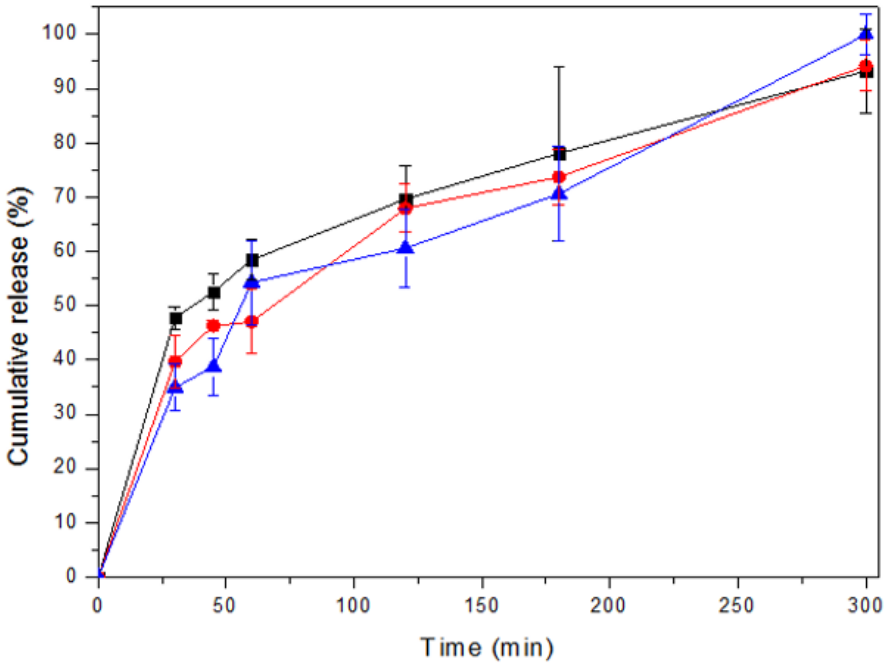

Figure 2. 8. Drug release profiles of PVA/CS 2 (■), PVA/CS/BG 2/0.5 (●) and PVA/CS/BG 2/1.5 (▲) samples immersed into 100 ml of PBS (pH 7.4) at 37°C for 5 hours.

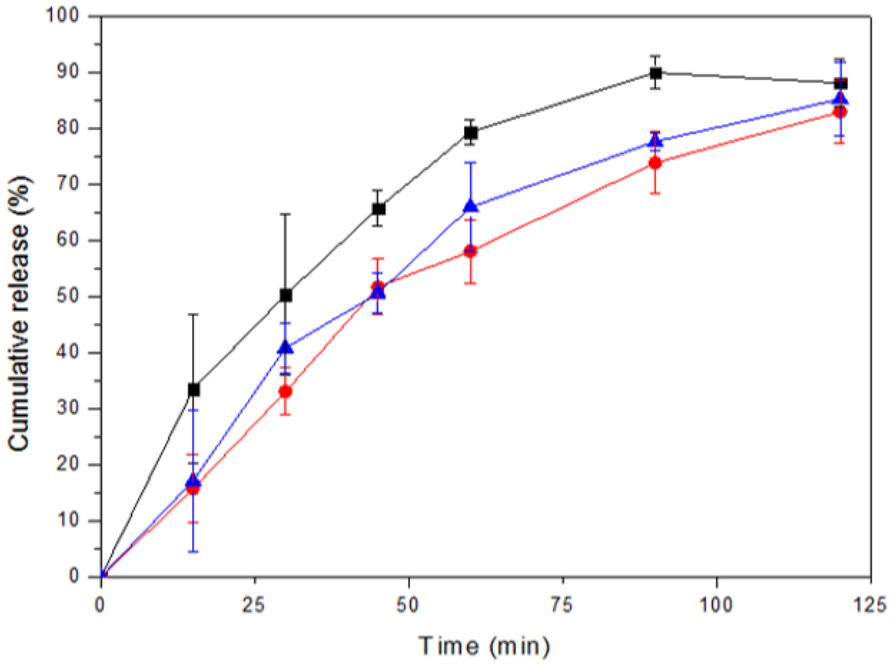

Figure 2. 9. Drug release profiles of PVA/CS 4 (■), PVA/CS/BG 4/0.5 (●) and PVA/CS/BG 4/1.5 (▲) samples immersed into 100 ml of PBS (pH 7.4) at 37°C for 5 hours.

In order to shed further light on the results obtained, the kinetics of release were fitted to different kinetic equations used to study the mechanism of drug release. Table 2.2. shows the regression coefficients. PVA/CS 2 and PVA/CS 4, the two systems without added bioactive glass fit with Korsmeyer-Peppas model, with correlation coefficients of 0.968 and 0.998, respectively. However, their release exponents show different release mechanisms. The release exponent for PVA/CS 2 is 0.29, too low to fit the mechanisms that were previously mentioned. This could happen due to the pore size distribution of the matrix, leading to a deviation of the diffusion laws [35]. Analyzing the correlation coefficients of the rest of the models, the release mechanism of this system could be closer to first order kinetics that to Fick's law. On the other hand, the release exponent for PVA/CS 4 is 0.61, which indicates abnormal transport, but predominantly controlled by Fick's diffusion. PVA/CS/BG 2/0.5 and PVA/CS/BG 2/1.5 systems fit Higuchi model, thus, the release is based in Fick's law, so the rate of diffusion is directly proportional to concentration gradient across the membrane [36]. However, PVA/CS/BG4/0.5 and PVA/CS/BG 4/1.5 follow first order kinetics. In this case, the release depends on drug concentration. This could be due to the difficulty of the drug to go through the matrix when the pore size is smaller, in addition to the obstruction caused by bioactive glass

particles. When the drug concentration is higher, there is a bigger amount closer to the surface, which makes the release faster.

Table 2. 2. Fitting of the release data to the mathematical models for drug release kinetics. R2 is the correlation coefficient, and n is the release exponent.

	Zero order	***First order***	***Higuchi***	***Korsmeyer-Peppas***	
	R^2	**R^2**	**R^2**	**R^2**	**n**
PVA/CS 2	0.65	0.955	0.92	*0.968*	*0.29*
PVA/CS/BG 2/0.5	0.773	0.958	*0.974*	0.933	0.38
PVA/CS/BG 2/1.5	0.832	0.872	*0.972*	0.804	0.42
PVA/CS 4	0.765	0.901	0.955	*0.998*	*0.61*
PVA/CS/BG 4/0.5	0.916	*0.996*	0.961	0.978	0.97
PVA/CS/BG 4/1.5	0.888	*0.993*	0.963	0.961	0.96

2.4. CONCLUSIONS

In the present work, CS/PVA hydrogels were reinforced with inorganic bioactive glass particles, in order to improve their mechanical properties and bioactivity. The effect of the chitosan and bioactive glass concentration on the swelling and mechanical properties was studied. After the satisfactory formation of the hydrogels, it was found that the increase of chitosan concentration results in a lower swelling index for all the samples regardless bioactive glass concentration. For samples with 2% (w/v) chitosan concentration, the addition of BG particles decreases the swelling index without increasing the elastic moduli. This is not the case for the samples prepared with 4% (w/v) chitosan concentration for which the swelling index is not affected by the addition of BG particles, however, the elastic modulus largely increases with the addition of 1.5% (w/v) BG particles. The results point on the one hand, to the decrease of effective crosslinking points in between polymer chains as a result of the BG incorporation, and on the other hand, to a reinforcement effect of the BG particles as previously seen for other composite gels. Bioactivity of the hydrogels containing BG particles was confirmed after immersion of the hydrogels in SBF for one month at physiological temperature, being able to appreciate the formation of a layer of apatite on the surface of hydrogels through SEM carried out on lyophilized samples. XRD further confirmed the formation of crystalline hydroxyapatite. The potential application of CS/PVA hydrogels with inorganic

BG particles as drug delivery matrixes was also proven employing levofloxacin as a model drug. The presence of bioactive glass particles does not influence the kinetics of the release in the case of hydrogels with 2% (w/v) concentration of chitosan, however, it slows the release when the concentration of chitosan is increased to 4% (w/v) in agreement with the lower swelling index found for these samples.

2.5. REFERENCES

[1] T. R. Hoare and D. S. Kohane, "Hydrogels in drug delivery: Progress and challenges," *Polymer*, vol. 49, no. 8. Elsevier BV, pp. 1993–2007, Apr. 15, 2008. doi: 10.1016/j.polymer.2008.01.027.

[2] N. A. Peppas, J. Z. Hilt, A. Khademhosseini, and R. Langer, "Hydrogels in biology and medicine: From molecular principles to bionanotechnology," *Advanced Materials*, vol. 18, no. 11. John Wiley & Sons, Ltd, pp. 1345–1360, Jun. 06, 2006. doi: 10.1002/adma.200501612.

[3] R. Langer and N. A. Peppas, "Advances in Biomaterials, Drug Delivery, and Bionanotechnology," *AIChE Journal*, vol. 49, no. 12, pp. 2990–3006, 2003, doi: 10.1002/aic.690491202.

[4] R. Barbucci, B. Zavan, R. Cortivo, and G. Abatangelo, "Hydrogels and Tissue Engineering," in *Hydrogels*, Springer Milan, 2009, pp. 1–8. doi: 10.1007/978-88-470-1104-5_1.

[5] J. L. Drury and D. J. Mooney, "Hydrogels for tissue engineering: Scaffold design variables and applications," *Biomaterials*, vol. 24, no. 24. Elsevier BV, pp. 4337–4351, Nov. 01, 2003. doi: 10.1016/S0142-9612(03)00340-5.

[6] J. Escobar, D. García, D. Zaldivar, and I. Katime, "Hidrogeles. Principales Características en el Diseño de Sistemas de Liberación Controlada de Fármacos," *Revista Iberoamericana de Polímeros*, vol. 3, no. 3, pp. 36–60, 2002.

[7] N. A. Peppas, P. Bures, W. Leobandung, and H. Ichikawa, "Hydrogels in pharmaceutical formulations," *European Journal of Pharmaceutics and Biopharmaceutics*, vol. 50, no. 1. Elsevier, pp. 27–46, Jul. 03, 2000. doi: 10.1016/S0939-6411(00)00090-4.

[8] M. Kong, X. G. Chen, K. Xing, and H. J. Park, "Antimicrobial properties of chitosan and mode of action: A state of the art review," *International Journal of Food Microbiology*, vol. 144, no. 1. Elsevier, pp. 51–63, Nov. 15, 2010. doi: 10.1016/j.ijfoodmicro.2010.09.012.

[9] F. Croisier and C. Jérôme, "Chitosan-based biomaterials for tissue engineering," *European Polymer Journal*, vol. 49, no. 4. Elsevier Ltd, pp. 780–792, Apr. 01, 2013. doi: 10.1016/j.eurpolymj.2012.12.009.

[10] A. Bernkop-Schnürch and S. Dünnhaupt, "Chitosan-based drug delivery systems," *European Journal of Pharmaceutics and Biopharmaceutics*, vol. 81, no. 3. Elsevier, pp. 463–469, Aug. 01, 2012. doi: 10.1016/j.ejpb.2012.04.007.

[11] V. Patrulea, V. Ostafe, G. Borchard, and O. Jordan, "Chitosan as a starting material for wound healing applications," *European Journal of Pharmaceutics and Biopharmaceutics*, vol. 97. Elsevier, pp. 417–426, Nov. 01, 2015. doi: 10.1016/j.ejpb.2015.08.004.

[12] X. Li *et al.*, "In situ injectable nano-composite hydrogel composed of curcumin, N,O-carboxymethyl chitosan and oxidized alginate for wound healing application," *International Journal of Pharmaceutics*, vol. 437, no. 1–2, pp. 110–119, Nov. 2012, doi: 10.1016/j.ijpharm.2012.08.001.

[13] T. Santos *et al.*, "Nanocomposite chitosan hydrogels based on PLGA nanoparticles as potential biomedical materials," *European Polymer Journal*, vol. 99, pp. 456–463, 2018, doi: 10.1016/j.eurpolymj.2017.12.039.

[14] H. D. M. Follmann *et al.*, "Advanced fibroblast proliferation inhibition for biocompatible coating by electrostatic layer-by-layer assemblies of heparin and chitosan derivatives," *Journal of Colloid and Interface Science*, vol. 474, pp. 9–17, Jul. 2016, doi: 10.1016/j.jcis.2016.04.008.

[15] G. Paradossi, F. Cavalieri, E. Chiessi, C. Spagnoli, and M. K. Cowman, "Poly(vinyl alcohol) as versatile biomaterial for potential biomedical applications," in *Journal of Materials Science: Materials in Medicine*, Aug. 2003, vol. 14, no. 8, pp. 687–691. doi: 10.1023/A:1024907615244.

[16] J. H. Sung *et al.*, "Gel characterisation and in vivo evaluation of minocycline-loaded wound dressing with enhanced wound healing using polyvinyl alcohol and chitosan," *International Journal of Pharmaceutics*, vol. 392, no. 1–2, pp. 232–240, Jun. 2010, doi: 10.1016/j.ijpharm.2010.03.024.

[17] A. Popov, E. Enlow, J. Bourassa, and H. Chen, "Mucus-penetrating nanoparticles made with 'mucoadhesive' poly(vinyl alcohol)," *Nanomedicine: Nanotechnology, Biology, and Medicine*, vol. 12, no. 7, pp. 1863–1871, Oct. 2016, doi: 10.1016/j.nano.2016.04.006.

[18] Y. Qiu and K. Park, "Environment-sensitive hydrogels for drug delivery," *Advanced Drug Delivery Reviews*, vol. 53, no. 3. Elsevier, pp. 321–339, Dec. 31, 2001. doi: 10.1016/S0169-409X(01)00203-4.

[19] M. McKenzie, D. Betts, A. Suh, K. Bui, L. Kim, and H. Cho, "Hydrogel-Based Drug Delivery Systems for Poorly Water-Soluble Drugs," *Molecules*, vol. 20, no. 11, pp. 20397–20408, Nov. 2015, doi: 10.3390/molecules201119705.

[20] V. Sáez, E. Hernáez, and L. Sanz Angulo, "Liberación Controlada de Fármacos. Hidrogeles.," *Revista Iberoamericana de Polímeros*, vol. 4, no. 1, pp. 21–91, 2003.

[21] A. Lejardi *et al.*, "Novel hydrogels of chitosan and poly(vinyl alcohol)-g-glycolic acid copolymer with enhanced rheological properties," *Carbohydrate Polymers*, vol. 103, no. 1, pp. 267–273, Mar. 2014, doi: 10.1016/j.carbpol.2013.12.040.

[22] A. Anitha *et al.*, "Chitin and chitosan in selected biomedical applications," *Progress in Polymer Science*, vol. 39, no. 9. Elsevier Ltd, pp. 1644–1667, Sep. 01, 2014. doi: 10.1016/j.progpolymsci.2014.02.008.

[23] L. L. Hench, "The story of Bioglass®," in *Journal of Materials Science: Materials in Medicine*, Nov. 2006, vol. 17, no. 11, pp. 967–978. doi: 10.1007/s10856-006-0432-z.

[24] A. Larrañaga, P. Aldazabal, F. J. Martin, and J. R. Sarasua, "Hydrolytic degradation and bioactivity of lactide and caprolactone based sponge-like scaffolds loaded with bioactive glass particles," *Polymer Degradation and Stability*, vol. 110, no. 110, pp. 121–128, 2014, doi: 10.1016/j.polymdegradstab.2014.08.021.

[25] Y. F. Tang, Y. M. Du, X. W. Hu, X. W. Shi, and J. F. Kennedy, "Rheological characterisation of a novel thermosensitive chitosan/poly(vinyl alcohol) blend hydrogel," *Carbohydrate Polymers*, vol. 67, no. 4, pp. 491–499, Feb. 2007, doi: 10.1016/j.carbpol.2006.06.015.

[26] E. Sanchez-Rexach, I. Martínez de Arenaza, J. R. Sarasua, and E. Meaurio, "Antimicrobial poly(ε-caprolactone)/thymol blends: Phase behavior, interactions and drug release kinetics," *Eur Polym J*, vol. 83, pp. 288–299, 2016, doi: 10.1016/j.eurpolymj.2016.08.029.

[27] P. Costa and J. M. Sousa Lobo, "Modeling and comparison of dissolution profiles," *European Journal of Pharmaceutical Sciences*, vol. 13, no. 2. Elsevier, pp. 123–133, May 01, 2001. doi: 10.1016/S0928-0987(01)00095-1.

[28] J. A. Killion *et al.*, "Hydrogel/bioactive glass composites for bone regeneration applications: Synthesis and characterisation," *Materials Science and Engineering: C*, vol. 33, no. 7, pp. 4203–4212, Oct. 2013, doi: 10.1016/j.msec.2013.06.013.

[29] K. S. Anseth, C. N. Bowman, and L. Brannon-Peppas, "Mechanical properties of hydrogels and their experimental determination," *Biomaterials*, vol. 17, no. 17. Elsevier Science Ltd, pp. 1647–1657, Jan. 01, 1996. doi: 10.1016/0142-9612(96)87644-7.

[30] V. Zamora-Mora, P. Soares, C. Echeverria, R. Hernández, and C. Mijangos, "Composite Chitosan/Agarose Ferrogels for Potential Applications in Magnetic Hyperthermia," *Gels*, vol. 1, no. 1, pp. 69–80, Jul. 2015, doi: 10.3390/gels1010069.

[31] C. D. F. Moreira, S. M. Carvalho, H. S. Mansur, and M. M. Pereira, "Thermogelling chitosan-collagen-bioactive glass nanoparticle hybrids as potential injectable systems for tissue engineering," *Materials Science and Engineering C*, vol. 58, pp. 1207–1216, Jan. 2016, doi: 10.1016/j.msec.2015.09.075.

[32] R. Kocen, M. Gasik, A. Gantar, and S. Novak, "Viscoelastic behaviour of hydrogel-based composites for tissue engineering under mechanical load," *Biomedical Materials (Bristol)*, vol. 12, no. 2, p. 25004, Mar. 2017, doi: 10.1088/1748-605X/aa5b00.

[33] D. S. Couto, Z. Hong, and J. F. Mano, "Development of bioactive and biodegradable chitosan-based injectable systems containing bioactive glass nanoparticles," *Acta Biomaterialia*, vol. 5, no. 1, pp. 115–123, Jan. 2009, doi: 10.1016/j.actbio.2008.08.006.

[34] A. Gantar *et al.*, "Nanoparticulate bioactive-glass-reinforced gellan-gum hydrogels for bone-tissue engineering," *Materials Science and Engineering C*, vol. 43, pp. 27–36, Oct. 2014, doi: 10.1016/j.msec.2014.06.045.

[35] J. Saurí *et al.*, "Quality by Design approach to understand the physicochemical phenomena involved in controlled release of captopril SR matrix tablets," *International Journal of Pharmaceutics*, vol. 477, no. 1–2, pp. 431–441, Dec. 2014, doi: 10.1016/j.ijpharm.2014.10.050.

[36] R. Gouda, H. Baishya, and Z. Qing, "Application of Mathematical Models in Drug Release Kinetics of Carbidopa and Levodopa ER Tablets," *J Dev Drugs*, vol. 6, no. 2, pp. 1–8, 2017, doi: 10.4172/2329-6631.1000171.

CHAPTER 3. POLY(ε-CAPROLACTONE) BASED POLYMER/DRUG AMORPHOUS SOLID DISPERSIONS

3a. Introduction and miscibility prediction

3b. Amorphous solid dispersions in poly (ε-caprolactone)/xanthohumol bioactive blends: physicochemical and mechanical characterization

3c. Miscibility, interactions and possible anti-cancer activity of poly(ε-caprolactone)/mycophenolic acid blends

3a. INTRODUCTION AND MISCIBILITY PREDICTION

3a.1. INTRODUCTION

The aim of this chapter is to study possible combinations of biodegradable polymer/active pharmaceutical ingredient (API) that result in stable mixtures for their antimicrobial application, in addition to being able to seek medical benefits beyond the inhibition of infections. One of the biggest problems that appear when obtaining these systems is the crystallinity and low solubility of most of the active molecules (in this case, most of them of vegetal origin). These characteristics mean that the bioavailability of the active agent is reduced, causing less absorption by the body, especially in the case of oral applications, since the percentage that can be dissolved in the gastrointestinal tract is reduced.

In order to solve this situation, one of the approaches that is being successful is the formation of amorphous solid dispersion (ASDs). In this kind of system, the drug can be kept in an amorphous state within a polymeric matrix, thus improving its solubility and, therefore, its bioavailability. The key to these systems lies in the formation of a single phase through the formation of favorable interactions between the API in an amorphous state and the polymer, thus being able to inhibit the formation of API crystals inside the polymeric matrix. However, for these mixtures to be successful, it is essential that they remain stable, therefore, it is desirable that there is a miscibility between both components, creating a single phase [1].

In order to confirm that a polymer/drug blend is miscible, it is essential to verify that the free energy of mixing is negative ($\Delta G_{mix}<0$) [2], and this free energy can be calculated using the Flory-Huggins theory (eq. (3a.1)):

$$\frac{\Delta G_{mix}}{kT} = n_{drug} \ln \phi_{drug} + n_{polymer} \ln \phi_{polymer} + n_{drug} \phi_{polymer} \chi \qquad (3a.1)$$

where *n* is the number of molecules, ϕ is the volume fraction, χ is the Flory-Huggins interaction parameter, *k* is Boltzmann's constant and *T* is the absolute temperature. The first two terms represent the entropic contribution (which will have a negative but small value) and the third term represents the enthalpic contribution to the free energy of

mixing. To determine the miscibility of polymer/API blends the interaction parameter must be negative (χ<0) or lower than 0.5 [3], since this will imply a negative enthalpic contribution, resulting in a free energy of negative value.

However, obtaining a miscible blend is not an easy task, since it is common to have to study several mixtures before finding one that has the desired characteristics, this being a long and tedious task.

In order not to have to study the free energy in each of the blends, a preliminary filter can be performed. One of the properties expected when two components are miscible is a single glass transition temperature (T_g) intermediate between those of the two pure components. To theoretically calculate the T_g that would correspond to each blend, there are different methods, such as Gordon-Taylor (GT), Couchman-Karasz (CK) or the Fox equation. In this case, considering that the polymer and drug densities are similar, the Fox equation [4] can be derived as (eq. (3a.2)):

$$\frac{1}{T_{gb}} = \frac{w_1}{T_{g1}} + \frac{w_2}{T_{g2}} \qquad \text{(3a.2)}$$

where w_1 and w_2 are the weight fractions of components 1 and 2 respectively, T_{g1} and T_{g2} are the glass transition temperatures of the pure components and T_{gb} is the glass transition temperature of the blend (values in Kelvin). That is, for a 50/50 blend of polymer and drug, the T_g would approach an intermediate value between the T_g of the polymer and that of the drug. It is worth mentioning that in the case of many of the drugs used, being mostly crystalline, it is impossible to measure their T_g experimentally, so their T_g has been estimated according to the following formula (eq. (3a.3.)) [5]:

$$T_{gt} = \frac{2}{3} T_m \qquad \text{(3a.3)}$$

The following section presents the first approach to the study of miscibility between the selected polymers and drugs by studying the intermediate glass transition temperature.

3a.2. MISCIBILITY PREDICTION: INTERMEDIATE GLASS TRANSITION TEMPERATURE

As mentioned in the introduction to this chapter, an initial filter has been performed, with poly(D,L-lactide) (PDLLA) and poly(ε-caprolactone) (PCL) being the polymers selected for mixing with a wide variety of drugs.

PDLLA is one of the four chiral macromolecules of PLA (Poly (lactic acid)), which is one of the most studied biodegradable polyesters for medical and environmental applications since the U.S. Food and Drug Administration (FDA) approved it in 1970 for use in contact with human biological fluids [6]. PDLLA is one of the most widely used chiral macromolecules due to its amorphous nature, having a more controllable *in vivo* degradation profile than PLLA, with a half-life of around 2-3 months under physiological conditions. The mechanical, thermal, rheological and biological properties of PDLLA can be modulated based on the different proportions of L- and D- isomers in its formulations. Higher proportion of the D- isomer lead to faster resorption and a less crystalline structure, while the L- isomer is characterized by slower resorption and higher crystallinity [7], [8]. The ratio of the isomers can also vary the glass transition temperature, which can be between 40°C – 50°C. This polymer is widely used in fields such as tissue engineering or drug delivery, as the products generated from its degradation are not toxic to the human body. This degradation occurs in two phases. First, the longer polymer chains are hydrolyzed by water molecules, separating into shorter segments. In the second phase, these shorter fragments are phagocytosed and metabolized by macrophages, in a physiological response of the body [7].

Poly (ε-caprolactone) is a biodegradable semicrystalline polyester, also approved by the U.S. Food and Drug Administration (FDA) with a very wide use in biomedical applications, especially in drug delivey and tissue engineering. It has a glass transition temperature of around -60°C, and its melting temperature is between 55°C-70°C [8], [9]. Its degradation can take from a few months to years depending on the environment, and the products generated are not toxic to the body or the environment. Like PDLLA, there is a first phase of degradation by hydrolysis, in which there is a decrease in its molecular weight with its corresponding macroscopic changes, to later increase this

fragmentation of the chains through metabolism and phagocytosis [10]. Despite having interesting properties for biomedical applications, it also has limitations, such as low mechanical properties or poor bioactivity. For this reason, there is great interest in improving these properties by mixing it with other components, or adding nanofillers, especially those of natural origin [11].

In order to perform the search for miscible polymer/API blends, a wide variety of active molecules have been selected, mostly coming from essential oils or plants. Most of them are plant polyphenols (Figure 3a.1.), basically composed of aromatic rings and hydroxyl groups, facilitating hydroxyl-hydroxyl and hydroxyl-carbonyl interactions with the polymers. The drugs, that can be seen in Table 3a.1., have been selected from the book *Encyclopedia of Traditional Chinese Medicines – Molecular Structures, Pharmacological Activities, Natural Sources and Applications* [12].

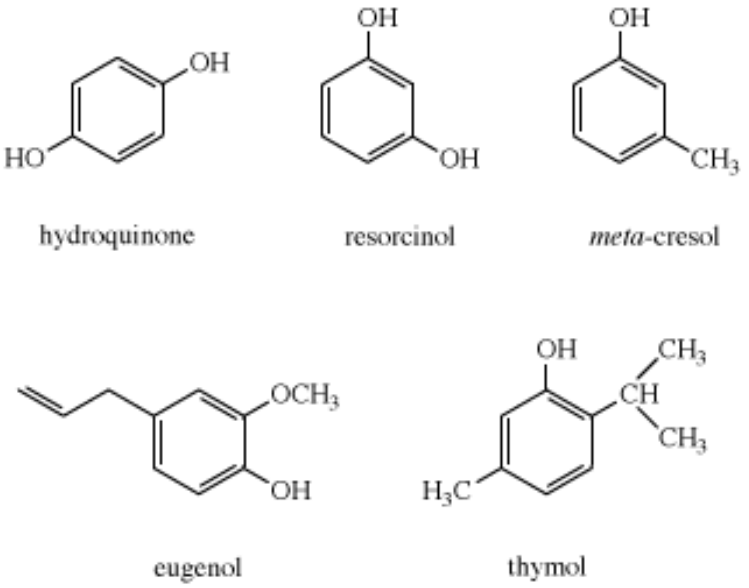

Figure 3a. 1. Different polyphenol examples.

Once the polymers and drugs had been chosen, films with 50/50 polymer/drug compositions were formed, mixing each polymer with each of the drugs. These were manufactured using the solvent casting procedure, dissolving the polymer and the active

molecule together and letting them to air dry in a petri dish. Most of them were dissolved in dichloromethane (DCM) or tetrahydrofuran (THF).

Having obtained the films, the thermal measurements were performed in a Modulated DSC Q200 (TA Instruments), using samples of between 5 and 10 mg of each of the blends in hermetic aluminum pans, in a nitrogen atmosphere. Two consecutive scans were performed for each sample. The first, coming to melt the polymeric part without degrading it or the drug, and the second up to higher temperatures, regardless of its degradation. The glass transition temperatures were measured in the second scan as the midpoint of the specific heat increment. It is worth mentioning that before measuring the blends, the same was done with the polymers and with each drug in its pure state. Thus, it was possible to obtain the experimental T_g of some drugs, while in other it was necessary to estimate it theoretically, using (Eq. (3a.3)).

In order to analyze the miscibility of the blends, two consequtive DSC scans were carried out in properly dry samples. Thermally unstable drugs tend to degrade fast after melting, and in these cases the first scan was stopped below the melting temperature of the drug. In the case of thermally stable drugs, the first scan was performed up to the melting point of the bioactive molecule. In general, our experimental results followed the following trends (though some exceptions were also observed). In most cases, the first scan showed negligible variations in the locations of the characteristic thermal transitions (the melting points of the polymer and the drug and the glass transition of the polymer), and miscibility was discarded. However, in some of these systems containing thermally stable drugs (which were melted during the first scan), the second scan showed clear displacements in the characteristic thermal transitions, indicating the possibility to use quenching procedures to obtain ASDs that are probably unstable and in which the drug is expected to crystallize over time. In the case of the thermally unstable drugs with negligible changes in the features present in the first scan, the second scan was also similar to the first one, discarding the possibility of using thermal treatments to obtain ASDs. In other systems, significative variations of the characteristic thermal transitions were observed from the first scan, indicating some degree of miscibility in the system. A second scan was also carried out to erase the thermal history of the system and to analyze the effect of quenching from the melt on the degree of dispersion

of the drug. Finally, the experimental T_g obtained during the second scan for the polymer rich phase were then compared with the theoretical T_g obtained by means of the Fox equation (Eq. (3a.2)). However, these theoretical T_g may present large deviations particularly in cases where T_g of the drug has been estimated using (eq. (3a.3)), in addition to taking into account that the Fox equation (Eq. (3a.2)) is more reliable in systems with weak interactions than in systems with specific interactions. Taking all these considerations together, systems were classified as partially miscible blends (PM) and not miscible ones (NM), which can be seen in Table 3a.1.

Table 3a. 1. Miscibility prediction for different polymer/API blends. Partially miscible (PM, in green) or Not miscible (NM, in red).

API	PCL	PDLLA
Vanillic acid	NM	PM
ρ-coumaric acid crystalline	PM	NM
5-Hydroxy-1,4-Naphthoquinone 97%	PM	NM
Trans-cinnamic acid 99%	NM	NM
Trans-ferulic acid 99%	NM	NM
Mycophenolic acid	PM	-
Succinic acid bioxtra	NM	NM
Gallic acid	PM	NM
Caffeic acid	PM	NM
Octyl gallate, antioxidant, >=99%	PM	-
Sclareol	NM	NM
Cholic acid from bovine or ovine	NM	NM
Xanthohumol	PM	NM
Tannic acid	-	NM
3,4-dihydroxybenzoic acid >=97%	-	NM
Methyl 3,4,5-trihydroxybenzoate 98%	PM	NM
Salicylic acid extra pure	PM	PM
2,5-dihydroxybenzoic acid	-	NM
(+/-) – Isoborneol, 95%	NM	NM
β-Thujaplicin 99%	NM	PM
8-Hydroxyquinoline 99%	NM	NM
Isoliquiritigenin	PM	NM

Dihydromyricetin	PM	NM
Metronidazole	-	NM
Doxycycline monohydrate	-	NM
Sulfanilamide	NM	NM
Pyrazinamide	NM	NM
(+) – Catechin hydrate >=96%	PM	NM
Methylhydroquinone 99%	PM	PM
L-ascorbic acid	NM	NM
Ellagic acid from chestnut bark	-	NM
Chlorogenic acid crystalline	NM	NM

3a.3. MISCIBILITY PREDICTION: BAGLEY PLOTS

As much as experimental prediction by measuring T_g facilitates the search for miscible blends, ideally one should be able to predict it theoretically. An approximation can be obtained knowing its solubility parameters, as is done to find out the solubility of polymers in certain solvents, or to predict the miscibility between two polymers [13]. It is worth mentioning that even so it is complex to predict, and the reliability is limited. However, the test has been performed to see if it is possible to find any connection between the experimental prediction and the theoretical prediction.

To predict the miscibility between a polymer and a drug, the solubility parameter difference between both must be calculated, determining the cohesive energy density (CED) of each component. The lower the cohesive energy density difference between two substances , the higher the chance of obtaining a miscible blend. There are different ways to calculate the solubility parameters, one of the most used is the so-called Hansen approach [14], [15], which can be seen below (Eq.(3a.4.)):

$$\delta^2 = \delta_d^2 + \delta_p^2 + \delta_h^2 \qquad (3a.4)$$

where δ is the total solubility parameter, δ_d refers to the contribution of dispersion forces, δ_h represents the contribution of hydrogen bonding and δ_p refers to the contribution of the polar forces.

One of the methods to estimate solubility parameters apart from experimental techniques is to use group contribution (GC) method, one of the most widely used classical methods being the Hoftyzer-Van Krevelen (HVK) method [16]. Hoftyzer and Van Krevelen proposed the following equations (Eq. (3a.5-7)) to estimate the three partial solubility parameters:

$$\delta_d = \frac{\sum F_{di}}{V} \tag{3a.5}$$

$$\delta_p = \frac{\sqrt{\sum F_{pi}^2}}{V} \tag{3a.6}$$

$$\delta_h = \sqrt{\frac{\sum E_{hi}}{V}} \tag{3a.7}$$

where F_{di} and F_{pi} are the molar attraction constants, E_{hi} is the molar energy of hydrogen bonding and V is the molar volume of the compound.

One of the most widely used resources to represent solubility parameters are solubility maps, which represent the three parameters (δ_d. δ_p, δ_h) experimentally. However, Bagley et al. concluded that a two-dimensional map with two parameters would be sufficient, since the effect of δ_d and δ_p is similar, while the effect of δ_h presents a different nature [13], [16] Therefore, δ_v parameter was introduced (Eq. (3a.8)):

$$\delta_v^2 = \delta_d^2 + \delta_p^2 \tag{3a.8}$$

One of the parameters to represent would be δ_v, which corresponds to "physical" interactions (polar and nonpolar effects) and the other would be δ_h, corresponding to "chemical" interactions (hydrogen bonding effects). Thus, plotting these two parameters the solubility parameter of each component would be displayed. In order to calculate the distances between two components and thus know if they are in the miscible area, the following equation is used (Eq. (3a.9)):

$$D_{12} = \sqrt{\left(\delta_{1,v} - \delta_{2,v}\right)^2 + \left(\delta_{1,h} - \delta_{2,h}\right)^2} \quad \text{(3a.9)}$$

The radius of the area is delimited by the maximum difference between solubility parameters (Δδ) for two components to be considered miscible. According to Greenhalgh et al, in amorphous solid dispersions the blends that show a solubility parameter difference of <7 $MPa^{1/2}$ between the polymer and the drug are more likely to be miscible, while the mixtures whose solubility parameters show a greater difference that 10 $MPa^{1/2}$ are generally immiscible [17]–[19]. Table 3a.2. shows the results that were obtained for δ_v and δ_h.

In Figure 3a.2. the Bagley plot resulting from the solubility parameters of PDLLA and the drugs is shown. With PDLLA as the center, two radii, R1 and R2, corresponding to the limits of 7 $MPa^{1/2}$ and 10 $MPa^{1/2}$ respectively, were extended.

According to the results of the experimental measurements, only four drugs show partial miscibility with PDLLA: vanillic acid, β-thujaplicin, salicylic acid and methylhydroquinone (Figures 3a.3-6). The Bagley plot show how vanillic acid and β-thujaplicin are within the radius R1, that is, within the miscible area. Salicylic acid and methylhydroquinone, on the other hand, are on the edge or close to the R2 radius, so the possibility of showing miscibility is at the limit. However, the graph also shows that most of the drugs are in the miscible region, while the experimental results do not agree with this. It should be mentioned that this difference between the experimental and the theoretical results is explainable. The group contribution methods used to obtain the solubility parameters were obtained from substances in a liquid state. However, these drugs are in a crystalline state, so it is likely that the cohesive energy density of the drug is higher than calculated in this case, making miscibility less likely, since miscibility is a

balance between the strength of the interassociation interactions and the autoassociation ones.

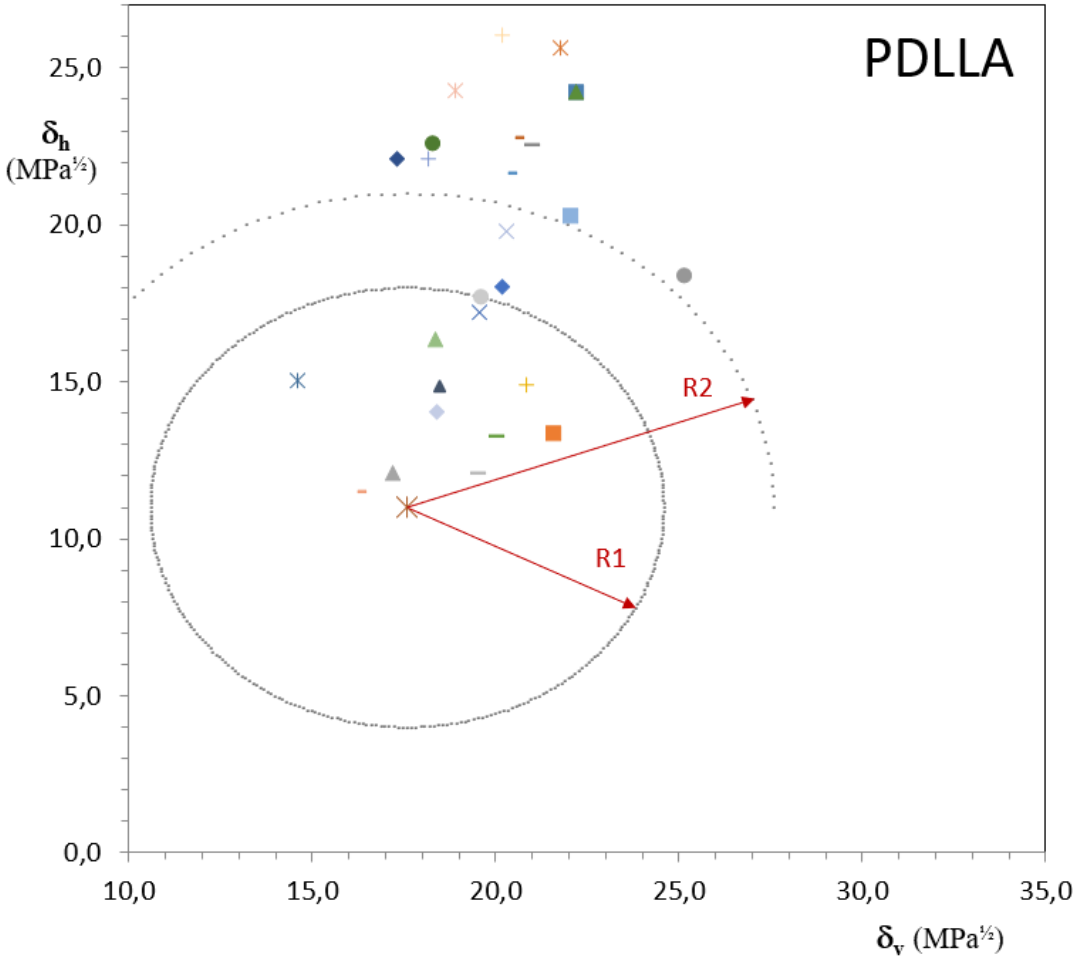

Figure 3a. 2. Bagley plot resulting from the solubility parameters of PDLLA and the drugs. R1 and R2 correspond to 7 $MPa^{1/2}$ and 10 $MPa^{1/2}$, respectively. The compound corresponding to each symbol can be seen in Table 3a.2.

Table 3a. 2. Solubility parameters and symbols for each of the compounds.

Symbol		Name of the compound	δ_v (x axis) ($MPa^{1/2}$)	δ_h (y axis) ($MPa^{1/2}$)
Fig. 3a.2	Fig.3a.7			
	✳	Poly(ε-caprolactone)	17.1	8.1
✳		Poly(D,L-lactide)	17.6	11
+	+	Vanillic acid	20.9	14.9
◆	◆	ρ-coumaric acid crystalline	20.2	18.1
■	■	5-Hydroxy-1,4-Naphthoquinone 97%	21.6	13.4
–	–	Trans-cinnamic acid 99%	20	13.3
✕	■	Trans-ferulic acid 99%	19.6	17.2
◆	◆	Mycophenolic acid	18.4	14.1

		Succinic acid bioxtra	25.2	18.4
		Gallic acid	21.8	25.7
		Caffeic acid	20.4	21.6
		Octyl gallate, antioxidant, >=99%	18.4	16.4
		Sclareol	16.3	11.5
		Cholic acid from bovine or ovine	14.6	15
		Xanthohumol	18.5	14.9
		Tannic acid	18.3	22.6
		3,4-dihydroxybenzoic acid >=97%	22.2	24.3
		Methyl 3,4,5-trihydroxybenzoate 98%	21	22.5
		Salicylic acid extra pure	22	20.3
		2,5-dihydroxybenzoic acid	22.2	24.3
		(+/-) – Isoborneol, 95%	17.2	12.1
		β-Thujaplicin 99%	19.5	12.1
		Isoliquiritigenin	19.6	17.7
		Dihydromyricetin	18.9	24.3
		(+) – Catechin hydrate >=96%	18.1	22.1
		Methylhydroquinone 99%	20.3	19.8
		L-ascorbic acid	20.2	26.0
		Ellagic acid from chestnut bark	20.6	22.8
		Chlorogenic acid crystalline	17.3	22.1

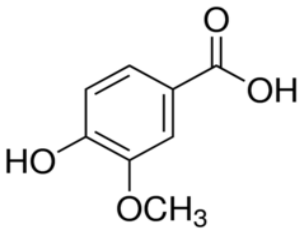

Figure 3a. 3. Vanillic acid

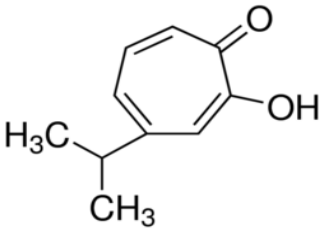

Figure 3a. 4. β-Thujaplicin

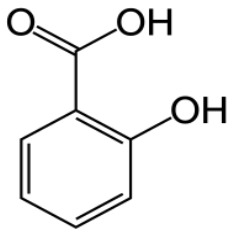

Figure 3a. 5. Salicylic acid

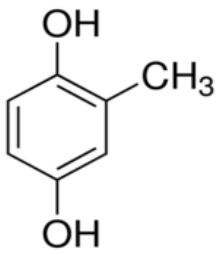

Figure 3a. 6. Methylhydroquinone

Taking a look at the Bagley plot for PCL and the drugs shown in Figure 3a.7., it can be seen that, applying the same R1 and R2 limits, the result is quite different from that of PDLLA.

The number of drugs that have shown a favorable result in experimental prediction is high: dihydromyricetin, catechin hydrate, methylhydroquinone, isoliquiritigenin, octyl gallate, xanthohumol, mycophenolic acid, gallic acid, methyl 3,4,5-trihydroxybenzoate, caffeic acid, salicylic acid, P-coumaric acid and 5-hydroxy-1,4-naphtoquinone (Figure 3a.8-20). However, in this graph only three of them are within the miscible region of <7 $MPa^{1/2}$, and another three between the limits of 7 and 10 $MPa^{1/2}$. In general, a connection between experimental and theoretical results cannot be defined, since the drugs are scattered throughout the graph. Even so, it would be interesting to analyze the blends of each of the drugs with the polymer experimentally in more depth, in order to see if the degree of miscibility of each of them is related to their position in the graph.

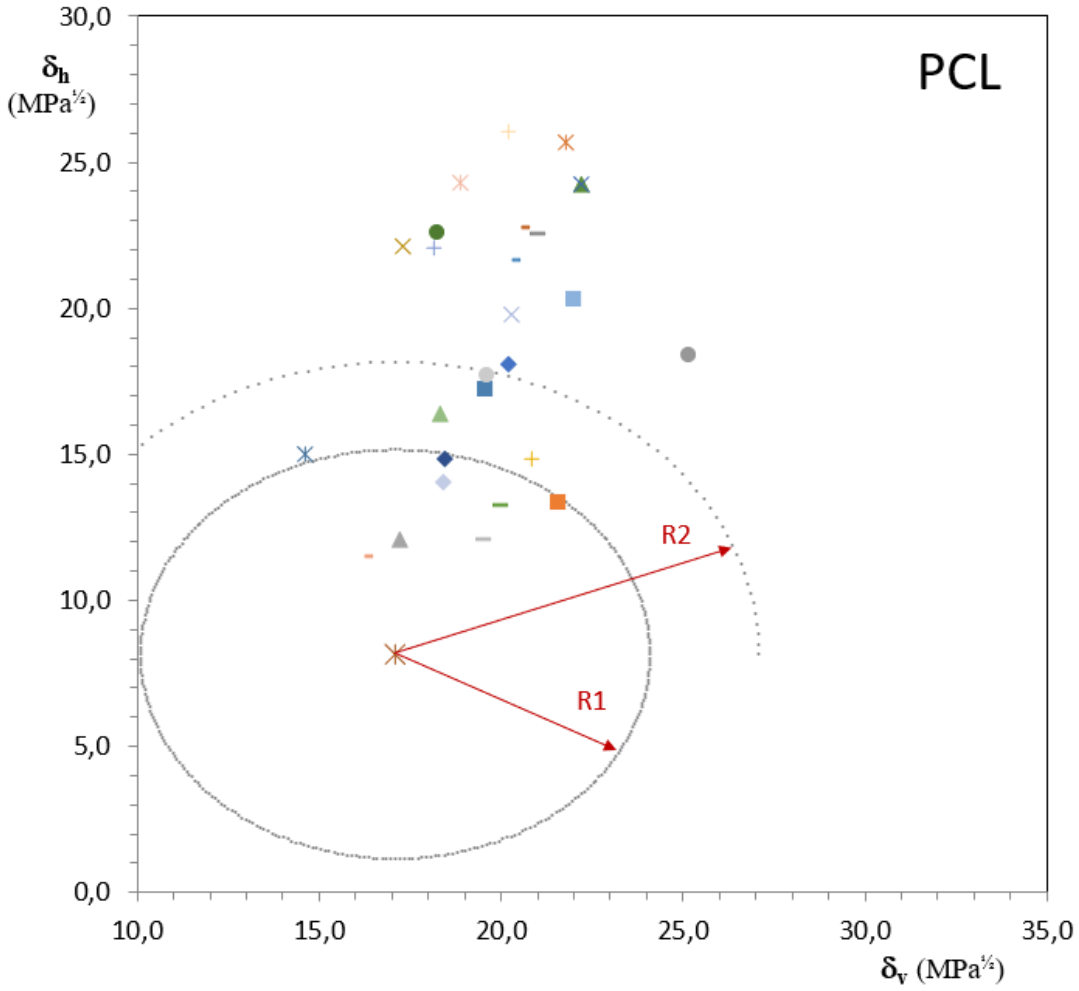

Figure 3a. 7. Bagley plot resulting from the solubility parameters of PCL and the drugs. R1 and R2 correspond to 7 MPa$^{1/2}$ and 10 MPa$^{1/2}$, respectively. The compound corresponding to each symbol can be seen in Table 3a.2.

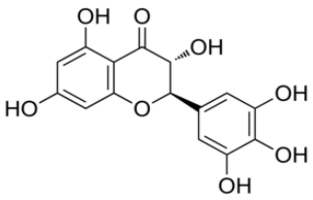

Figure 3a. 8. Dihydromyricetin

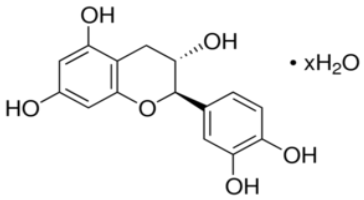

Figure 3a. 9. Catechin hydrate

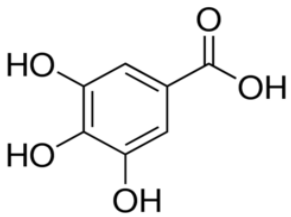

Figure 3a. 10. Gallic acid

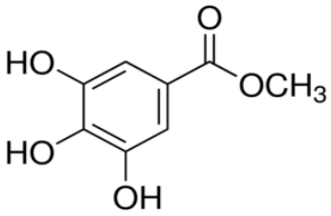

Figure 3a. 11. Methyl-3,4,5-trihydroxybenzoate

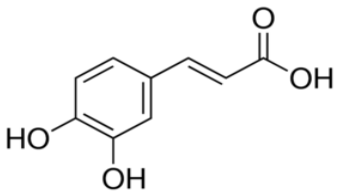

Figure 3a. 12. Caffeic acid

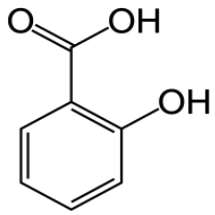

Figure 3a. 13. Salicylic acid

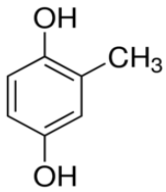

Figure 3a. 14. Methylhydroquinone

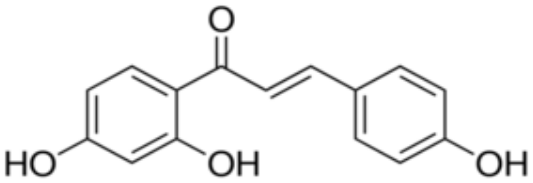

Figure 3a. 15. Isoliquiritigenin

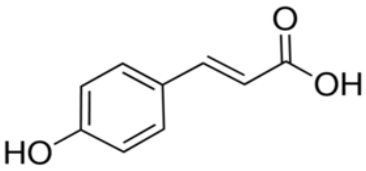

Figure 3a. 16. P-coumaric acid

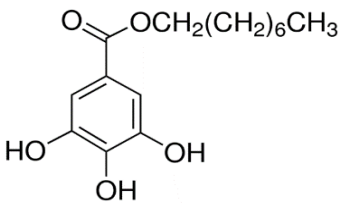

Figure 3a. 17. Octyl gallate

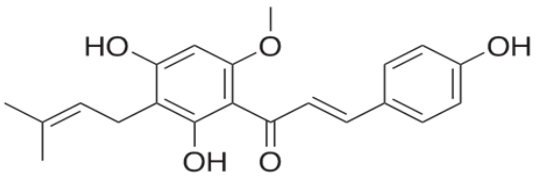

Figure 3a. 18. Xanthohumol

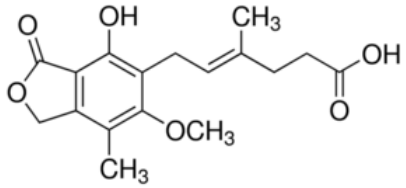

Figure 3a. 19. Mycophenolic acid

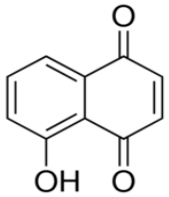

Figure 3a. 20. 5-Hydroxy-1,4-Naphtoquinone

For this work, after seeing both the theoretical and experimental results, it was decided to develop two specific blends: poly (ε-caprolactone)/xanthohumol (PCL/XH) and poly (ε-caprolactone)/mycophenolic acid (PCL/MPA). Regarding drugs, both xanthohumol and mycophenolic acid have been raising great interest lately, and both showed a better miscibility than the rest of the compounds. Apart from working against bacteria, both display remarkable medical properties, which will be explained in the following sections of this chapter. In addition, they are two of the three drugs that are in the miscible region of the Bagley plot, so it is interesting to verify if the theoretically predicted miscibility is fulfilled in both cases. But even if it does, it should be taken into account that these predictions should be applied to liquid blends, so it would be a better approximation if the drugs were in a liquid state, above their melting temperature. However, the temperature difference could also cause wrong results, as theoretical CEDs are valid at room temperature.

3a.4. REFERENCES

[1] E. Sanchez-Rexach, I. Martínez de Arenaza, J. R. Sarasua, and E. Meaurio, "Antimicrobial poly(ε-caprolactone)/thymol blends: Phase behavior, interactions and drug release kinetics," *Eur Polym J*, vol. 83, no. 83, pp. 288–299, Oct. 2016, doi: 10.1016/j.eurpolymj.2016.08.029.

[2] M. A. Altamimi and S. H. Neau, "Drug Development and Industrial Pharmacy Use of the Flory-Huggins theory to predict the solubility of nifedipine and sulfamethoxazole in the triblock, graft copolymer Soluplus", doi: 10.3109/03639045.2015.1075033.

[3] E. Meaurio, N. Hernandez-Montero, E. Zuza, and J. R. Sarasua, "Miscible Blends Based on Biodegradable Polymers," *Characterization of Polymer Blends: Miscibility, Morphology and Interfaces*, vol. 9783527331536, pp. 7–92, Feb. 2015, doi: 10.1002/9783527645602.CH02.

[4] J. A. Baird and L. S. Taylor, "Evaluation of amorphous solid dispersion properties using thermal analysis techniques," *Adv Drug Deliv Rev*, vol. 64, no. 5, pp. 396–421, Apr. 2012, doi: 10.1016/J.ADDR.2011.07.009.

[5] H. Kanno, "A simple derivation of the empirical rule TGTM = 23," *J Non Cryst Solids*, vol. 44, no. 2–3, pp. 409–413, Jun. 1981, doi: 10.1016/0022-3093(81)90047-8.

[6] E. Silva *et al.*, "PDLLA honeycomb-like scaffolds with a high loading of superhydrophilic graphene/multi-walled carbon nanotubes promote osteoblast in vitro functions and guided in vivo bone regeneration," *Materials Science and Engineering: C*, vol. 73, pp. 31–39, Apr. 2017, doi: 10.1016/J.MSEC.2016.11.075.

[7] M. Annunziata, L. Nastri, G. Cecoro, and L. Guida, "The Use of Poly-d,l-lactic Acid (PDLLA) Devices for Bone Augmentation Techniques: A Systematic Review," *Molecules 2017, Vol. 22, Page 2214*, vol. 22, no. 12, p. 2214, Dec. 2017, doi: 10.3390/MOLECULES22122214.

[8] K. Fukushima, J. L. Feijoo, and M. C. Yang, "Comparison of abiotic and biotic degradation of PDLLA, PCL and partially miscible PDLLA/PCL blend," *Eur Polym J*, vol. 49, no. 3, pp. 706–717, Mar. 2013, doi: 10.1016/J.EURPOLYMJ.2012.12.011.

[9] I. Fortelny, A. Ujcic, L. Fambri, and M. Slouf, "Phase Structure, Compatibility, and Toughness of PLA/PCL Blends: A Review," *Front Mater*, vol. 6, p. 206, Aug. 2019, doi: 10.3389/FMATS.2019.00206/BIBTEX.

[10] M. Bartnikowski, T. R. Dargaville, S. Ivanovski, and D. W. Hutmacher, "Degradation mechanisms of polycaprolactone in the context of chemistry, geometry and environment," *Prog Polym Sci*, vol. 96, pp. 1–20, Sep. 2019, doi: 10.1016/J.PROGPOLYMSCI.2019.05.004.

[11] S. Homaeigohar and A. R. Boccaccini, "Nature-Derived and Synthetic Additives to poly(ε-Caprolactone) Nanofibrous Systems for Biomedicine; an Updated Overview," *Front Chem*, vol. 9, p. 1212, Jan. 2022, doi: 10.3389/FCHEM.2021.809676/BIBTEX.

[12] J. Zhou, G. Xie, and X. Yan, *Encyclopedia of Traditional Chinese Medicines - Molecular Structures, Pharmacological Activities, Natural Sources and Applications*, 1st ed. Springer Berlin, Heidelberg, 2011.

[13] E. Meaurio, E. Sanchez-Rexach, E. Zuza, A. Lejardi, A. del P. Sanchez-Camargo, and J. R. Sarasua, "Predicting miscibility in polymer blends using the Bagley plot: Blends with poly(ethylene oxide)," *Polymer (Guildf)*, vol. 113, pp. 295–309, 2017, doi: 10.1016/j.polymer.2017.01.041.

[14] C. M. Hansen, "The universality of the solubility parameter," *Industrial and Engineering Chemistry Product Research and Development*, vol. 8, no. 1, pp. 2–11, Mar. 1969, doi: 10.1021/I360029A002/ASSET/I360029A002.FP.PNG_V03.

[15] F. Meng, V. Dave, and H. Chauhan, "Qualitative and quantitative methods to determine miscibility in amorphous drug-polymer systems," *European Journal of Pharmaceutical Sciences*, vol. 77, pp. 106–111, 2015, doi: 10.1016/j.ejps.2015.05.018.

[16] D. W. van Krevelen and K. te Nijenhuis, *Properties of Polymers: Their Correlation with Chemical Structure; their Numerical Estimation and Prediction from Additive Group Contributions*, Fourth, Co. Amsterdam: Elsevier, 2009. doi: 10.3303/CET1543248.

[17] D. J. Greenhalgh, A. C. Williams, P. Timmins, and P. York, "Solubility parameters as predictors of miscibility in solid dispersions," *J Pharm Sci*, vol. 88, no. 11, pp. 1182–1190, 1999, doi: 10.1021/js9900856.

[18] S. Baghel, H. Cathcart, and N. J. O'Reilly, "Theoretical and experimental investigation of drug-polymer interaction and miscibility and its impact on drug supersaturation in aqueous medium," *European Journal of Pharmaceutics and Biopharmaceutics*, vol. 107, pp. 16–31, 2016, doi: 10.1016/j.ejpb.2016.06.024.

[19] K. Bansal, U. S. Baghel, and S. Thakral, "Construction and Validation of Binary Phase Diagram for Amorphous Solid Dispersion Using Flory–Huggins Theory," *AAPS PharmSciTech*, vol. 17, no. 2, pp. 318–327, 2016, doi: 10.1208/s12249-015-0343-8.

3b. AMORPHOUS SOLID DISPERSIONS IN POLY (ε-CAPROLACTONE)/XANTHOHUMOL BIOACTIVE BLENDS: PHYSICOCHEMICAL AND MECHANICAL CHARACTERIZATION

ABSTRACT

This paper reports the obtention of amorphous solid dispersions (ASDs) of Xanthohumol (XH) into poly (ε-caprolactone) (PCL) containing up to 50 wt% of the bioactive compound in amorphous form thanks to the advantageous specific interactions stablished in this system. The miscibility of the PCL/XH blends was investigated using DSC. The melting point depression analysis yielded a negative interaction parameter indicating the occurrence of favorable inter-association interactions. XRD analyses performed at room temperature agree with the crystallinity results obtained on the heating runs performed by DSC. FTIR spectroscopy reveals strong C=O···O-H specific interactions between the hydroxyl groups of XH and the carbonyl groups of PCL. The AFM analysis of the blends obtained by spin-coating shows the variation of crystalline morphology with composition. Finally, tensile tests reveal high toughness retention for the blends in which XH can be dispersed in amorphous form (containing up to 50 wt% XH). In summary, PCL is a convenient matrix to disperse XH in amorphous form, bringing the possibility to obtain completely amorphous bioactive materials suitable for the development of non-stiff biomedical devices.

3b.1. INTRODUCTION

The successful therapeutic use of medical devices can be compromised by the risk of bacterial infection, that usually begin through biofilm formation. Biofouling is an undesirable process by which harmful microorganisms and their subproducts attach to surfaces, producing extracellular polymers that facilitate adhesion and provide a structural matrix, the so-called biofilm. These biofilms represent a huge risk for public health, as they are responsible for several device-related infections caused by gram-positive or gram-negative bacteria composed biofilms on indwelling medical devices, such as prosthetic heart valves, central venous catheters or urinary catheters, among others [1]–[3]. According to EPINE (Study of the prevalence of nosocomial infections in Spain), urinary infections caused by urinary catheters represent 20.8% of the total nosocomial infections, while vascular catheterization associated bacteremias represent 15.9% [4]. According to World Health Organization (WHO), 8.7% of hospitalized patients present nosocomial infections [5]. Furthermore, biofilms are highly resistant to antibiotic

treatment. Antibiotic therapies can reverse symptoms caused by biofilms, but the sessile population of the biofilm remains, having to remove it surgically from the body. This causes a need for removal of any foreign-body material, in addition to long-term, high-dose antibiotic therapies [6]–[8].

Mimicking the defense mechanisms present in nature has been proposed to prevent bioaccumulation, inhibiting both adhesion and growth of microorganisms [9]–[13]. Within this strategy, the antifouling mechanisms of many plant species have aroused great interest, paying attention to the flavonoids that are obtained from their extracts and essential oils. Flavonoids are part of the defense of plants against external aggressions, and works in which their antifouling properties are investigated have been published recently [14]–[18]. In recent years, the interest in Xanthohumol (XH), a natural polyphenol obtained from *Humulus lupulus* has received growing attention due to its wide spectrum of biological activities with beneficial effects on human health [19]. According to recent studies, it presents anti-inflammatory, antioxidant or anti-cancer properties, among others [19]–[25]. In addition, Xanthohumol displays a broad spectrum of anti-infective activities against different bacteria, such as *Staphylococcus aureus* and *Streptococcus mutans*, with a powerful anti-adherent and antibiofilm activity [26], [27].

Xanthohumol has been reported to inhibit the growth of the Gram-positive bacteria *Staphylococcus aureus* (with a minimal inhibitory concentration MIC of 17.7 μM) and *Streptococcus mutans* (with MIC of 35.3 μM) [28]. Antiviral activity of xanthohumol, in combination with interferon α-2b, was demonstrated against the virus that causes bovine diarrhea (bovine viral diarrhea virus, BVDV E2), which shows considerable similarities with the human hepatitis C virus, and against herpes virus (herpes simplex virus HSV 1 and HSV 2), cytomegalovirus (CMV) and rhinovirus [29]. The xanthohumol concentrations required for antiviral activity (IC_{50}) were in a range of 4.2-7.6 μM. Wang et al. investigated the activity of xanthohumol to suppress several crucial steps in the replication of HIV-1 to treat AIDS patients [30]. A recent review on the antiinfective properties of hop constituents, describes xanthohumol as a broad spectrum anti-infective agent against Gram-positive bacteria, several viruses, fungi (*trichophyton spp.*) and malarial protozoa (*plasmodium falciparum*) [28]. The mechanism/s of the observed inhibitory activities are still under investigation. However, no influence has been

reported on Gram-negative bacteria (e.g. *Escherichia coli*) or the *Candida albicans* fungus [31].

Xanthohumol is a prenylated chalcone, a subclass of the flavonoids family [25]. Flavonoids are sparingly soluble compounds, making difficult their obtention and handling [32]. In particular, the solubility reported for xanthohumol in common organic solvents is about 10 mg/ml in ethanol and 35 mg/ml in DMSO (approx. 1 and 3.5 wt% respectively) [33], [34]. This low solubility could be related to comparatively larger intermolecular crystal forces than in other compounds [35]. A priori, compounds poorly soluble in organic solvents are not good candidates to obtain miscible blends with polymeric materials, since increasing the molecular size decreases the favorable entropic contribution to miscibility. But, on the other hand, polymer matrixes can delay the crystallization process of amorphous drugs in the metastable region of the binary phase diagram, increasing the composition range available to obtain useful ASDs [36]–[38]. Using polymers with high glass transition temperatures may further favor ASD obtention due to the vitrification of the system upon cooling [38]; but this property may hardly allow extending the composition range to the unstable region of the miscibility diagram because glassy systems also evolve with time and the unstable amorphous drug will tend to crystallize [39], [40]. Consequently, miscibility is considered a key requisite to obtain stable enough ASDs for practical applications [41]. Unfortunately, polymer-drug interactions cannot be currently accurately predicted, hence obtaining ASDs is nowadays a trial-and-error effort [42]. Hence, the number of formulations containing drug in the amorphous form that have made it through to the market is limited due to the generally poor physical stability of the amorphous form [39]. This reveals the need of attention in this research area, particularly considering that about 50% of the new molecules discovered are estimated to have solubility problems [41].

In addition, due to its non-polar, highly hydrophobic nature, XH is nearly insoluble in water. Dispensing the drug in the form of an amorphous solid dispersion (ASD) is usually a good strategy to improve its bioavailability [43], [44]. In this paper, poly (ε-caprolactone) (PCL) has been selected as a suitable matrix to disperse Xanthohumol in the amorphous form based on the hypothesis of the occurrence of favorable hydrogen bonding interactions between the OH groups of XH and the C=O groups in PCL (see

Figures 3b.1-2). PCL is a biodegradable semicrystalline polyester, with glass transition temperature located at about -60° C, and melting point at about 60° C. This polymer is suitable for long-term biomedical applications, as the degradation can last from several months to years [45].

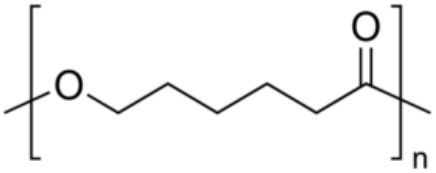

Figure 3b. 1. Poly(ε-caprolactone)

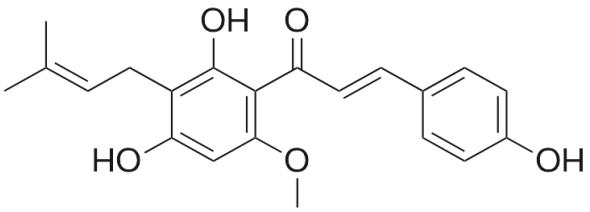

Figure 3b. 2. Xanthohumol

3b.2. EXPERIMENTAL SECTION

3b.2.1. Starting materials

Poly(ε-caprolactone) (PURASORB® PC12 trade name) with an average molecular weight (M_w) of $1.3 \cdot 10^5$ g mol^{-1} and M_w/M_n = 1.76 was purchased from Purac Biochem (The Netherlands). Xanthohumol (purity 98%) was obtained from Chengdu Biopurify Phytochemicals (China) and tetrahydrofuran (THF) was supplied by Labkem.

3b.2.2. Blend preparation

Films were prepared by solvent casting at room temperature from tetrahydrofuran (THF) solutions containing 2.5 wt% of PCL/XH blend.

3b.2.3. Differential Scanning Calorimetry (DSC)

Thermal analyses were conducted on a Modulated DSC Q200 from TA Instruments. All the scans were carried out in hermetic aluminum pans under nitrogen atmosphere with sample weights between 5 and 10 mg. In order to study the glass transition temperatures, two consecutive scans were performed with a scan rate of 20°C/min: the first one from -90°C to 130°C to ensure complete melting of the polymeric phase and the second one from -90°C to 300°C. In the case of neat XH, the sample was heated up to 175ºC during the first scan in order to be able to observe the glass transition heat jump during the consecutive DSC scan with minimal sample degradation. The glass transition temperatures (T_g) were measured in the second scan as the midpoint of the specific heat increment.

3b.2.4. Melting Point Depression

The melting point depression of XH was analyzed in XH-rich blends containing 0-20% PCL. To obtain the melting temperature of XH crystals, samples were heated in the DSC with a scan rate of 1°C/min. Three samples were measured for each composition. No weight loss was observed during the thermal treatments.

3b.2.5. Fourier Transform Infrared Spectroscopy (FTIR)

A Nicolet AVATAR 370 Fourier transform infrared spectrophotometer was used to record FTIR spectra of the blends, averaged over 64 scans in the 400-4000 cm^{-1} range with a resolution of 2 cm^{-1}. Tetrahydrofuran solutions containing 2 wt% PCL/XH blends were cast on KBr pellets by evaporation of the solvent at room temperature. Traces of tetrahydrofuran were removed placing the films into a heated vacuum oven for 24 h. The absorbance of the samples was within the range where Lambert-Beer law is obeyed. Second derivative spectra were smoothed using the Norris-Williams Gap Derivatives using maximum gap sizes and segment lengths of 5 points and 5 cm^{-1} respectively in the derivative transformations.

3b.2.6. Atomic Force Spectroscopy (AFM)

Atomic Force Microscopy was performed using a Nanoscope V controller multimode AFM (Veeco, Santa Barbara, USA). The images were recorded in tapping mode between 0.2 and 2 Hz. Silicon tip on nitride lever cantilevers of 0.4 N m^{-1} with reflective aluminum

back sides (Bruker AXS, Santa Barbara, USA) were used. The image processing was performed using the Nanoscope 9.2 program (Bruker AXS, Santa Barbara, USA).

3b.2.7. X-ray Diffraction (XRD)

To collect the X-ray diffraction patterns a Philips X'pert PRO automatic diffractometer was used, operating at 40 kV and 40 mA, in theta-theta configuration, secondary monochromator with Cu-Kα radiation (λ = 1.5418 Å) and a PIXcel solid state detector (active length in 2θ 3.347°). Data were collected from 4 to 70° 2θ (step size 0.026 and time per step = 72.42 s) at room temperature. A fixed divergence and antiscattering slit giving a constant volume of sample illumination was used.

3b.2.8. Tensile tests

Tensile tests were carried out in an Instron 5565 universal testing machine at a crosshead displacement rate of 5 mm/min at room temperature. Specimens 60 mm length and 10 mm wide were cut from films of 80 μm average thickness. Young's modulus (E), yield stress (σ_y) and strain at break (ε_b) were determined as the mean value of at least four determinations. Data were subjected to one-way analysis of variant (ANOVA) with the level of significance set at $p < 0.05$.

3b.2.9. In Vitro Release Studies (UV-Vis)

UV–Vis absorption spectra were recorded using a Perkin Elmer Lambda 265 UV-Visible spectrophotometer. Before performing the drug release experiments, a calibration curve was obtained measuring the absorbance at a wavelength of 370 nm for solutions of xanthohumol in 0.1 M PBS (pH 7.4) with concentrations ranging from 1 to 15 ppm. Three PCL/XH systems containing 2, 5 and 10 wt% XH were measured in triplicate using samples of about 3 mg (containing about 60, 150 and 300 μg XH) obtained by solvent casting. Samples were immersed in 4 ml of 0.1 M PBS buffer at 37º C. At fixed time intervals of 15 min., the whole solution was replaced with fresh one, and the solution taken out was used to measure the drug concentration by UV spectroscopy using the calibration curve.

3b.3. RESULTS AND DISCUSSION

3b.3.1. Miscibility analysis by DSC according to single glass transition criterion

When two components are miscible, the blend is expected to show a single glass transition temperature (T_g) located between the T_gs of the neat materials, which is expected to change progressively with composition [46], [47]. On the contrary, more than one single value could be detected if there is a separation into individual amorphous phases within the system. Figure 3b.3. shows the second scan DSC traces for PCL, XH and their blends. As can be seen, the glass transition temperature of pure XH is located at about 71°C, while the T_g of pure PCL occurs at about -62° C. All the PCL/XH blends show single intermediate glass transition temperatures, indicating miscibility in the amorphous phase in the whole composition range.

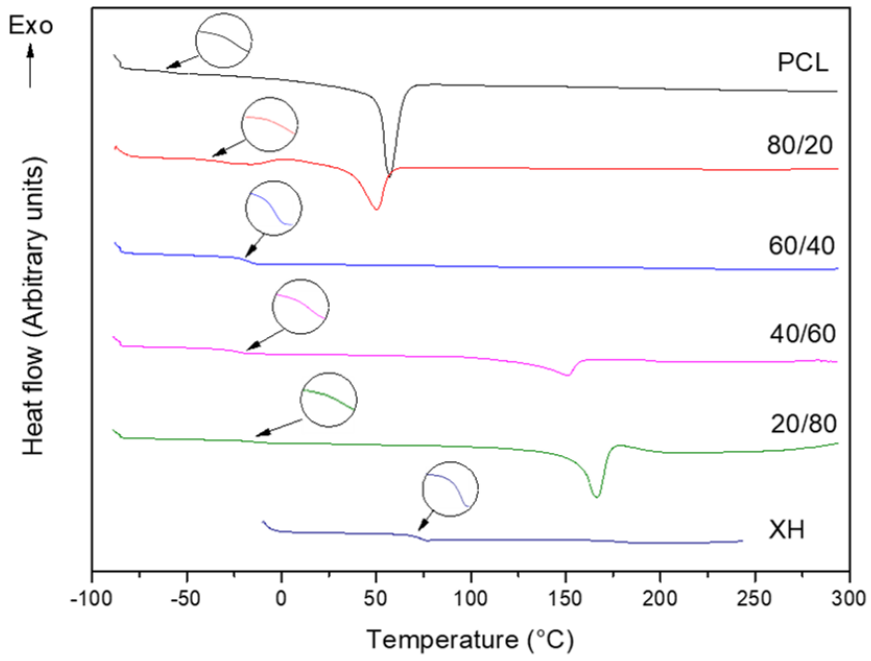

Figure 3b. 3. Second scan DSC traces for PCL, XH and PCL/XH blends.

Different methods, such as Gordon-Taylor (GT), Couchman-Karasz (CK) or Fox equations, have been employed to predict the glass transition temperature of amorphous binary systems. Particularly, the Gordon-Taylor equation was derived assuming ideal solution behavior; and considering also equal densities, the widely used Fox equation (Eq. (3b.1)) can be derived [48]:

$$\frac{1}{T_{gb}} = \frac{w_1}{T_{g1}} + \frac{w_2}{T_{g2}} \quad \text{(3b.1)}$$

where w_1 and w_2 are the weight fractions of components 1 and 2 respectively, T_{g1} and T_{g2} are the glass transition temperatures of the pure components, and T_{gb} is the glass transition temperature of the blend. As can be seen in Figure 3b.4., in the 0-40 XH wt% range the experimental values are close to the values predicted by the Fox law, while at higher XH concentrations the experimental T_gs lie below the predicted values. This behavior can be rationalized considering that XH is completely dissolved in the PCL rich blends, while partial XH crystallization occurs in the XH rich blends (see also Fig.3b.3) [46].

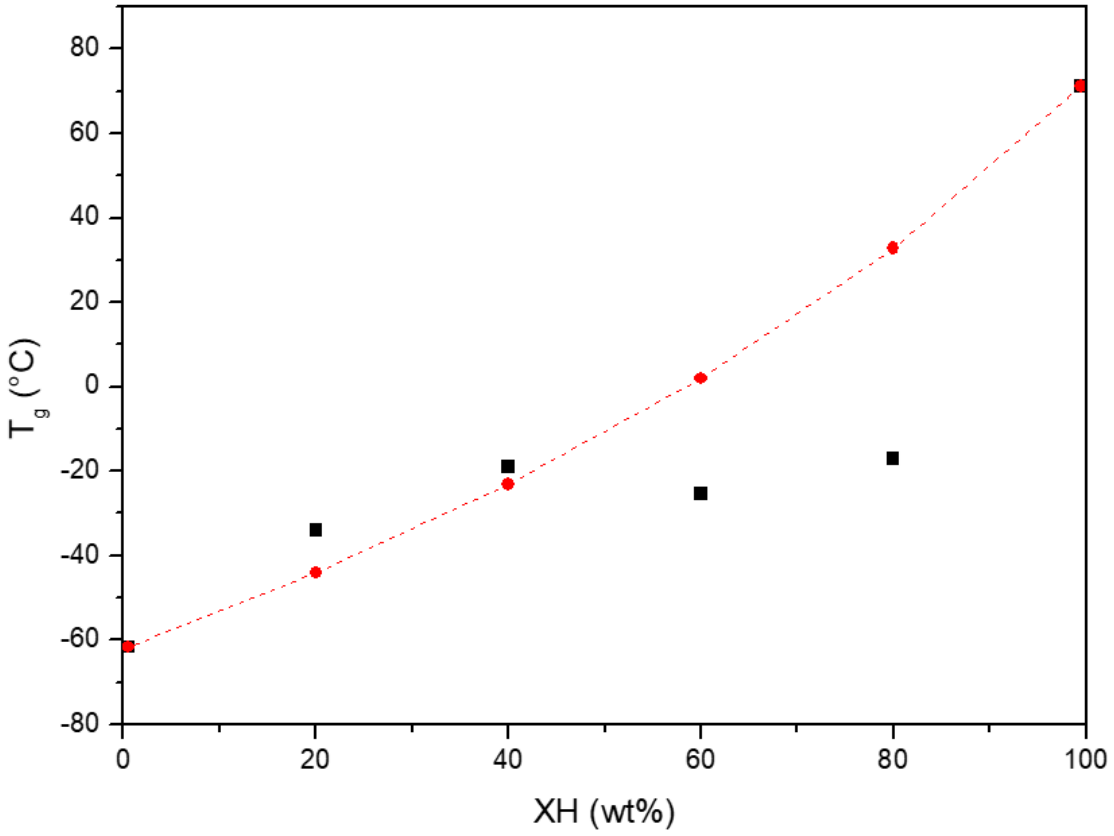

Figure 3b. 4. Glass transition temperature *versus* composition for the PCL/XH system: (■) experimental values (♦) Fox equation.

3b.3.2. Melting Point Depression Analysis

Table 3b.1. lists the melting properties of the pure components investigated in this work. As can be seen, PCL is a semicrystalline polymer melting at about 57°C, in good agreement with the values reported in the literature [45], [49]. However, the DSC scans performed on XH reveal an unusually large melting temperature dependence on heating rate, since its melting temperature increases by about 20°C when the heating rate increases from 1°C/min to 20°C/min. A revision of the literature also reveals a broad range of melting temperatures reported for XH, ranging from 148°C to 172°C [50]–[53]. The dependence of melting temperature on heating rate is typical of compounds exhibiting "apparent melting", a new term proposed by Lee et al. [54] to distinguish the loss of crystalline structure caused by kinetic processes (e.g., thermal decomposition, dehydration, and chemical interactions/reactions) from that caused by thermodynamic melting. The apparent melting of sucrose (and other related compounds) was initially attributed to the kinetic process of thermal decomposition [54], but Magoń et al. [55] have recently shown it to be actually due to superheating. The melting of crystalline sucrose was found to be kinetically slow and under heating rates faster than equilibrium conditions the melting of crystals occurred at higher temperatures [55]. A similar behavior is observed in this work for XH. Even though degradation of XH to isoxanthohumol can occur upon melting [50], our samples did not show weight loss or decoloration during the DSC experiments, and similarly to sucrose, the observed dependence of melting temperature with heating rate can be attributed to the superheating of the XH crystals. The recommendation to obtain the equilibrium transition parameters for this type of compounds is to perform extrapolations to zero heating rate [55]. In any case, superheating is reduced with decreasing heating rate, hence only the measurements performed at sufficiently low heating rate (1°C/min) will be used to analyze the melting point of XH in this section [56], [57].

Table 3b. 1. Melting properties of PCL and XH obtained from the first heating scans.

Compound (scan rate)	T_m *(°C)*	ΔH_m *(J/g)*
PCL	57.0	81
XH (20ºC/min)	173.2	121
XH (1ºC/min)	153.1	80

The melting point depression method, derived from the Flory-Huggins Theory, provides a thermodynamic description of the miscibility between two components. Essentially, a pure component melts when the entropic contribution ($T\Delta S_m$, arising from the increase in entropy upon melting) equals the enthalpic contribution (ΔH_m, arising from reduced intermolecular interactions in the liquid phase). However, in the presence of a second miscible component in liquid form, there is an additional entropic contribution arising for the combinatorial entropy, and an additional enthalpic contribution arising from intermolecular interactions with the second component. Both contributions shift the melting temperature of the pure component [58]. The Flory's relationship for the depression of the equilibrium melting point, ΔT_m, is (Eq. (3b.2)):

$$\frac{1}{T_m}-\frac{1}{T_m^0} = \frac{-R}{\Delta H_{2u}}\frac{V_{2u}}{V_{1u}}\left(\frac{\ln \phi_2}{m_2} + \left(\frac{1}{m_2} - \frac{1}{m_1}\right)\phi_1 + \chi_{12}\phi_1^2\right) \quad \text{(3b.2)}$$

where T_m^0 is the equilibrium melting point of the pure crystallizable component and T_m is the equilibrium melting point of its blends, the subscripts 1 and 2 refer to the amorphous and crystallizable components respectively. R is the universal gas constant, while ΔH_{2u} is the heat of fusion per mole of crystalline repeat units. V_u is the molar volume of the repeating unit, m is the degree of polymerization, ϕ is the volume fraction, and χ_{12} is the interaction parameter.

In order to analyze the melting point depression of XH (component 2) applying (Eq. (3b.2)), the molar volume of the lattice sites can be considered as the molar volume of XH ($V_2 = 285.8$ cm^3/mol, estimated from its crystalline density), and consequently $m_2 = 1$. To further simplify the equation, the same volume can be taken as the molar volume of the polymeric repeat unit ($V_2 = V_{1u}$). Since $m_1 = V_{pol}/V_{1u}$ is large, $1/m_1 \approx 0$. As a result, (Eq. (3b.3)) reduces to:

$$\frac{1}{T_m}-\frac{1}{T_m^0} = \frac{-R}{\Delta H_2}(\ln \phi_2 + \phi_1 + \chi\phi_1^2) \quad \text{(3b.3)}$$

where the first two terms in the right-hand side of (Eq. (3b.3)) represent the mixing entropy contribution to ΔT_m, and the third term the mixing enthalpy contribution. Substituting typical numbers for a polymer-monomer system in (Eq. (3b.3)), it is easy to show that the entropic term only accounts for a small depression (usually about 1–2°C) [44].

The average melting point of pure XH obtained at low heating rate (1°C/min) is $T_m^0 = 153.1$°C. The melting point decreases by about 5°C when 20 wt% PCL is added. Considering the average melting enthalpy of pure XH (ΔH_{XH} = 80 J/g), (Eq. (3b.4)) has been used in Figure 3b.5. to obtain the interaction parameter from the slope of the plot, χ = -1.3. This value confirms a thermodynamically miscible system, since negative values for the interaction parameter indicate an exothermic process, as expected when the interassociation interactions are stronger than the autoassociation interactions [58]. Additionally, it is possible to calculate the interaction energy density, B, at the melting temperature of XH according to (Eq. (3b.4)):

$$\chi = \frac{BV_r}{RT} \tag{3b.4}$$

where V_r is a reference volumen ($V_r = V_2 = 285.8$ cm^3/mol), yielding $B = -16$ J/cm^3.

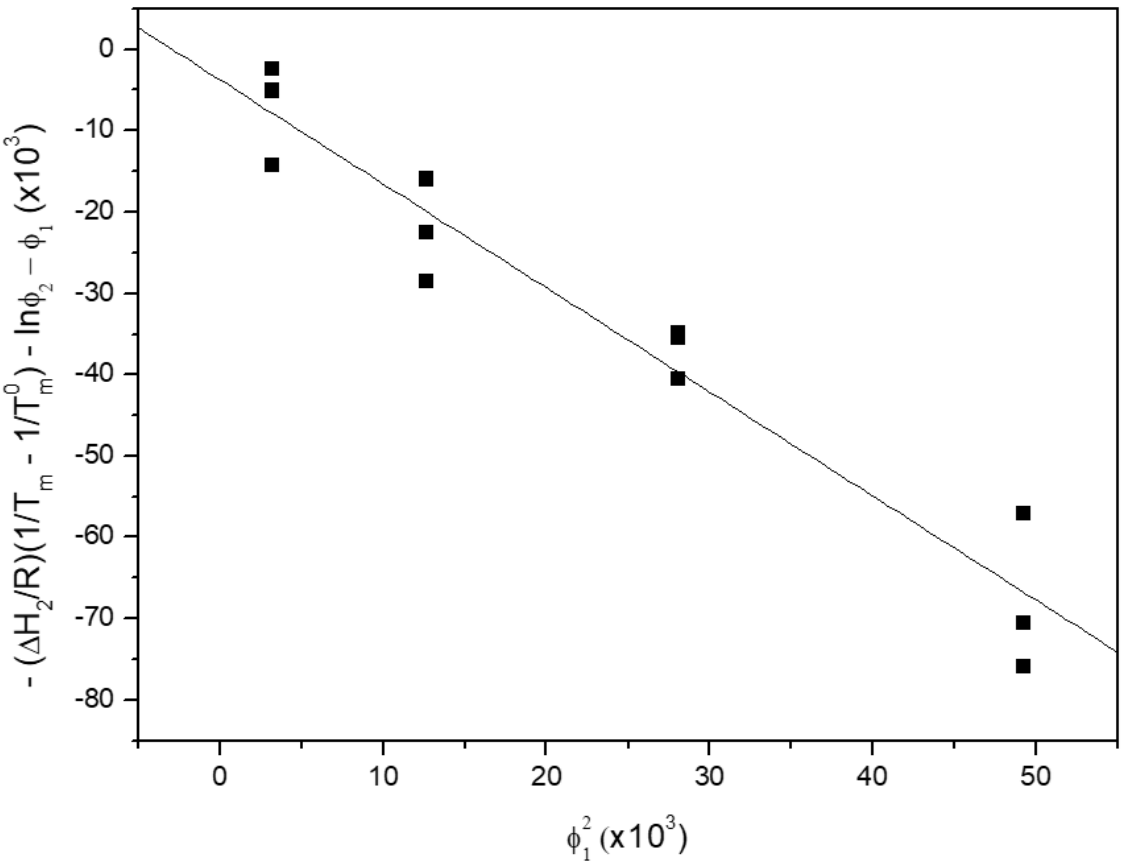

Figure 3b. 5. Analysis of the melting temperature of XH according to (Eq. (3b.3)) for the PCL/XH system. The slope of the plot gives the interaction parameter χ = -1.3.

3b.3.3. FTIR analysis of PCL/XH blends

Hydrogen bonding interactions between the hydroxyl groups of XH and the carbonyl groups of PCL can be expected considering the chemical structures of the species investigated in this paper (see Figures 3b.1-2), hence, the occurrence of specific interactions has been investigated by infrared spectroscopy. Figure 3b.6 shows the ester carbonyl stretching region of the pure components and their blends at room temperature (notice that the absorption region corresponding to the aromatic ketone present in XH occurs at lower wavenumbers and is not displayed in Fig. 3b.6.). The spectrum of pure PCL shows a peak at 1725 cm^{-1} attributable to crystalline PCL and a shoulder at 1735 cm^{-1} representing the amorphous phase [59]. As can be seen, blending with XH results in the occurrence of a new band located at about 1703 cm^{-1}, attributable to hydrogen bonded C=O groups in PCL[34]. The observed red shift (~32 cm^{-1}) is larger than those reported for blends of PCL with thymol [44] or chloramphenicol [60] (~25 cm^{-1}) indicating stronger hydrogen bonding interactions.

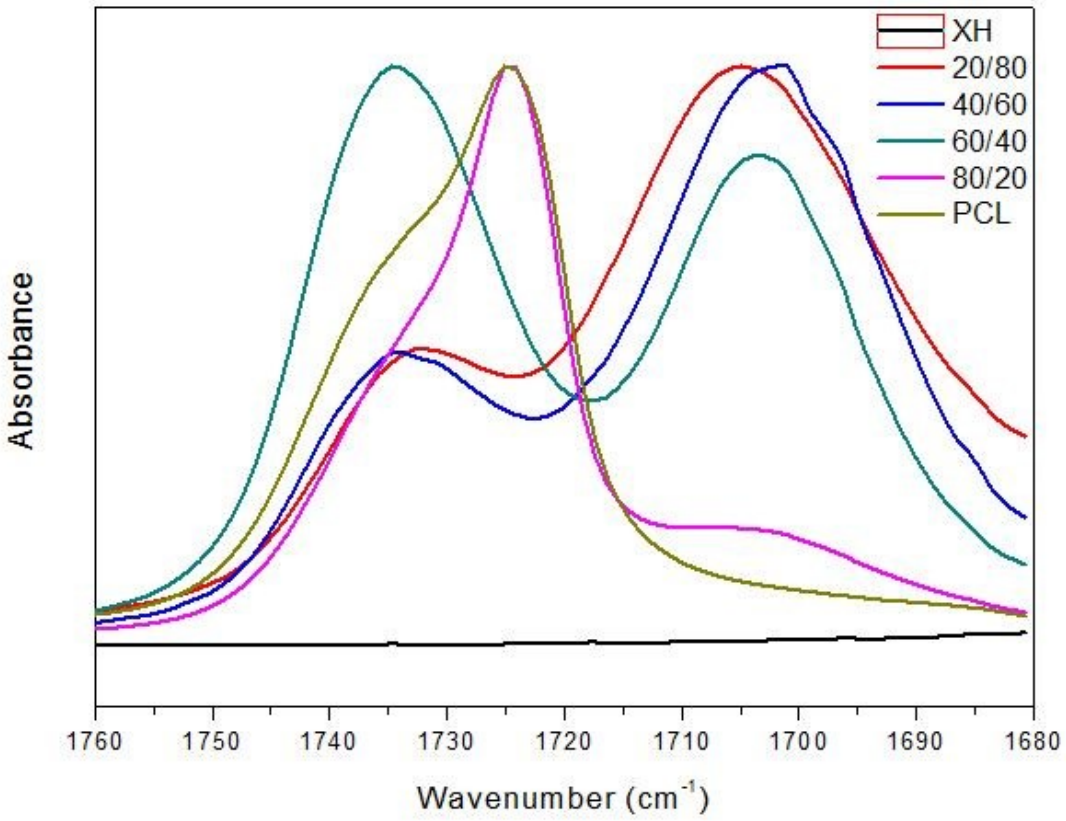

Figure 3b. 6. Carbonyl stretching region for pure PCL and XH and PCL/XH blends of different composition.

Figure 3b.7. displays the hydroxyl stretching region of PCL and PCL/XH blends. The spectrum of pure XH shows a very broad band, attributable to the overlap of bands corresponding to different hydrogen bonding interactions. The typical location reported for pure completely dry XH, about 3300 cm^{-1} [61] indicates the occurrence of cooperative O-H···O-H interactions [60], though the actual location observed can be affected by residual water or other compounds that may cocrystallize with the pure compound [62], [63]. As can be seen, the addition of PCL to XH shifts the band to higher wavenumbers, up to about 3350 cm^{-1} as the PCL content in the blend increases. Shifting to higher wavenumbers is usually attributed to the replacement of the cooperatively strengthened hydroxyl-hydroxyl interactions by the weaker hydroxyl-carbonyl interactions absorbing at higher wavenumbers [60], [64].

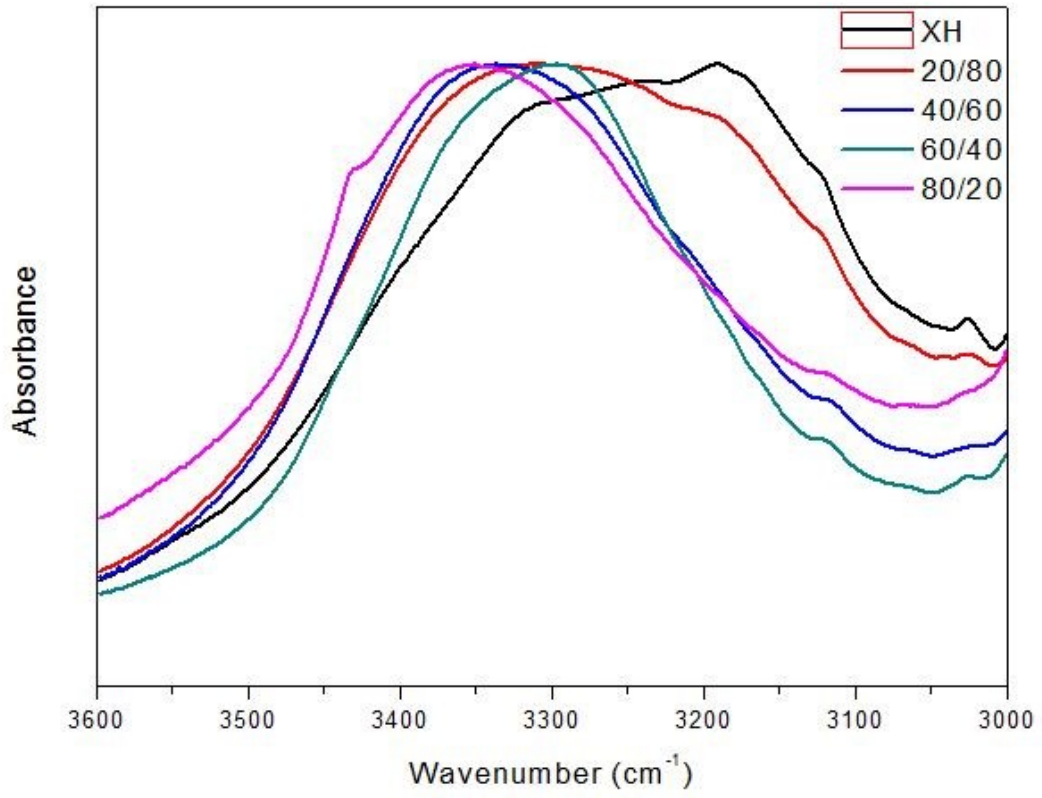

Figure 3b. 7. Hydroxyl stretching region for pure XH and PCL/XH blends of different composition.

3b.3.4. Crystallization Behavior Based on the X-ray Diffraction Analysis

The XRD patterns of the pure components are shown in Figure 3b.8.. XH exhibits characteristic peaks at 2θ = 5.8° and 7.7° with several peaks between 11° and 28°, while the characteristic peaks of PCL occur at 2θ = 21.7° and 24°. As can be seen, the intensity of the crystalline peaks of XH decreases with the addition of PCL. The same behavior is observed for the PCL peaks upon increasing the XH content. For the PCL/XH 60/40 composition, the material is an homogeneous, single phase blend. If the XH content is increased to 50 wt%, the XRD diffraction pattern shows a weak, broad peak centered at about 2θ = 6.6°, shifted form the locations corresponding to the pure XH crystals. This suggests that at this composition XH is still unable to form fully developed crystals, and the peak arises from small ordered regions intimately connected to the surrounding amorphous matrix [24]. Further increase of the XH content to 60 wt% results in the occurrence of a fully developed second phase consisting of pure XH crystals, though the mass fraction corresponding to this second phase is still small according to the intensity of the crystalline peaks.

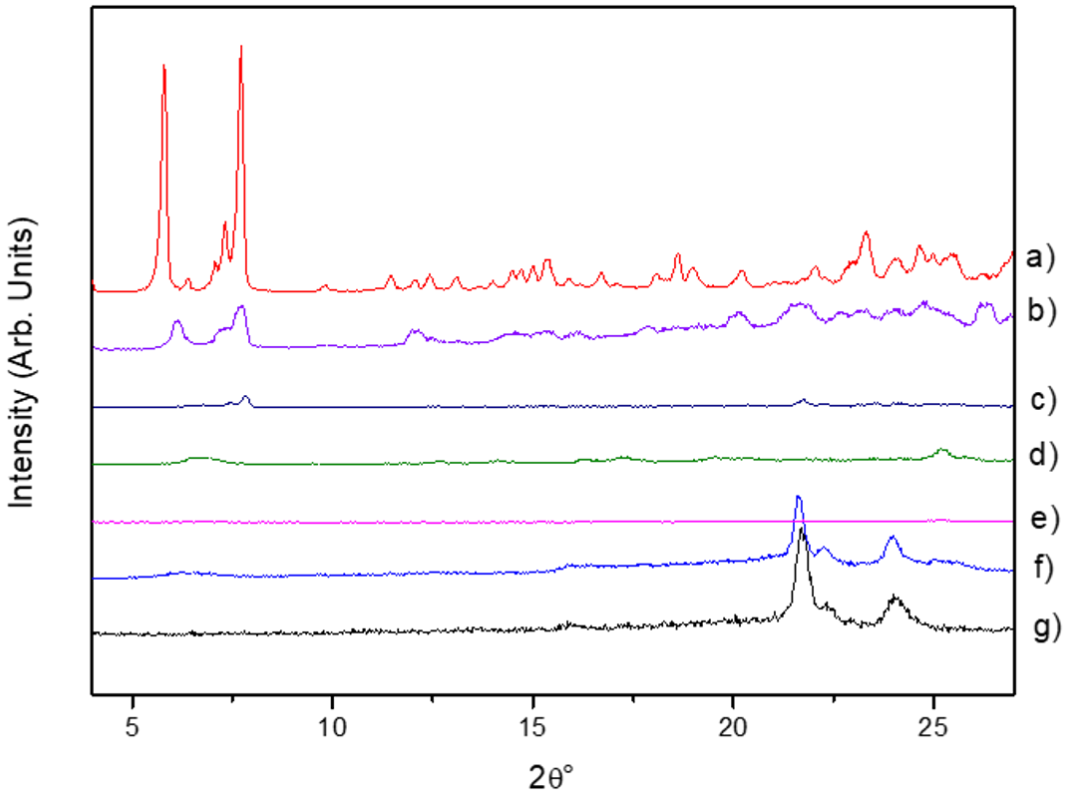

Figure 3b. 8. XRD patterns of: a) pure XH; b) PCL/XH 30/70; c) PCL/XH 40/60; d) PCL/XH 50/50; e) PCL/XH 60/40; f) PCL/XH 70/30 and g) pure PCL.

3b.3.5. AFM Analysis

Figure 3b.9. shows topographic images of thin films (400 nm) of pure PCL and PCL/XH blends of different composition obtained by Atomic Force Microscopy. As can be seen, pure PCL shows the characteristic spherulitic morphology of semicrystalline polymers. Upon addition of 20 wt% XH, spherulitic boundaries become less defined, and the crystalline phase shows a looser, less compact morphology, indicating that crystallization of PCL in the presence of XH creates a XH enriched amorphous phase that is displaced by the growing crystallites to the interlamellar region and to the spherulitic grain boundaries [65]. On the other hand, the PCL/XH 40/60 system shows discrete XH crystals dispersed in a smooth and homogeneous film. In case of the intermediate PCL/XH 60/40 composition, the topographic images obtained lack any crystalline morphology in agreement with the XRD analysis, but show a rough surface that suggests the occurrence of compositional heterogeneities attributable to a metaestable composition [66]. The analysis of the long term stability of this system is, however, beyond the scope of this paper.

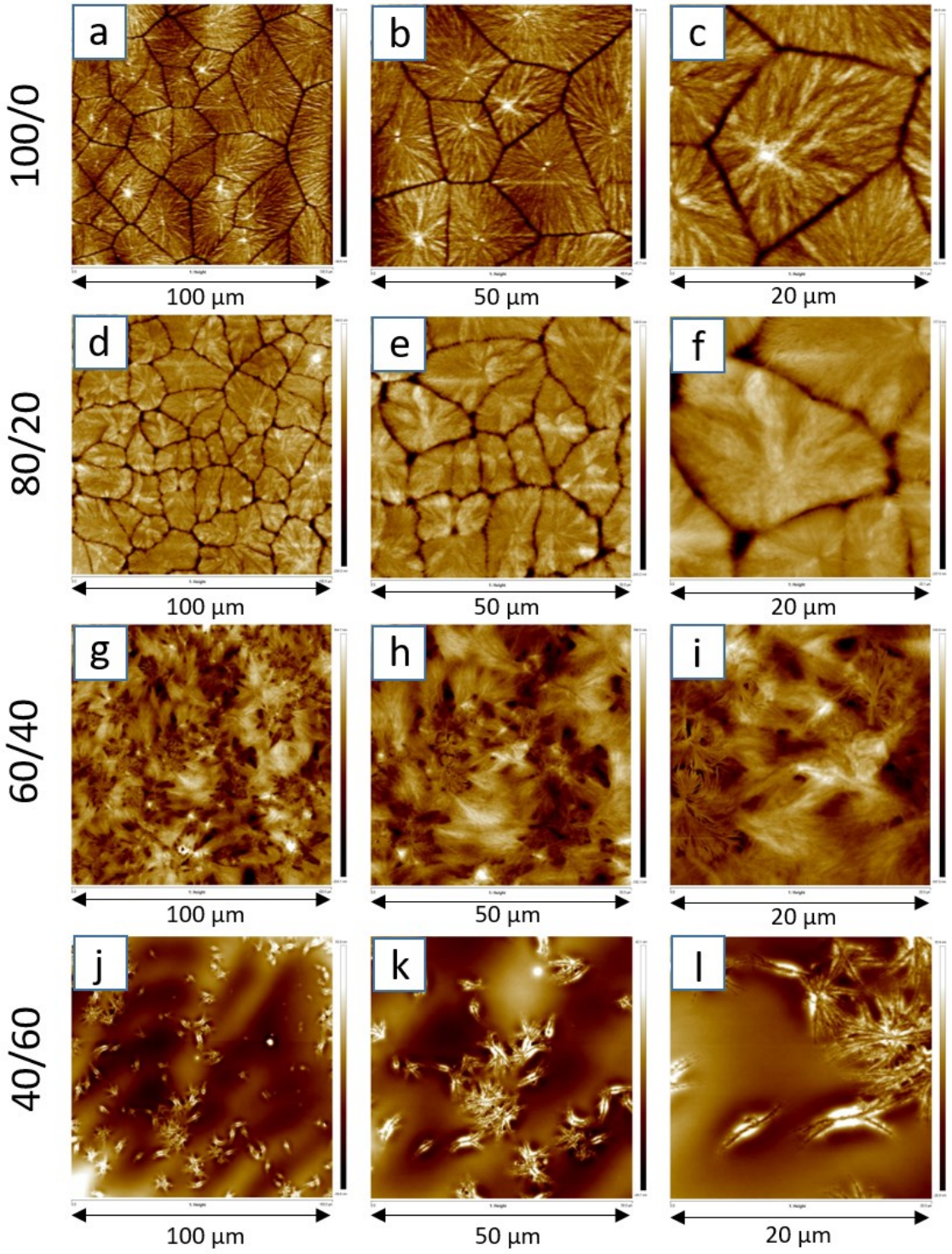

Figure 3b. 9. AFM topographic images for pure PCL and PCL/XH blends of different compsition.

3b.3.6. Tensile Behavior

The tensile behavior of PCLs is strongly dependent on molecular weight [67]. PCL oligomers (M_w below several thousands) are brittle and waxy, but both ductility and tensile modulus increase with increasing molecular weight [68]. Low molecular weight PCLs (M_w from 10^4 to a few tens of thousands) are soft and show increased ductility, while high molecular weight PCL achieves mechanical properties comparable to linear polyethylenes, reaching Young's modulus E = 700 MPa and elongation at break in the 700-1000% range [67], [69]. Figure 3b.10. shows the tensile curves obtained for the high molecular weight PCL sample investigated in this work and its blends containing up to 60 wt% XH. As can be seen, the tensile curves of the blends lie below that of pure PCL, indicating that the addition of XH reduces the resistive properties of the blends. This behavior should be attributed to the suppression of the crystallinity of PCL occurring upon the addition of XH rather than to a plasticizing effect, since the addition of XH actually increases the glass transition of the blends. Interestingly, the blends retain high ductilities within the composition range in which XH is dispersed in amorphous form. For example, adding 50 wt% XH to PCL reduces the strain at break from ε_b = 595 ± 25 % to ε_b = 374 ± 7 %, hence the films retain nearly 2/3 of the ductility in spite of containing half the polymer. However, a strong reduction of ductility is observed when the XH content increases further to 60 wt% (ε_b = 135 ± 21 %). The strong reduction of ductility observed upon increasing the XH content from 50 wt% to 60 wt% cannot be explained only in terms of the lower polymer content of the latter. In this case, the presence of a disruptive second crystalline phase in the sample containing 60 wt% XH must be considered as an additional detrimental effect.

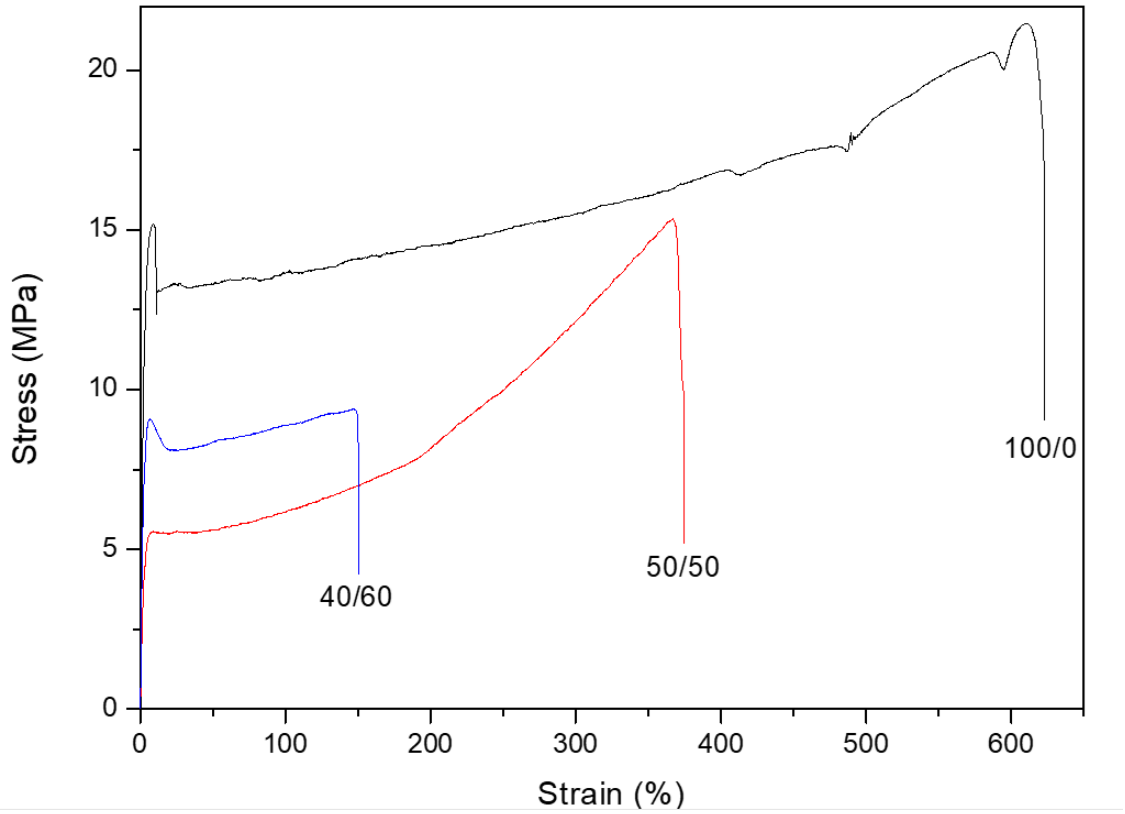

Figure 3b. 10. Tensile tests for the PCL/XH blends.

Figures 3b.11-12 show the Young's modulus and the yield stress for pure PCL and its blends with XH of different composition. The Young's modulus for the pure PCL used in this work is 686 ± 2 MPa (see Fig. 3b.11), in good agreement with values reported in the literature [60]. As can be seen, the addition of XH to PCL halves the stiffness of the films. In addition, the yield strength of pure PCL (15.4 ± 0.7 MPa, see Fig. 3b.12) is also halved upon the addition of XH. A dependence on composition cannot be established for these parameters from our results. In any case, the analysis of the mechanical properties shows that soft, flexible PCL/XH blends can be developed, particularly by considering also the possibility of tuning the molecular weight of PCL to achieve the desired mechanical properties.

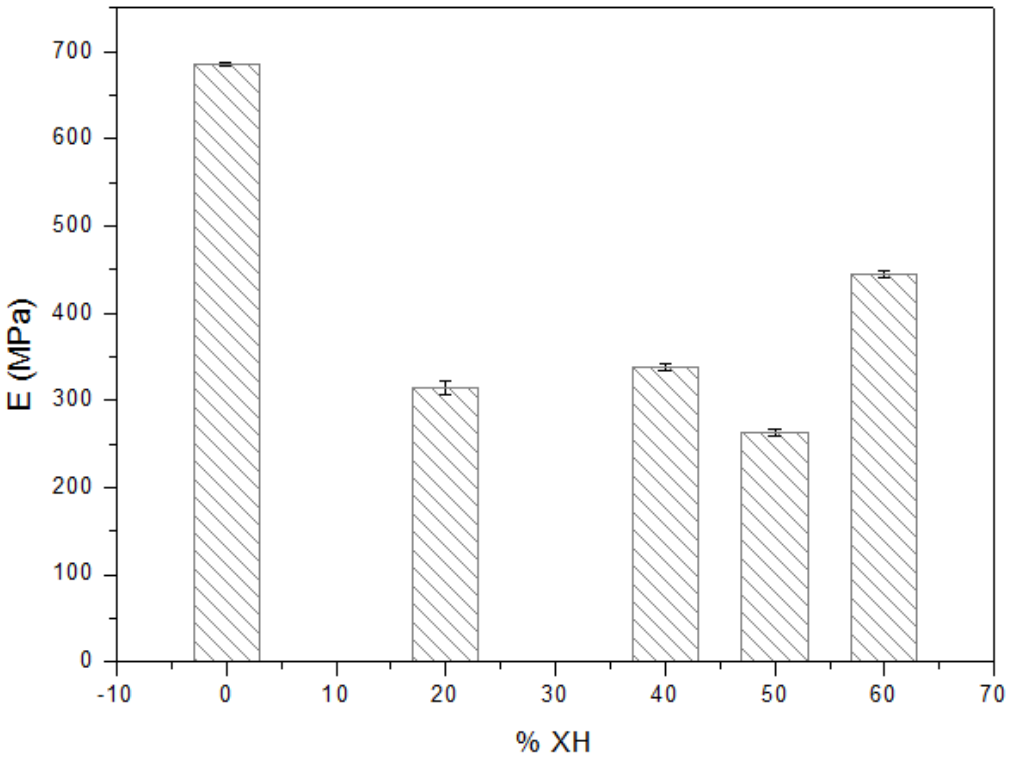

Figure 3b. 11. Young's modulus for PCL and PCL/XH blends.

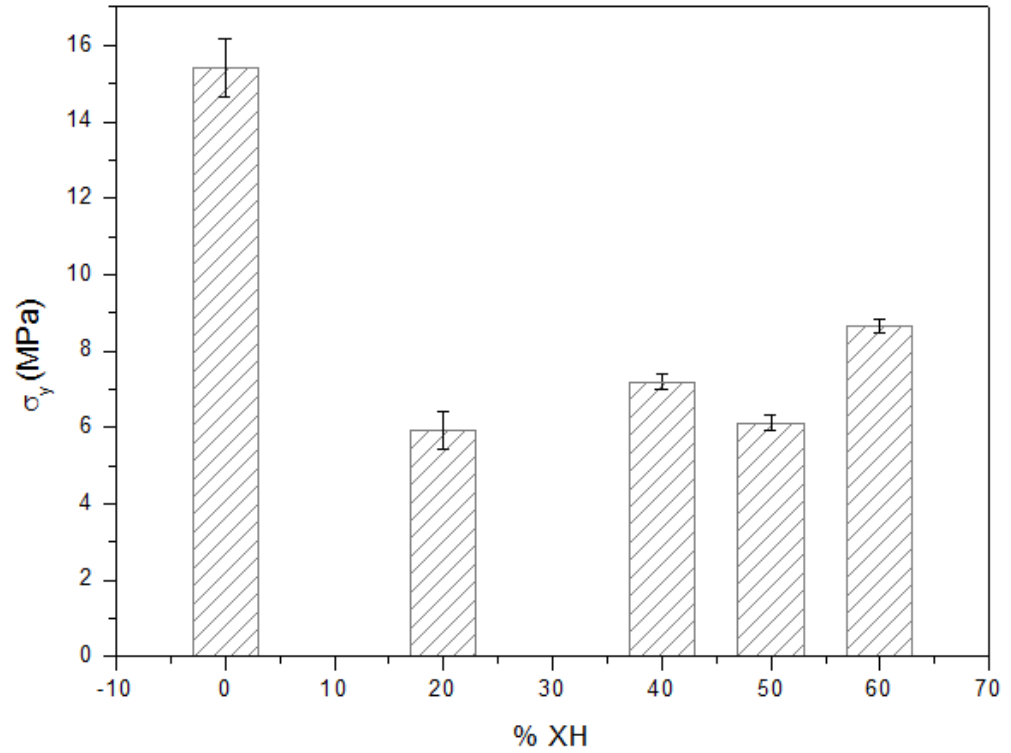

Figure 3b. 12. Yield stress values for PCL and PCL/XH blends.

Table 3b. 2. Statistical analysis results for the mechanical properties.

XH wt%	YOUNG'S MODULUS		YIELD STRENGTH	
	Average modulus (MPa)	Standard deviation	Average Yield strength (MPa)	Standard deviation
0	685.8	±2.0	15.4	±0.7
20	314.9	±8.3	5.9	±0.5
40	338.5	±4.6	7.2	±0.2
50	263.3	±3.1	6.1	±0.2
60	444.7	±3.9	8.6	±0.2

3b.3.7. Drug Release Behavior

As indicated in the introduction, XH is virtually insoluble in water due to its non-polar, highly hydrophobic nature. The solubility reported in aqueous media is 1.3 mg/L (about 1.3 ppm) at 23°C [70]. Such a low value limits its bioavalavility and makes difficult handling XH to perform both *in vivo* and *in vitro* pharmacological studies [62]. Hence, solubility and drug release studies have been usually carried out in 50:50 (v/v) ethanol–water solution, where the solubility of XH increases to 7.6 mg/L [62].

In an attempt to stick as close as possible to the physiological conditions, release experiments have been carried out in 0.1 M PBS (pH 7.4) medium. To avoid the precipitation of XH (usually occurring when the solutions reach the unstable region of the phase diagram), the total XH concentration has been limited by removing the whole solution before each addition of fresh PBS medium. Figure 3b.13 shows the *in vitro* drug release profiles for the PCL/XH blends containing 2, 5 and 10 wt% XH. As can be seen, in the experimental conditions chosen for this analysis, all the samples show quasi-linear release profiles, and the whole drug was released in short time lapses, of about 1 hour, 3 hours and 4.5 hours respectively. The XH released in each step reached 50 µg (in 4 ml of PBS solution), hence, XH concentrations of about 12 mg/L were achieved without precipitation in the release experiments. Both the larger XH concentrations and the short release times indicate that releasing from PCL/XH ASDs should increase the bioavailability of the drug.

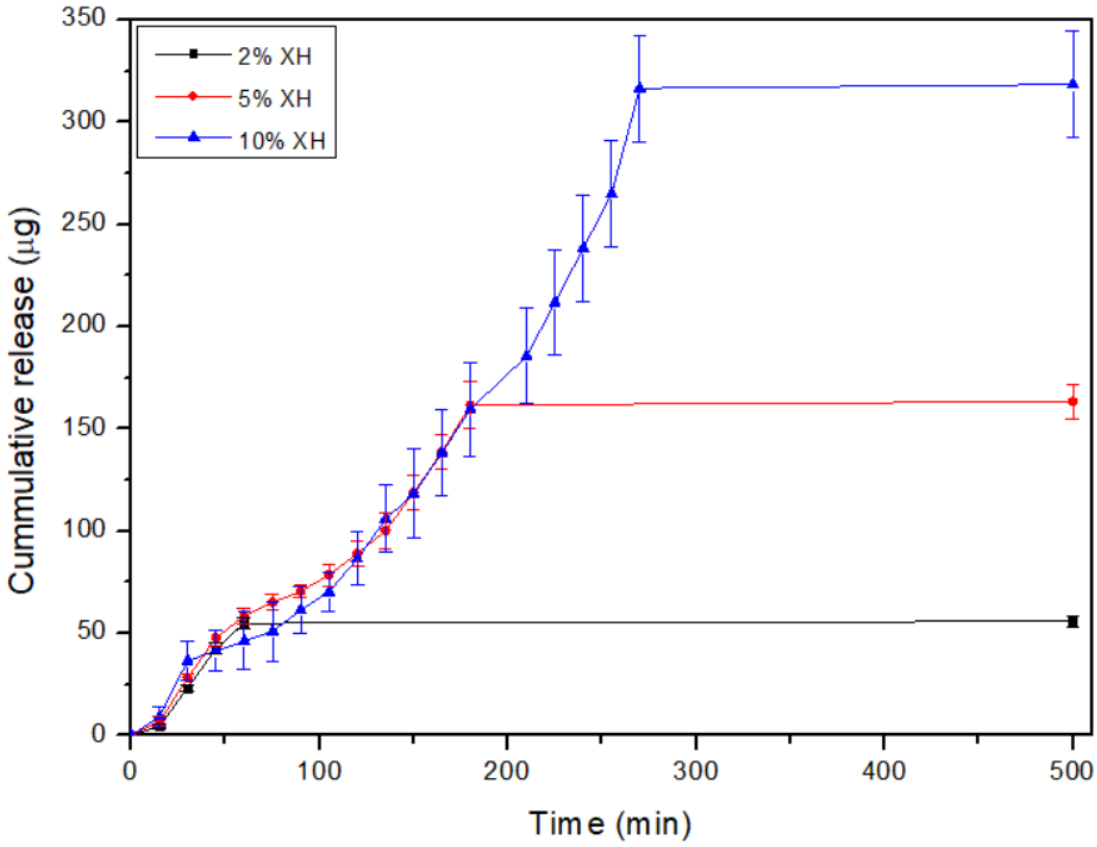

Figure 3b. 13. Drug release profiles of PCL/XH films containing 2, 5 and 10 wt% XH immersed into 0.1 M PBS buffer at 37º C.

3b.4. CONCLUSIONS

Miscibility is observed in the PCL/XH system according to the intermediate glass transition temperature criterion. The analysis of the melting point depression of the XH crystals results in a negative interaction parameter, χ = -1.3, indicating favorable interactions between the polymer and the bioactive molecule. Crystallization is suppressed for both PCL or XH in the presence of the second component. In fact, the PCL/XH 60/40 blend is completely amorphous according to both the DSC and X-Ray diffraction pattern analyses. PCL can be loaded with XH contents up to 50 wt% to obtain amorphous solid dispersions (ASDs) of the bioactive molecule.

The analysis by FTIR spectroscopy for the PCL/XH blends shows new bands in the C=O stretching region attributable to C=O···H-O interactions between the carbonyl groups of PCL and the hydroxyl groups of XH. In addition, the hydroxyl stretching band of XH shifts

to higher wavenumbers in the presence of PCL indicating the replacement of the cooperative H-O···H-O autoassociation interactions by C=O···H-O interassociation interactions.

The analysis of the spherulitic morphology of the blends by AFM shows that the addition of XH to PCL results in less defined spherulites, showing a looser, less compact morphology, characteristic of miscible systems. Tensile tests indicate that the resistant properties of PCL are reduced upon the addition of XH, but the materials maintain high ductilities even in the presence of XH contents up to 50 wt%. The PCL/XH system shows interesting properties for the development of biomedical devices based on soft materials.

3b.5. REFERENCES

[1] R. M. Donlan, "Biofilms: Microbial life on surfaces," *Emerg. Infect. Dis.*, vol. 8, no. 9, pp. 881–890, 2002, doi: 10.3201/eid0809.020063.

[2] R. M. Donlan, "Biofilms and device-associated infections," *Emerg. Infect. Dis.*, vol. 7, no. 2, pp. 277–281, 2001, doi: 10.3201/eid0702.010226.

[3] S. Aiola, G. Amico, P. Battaglia, and E. Battistelli, "The Large-Scale Polarization Explorer (LSPE)," *Clin. Microbiol. Rev.*, vol. 15, no. 2, pp. 167–193, 2002, doi: 10.1128/CMR.15.2.167.

[4] M. Palomar, J. Vaque, F. Álvarez Lerma, V. Pastor, P. Olaechea, and J. Fernández-Crehuet, "Indicadores de infección nosocomial," *Med. Clin. (Barc).*, vol. 131, pp. 48–55, 2008, doi: https://doi.org/10.1016/S0025-7753(08)76461-3.

[5] G. Ducel, J. Fabry, and L. Nicole, "Prevention of hospital-acquired infections: A practical guide," 2002. [Online]. Available: https://www.who.int/csr/resources/publications/WHO_CDS_CSR_EPH_2002_12/en/.

[6] J. W. Costerton, P. S. Stewart, and E. P. Greenberg, "Bacterial biofilms: A common cause of persistent infections," *Science (80-.).*, vol. 284, no. 5418, pp. 1318–1322, 1999, doi: 10.1126/science.284.5418.1318.

[7] M. R. Parsek and P. K. Singh, "Bacterial Biofilms: An Emerging Link to Disease Pathogenesis," *Annu. Rev. Microbiol.*, vol. 57, no. 1, pp. 677–701, 2003, doi: 10.1146/annurev.micro.57.030502.090720.

[8] C. A. Fux, J. W. Costerton, P. S. Stewart, and P. Stoodley, "Survival strategies of infectious biofilms," *Trends Microbiol.*, vol. 13, no. 1, pp. 34–40, 2005, doi: 10.1016/j.tim.2004.11.010.

[9] C. M. Kirschner and A. B. Brennan, "Bio-Inspired Antifouling Strategies," *Annu. Rev. Mater. Res.*, vol. 42, no. 1, pp. 211–229, 2012, doi: 10.1146/annurev-matsci-070511-155012.

[10] N. Fusetani, "Antifouling marine natural products," *Nat. Prod. Rep.*, vol. 28, no. 2, pp. 400–410, 2011, doi: 10.1039/c0np00034e.

[11] K. Bazaka, M. V. Jacob, W. Chrzanowski, and K. Ostrikov, "Anti-bacterial surfaces: Natural agents, mechanisms of action, and plasma surface modification," *RSC Adv.*, vol. 5, no. 60, pp. 48739–48759, 2015, doi: 10.1039/c4ra17244b.

[12] P. Y. Qian, Y. Xu, and N. Fusetani, "Natural products as antifouling compounds: recent progress and future perspectives.," *Biofouling*, vol. 26, no. 2, pp. 223–234, 2010, doi: 10.1080/08927010903470815.

[13] J. R. Almeida and V. Vasconcelos, "Natural antifouling compounds: Effectiveness in preventing invertebrate settlement and adhesion," *Biotechnol. Adv.*, vol. 33, no. 3–4, pp. 343–357, 2015, doi: 10.1016/j.biotechadv.2015.01.013.

[14] H. X. Xu and S. F. Lee, "Activity of plant flavonoids against antibiotic-resistant bacteria," *Phyther. Res.*, vol. 15, no. 1, pp. 39–43, 2001, doi: 10.1002/1099-1573(200102)15:1<39::AID-PTR684>3.0.CO;2-R.

[15] T. P. T. Cushnie and A. J. Lamb, "Antimicrobial activity of flavonoids," *Int. J. Antimicrob. Agents*, vol. 26, no. 5, pp. 343–356, 2005, doi: 10.1016/j.ijantimicag.2005.09.002.

[16] X. Zhou *et al.*, "Flavone and isoflavone derivatives of terrestrial plants as larval settlement inhibitors of the barnacle Balanus amphitrite," *Biofouling*, vol. 25, no.

1, pp. 69–76, 2009, doi: 10.1080/08927010802455941.

[17] S. Kumar and A. K. Pandey, “Chemistry and biological activities of flavonoids: An overview,” *Sci. World J.*, vol. 2013, no. 7, pp. 637–670, 2013, doi: 10.1155/2013/162750.

[18] A. Córdoba *et al.*, “Flavonoid-modified surfaces: Multifunctional bioactive biomaterials with osteopromotive, anti-inflammatory, and anti-fibrotic potential,” *Adv. Healthc. Mater.*, vol. 4, no. 4, pp. 540–549, 2015, doi: 10.1002/adhm.201400587.

[19] M. Liu *et al.*, “Pharmacological profile of xanthohumol, a prenylated flavonoid from hops (Humulus lupulus),” *Molecules*, vol. 20, no. 1, pp. 754–779, 2015, doi: 10.3390/molecules20010754.

[20] E. Sangiovanni *et al.*, “A bio-guided assessment of the anti-inflammatory activity of hop extracts (Humulus lupulus L. cv. Cascade) in human gastric epithelial cells,” *J. Funct. Foods*, vol. 57, no. April, pp. 95–102, 2019, doi: 10.1016/j.jff.2019.03.041.

[21] J. L. Bolton *et al.*, “The Multiple Biological Targets of Hops and Bioactive Compounds,” *Chem. Res. Toxicol.*, vol. 32, no. 2, pp. 222–233, 2019, doi: 10.1021/acs.chemrestox.8b00345.

[22] M. Ambrož, K. Lněničková, P. Matoušková, L. Skálová, and I. Boušová, “Antiproliferative effects of hop-derived prenylflavonoids and their influence on the efficacy of oxaliplatine, 5-fluorouracil and irinotecan in human colorectalC cells,” *Nutrients*, vol. 11, no. 4, 2019, doi: 10.3390/nu11040879.

[23] J. Sastre-Serra, Y. Ahmiane, P. Roca, J. Oliver, and D. G. Pons, “Xanthohumol, a hop-derived prenylflavonoid present in beer, impairs mitochondrial functionality of SW620 colon cancer cells,” *Int. J. Food Sci. Nutr.*, vol. 70, no. 4, pp. 396–404, 2019, doi: 10.1080/09637486.2018.1540558.

[24] J. M. Seliger, H. J. Martin, E. Maser, and J. Hintzpeter, “Potent inhibition of human carbonyl reductase 1 (CBR1) by the prenylated chalconoid xanthohumol and its related prenylflavonoids isoxanthohumol and 8-prenylnaringenin,” *Chem. Biol. Interact.*, vol. 305, no. January, pp. 156–162, 2019, doi:

10.1016/j.cbi.2019.02.031.

[25] A. Sławińska-Brych *et al.*, "Xanthohumol exhibits anti-myeloma activity in vitro through inhibition of cell proliferation, induction of apoptosis via the ERK and JNK-dependent mechanism, and suppression of sIL-6R and VEGF production," *Biochim. Biophys. Acta - Gen. Subj.*, vol. 1863, no. 11, 2019, doi: 10.1016/j.bbagen.2019.08.001.

[26] N. Yamaguchi, K. Satoh-Yamaguchi, and M. Ono, "In vitro evaluation of antibacterial, anticollagenase, and antioxidant activities of hop components (Humulus lupulus) addressing acne vulgaris," *Phytomedicine*, vol. 16, no. 4, pp. 369–376, 2009, doi: 10.1016/j.phymed.2008.12.021.

[27] S. Bhattacharya, S. Virani, M. Zavro, and G. J. Haas, "Inhibition of Streptococcus mutans and other oral Streptococci by hop (Humulus lupulus L.) constituents," *Econ. Bot.*, vol. 57, no. 1, pp. 118–125, 2003, doi: 10.1663/0013-0001(2003)057[0118:IOSMAO]2.0.CO;2.

[28] C. Gerhäuser, "Broad spectrum antiinfective potential of xanthohumol from hop (Humulus lupulus L.) in comparison with activities of other hop constituents and xanthohumol metabolites," *Mol. Nutr. Food Res.*, vol. 49, no. 9, pp. 827–831, Sep. 2005, doi: 10.1002/mnfr.200500091.

[29] N. Zhang, Z. Liu, Q. Han, J. Chen, and Y. Lv, "Xanthohumol enhances antiviral effect of interferon α-2b against bovine viral diarrhea virus, a surrogate of hepatitis C virus," *Phytomedicine*, vol. 17, no. 5, pp. 310–316, 2010, doi: https://doi.org/10.1016/j.phymed.2009.08.005.

[30] Q. Wang, Z.-H. Ding, J.-K. Liu, and Y.-T. Zheng, "Xanthohumol, a novel anti-HIV-1 agent purified from Hops Humulus lupulus," *Antiviral Res.*, vol. 64, no. 3, pp. 189–194, 2004, doi: https://doi.org/10.1016/j.antiviral.2004.08.005.

[31] C. R. Langezaal, A. Chandra, and J. J. C. Scheffer, "Antimicrobial screening of essential oils and extracts of someHumulus lupulus L. cultivars," *Pharm. Weekbl.*, vol. 14, no. 6, pp. 353–356, 1992, doi: 10.1007/BF01970171.

[32] Oyvind M. Andersen and K. R. Markham, *Flavonoids: Chemistry, Biochemistry and*

Applications - 1st Edition - O. .

[33] N. Sus *et al.*, "Validation of a rapid and sensitive reversed-phase liquid chromatographic method for the quantification of prenylated chalcones and flavanones in plasma and urine," *NFS J.*, vol. 10, pp. 1–9, Mar. 2018, doi: 10.1016/j.nfs.2017.11.001.

[34] N. López-Rodríguez, A. López-Arraiza, E. Meaurio, and J. R. Sarasua, "Crystallization, morphology, and mechanical behavior of polylactide/poly(ε-caprolactone) blends," *Polym. Eng. Sci.*, vol. 46, no. 9, pp. 1299–1308, 2006, doi: 10.1002/pen.20609.

[35] L. Di and E. H. Kerns, "Solubility," in *Drug-Like Properties*, Elsevier, 2016, pp. 61–93.

[36] P.-Y. Qian, Y. Xu, and N. Fusetani, "Natural products as antifouling compounds: recent progress and future perspectives," *Biofouling*, vol. 26, no. 2, pp. 223–234, 2009, doi: 10.1080/08927010903470815.

[37] B. T. Surikutchi, S. P. Patil, G. Shete, S. Patel, and A. K. Bansal, "Drug-excipient behavior in polymeric amorphous solid dispersions," *J. Excipients Food Chem. Vol 4 No 3*, Sep. 2013, [Online]. Available: https://ojs.abo.fi/ojs/index.php/jefc/article/view/214.

[38] M. M. Knopp, N. E. Olesen, Y. Huang, R. Holm, and T. Rades, "Statistical Analysis of a Method to Predict Drug-Polymer Miscibility," *J. Pharm. Sci.*, vol. 105, no. 1, pp. 362–367, Jan. 2016, doi: 10.1002/jps.24704.

[39] M. M. Knopp *et al.*, "Comparative Study of Different Methods for the Prediction of Drug–Polymer Solubility," *Mol. Pharm.*, vol. 12, no. 9, pp. 3408–3419, 2015, doi: 10.1021/acs.molpharmaceut.5b00423.

[40] J. Tao, Y. Sun, G. G. Z. Zhang, and L. Yu, "Solubility of small-molecule crystals in polymers: D-Mannitol in PVP, indomethacin in PVP/VA, and nifedipine in PVP/VA," *Pharm. Res.*, vol. 26, no. 4, pp. 855–864, Apr. 2009, doi: 10.1007/s11095-008-9784-z.

[41] P. J. Marsac, T. Li, and L. S. Taylor, "Estimation of Drug–Polymer Miscibility and Solubility in Amorphous Solid Dispersions Using Experimentally Determined Interaction Parameters," *Pharm. Res.*, vol. 26, no. 1, pp. 139–151, 2008, doi: 10.1007/s11095-008-9721-1.

[42] K. DeBoyace and P. L. D. Wildfong, "The Application of Modeling and Prediction to the Formation and Stability of Amorphous Solid Dispersions," *Journal of Pharmaceutical Sciences*, vol. 107, no. 1. Elsevier B.V., pp. 57–74, Jan. 01, 2018, doi: 10.1016/j.xphs.2017.03.029.

[43] T. Vasconcelos, B. Sarmento, and P. Costa, "Solid dispersions as strategy to improve oral bioavailability of poor water soluble drugs," *Drug Discov. Today*, vol. 12, no. 23–24, pp. 1068–1075, 2007, doi: 10.1016/j.drudis.2007.09.005.

[44] E. Sanchez-Rexach, I. Martínez de Arenaza, J. R. Sarasua, and E. Meaurio, "Antimicrobial poly(ε-caprolactone)/thymol blends: Phase behavior, interactions and drug release kinetics," *Eur. Polym. J.*, vol. 83, pp. 288–299, Oct. 2016, doi: 10.1016/j.eurpolymj.2016.08.029.

[45] E. Sanchez-Rexach *et al.*, "Miscibility, interactions and antimicrobial activity of poly(ε-caprolactone)/chloramphenicol blends," *Eur. Polym. J.*, vol. 102, pp. 30–37, 2018, doi: 10.1016/j.eurpolymj.2018.03.011.

[46] R. Pezzoli, J. G. Lyons, N. Gately, and C. L. Higginbotham, "Investigation of miscibility estimation methods between indomethacin and poly(vinylpyrrolidone-co-vinyl acetate)," *Int. J. Pharm.*, vol. 549, no. 1–2, pp. 50–57, 2018, doi: 10.1016/j.ijpharm.2018.07.039.

[47] N. Hernandez-Montero, J. M. Ugartemendia, H. Amestoy, and J. R. Sarasua, "Complex phase behavior and state of miscibility in Poly(ethylene glycol)/Poly(l-lactide-co-ε-caprolactone) Blends," *J. Polym. Sci. Part B Polym. Phys.*, vol. 52, no. 2, pp. 111–121, Jan. 2014, doi: 10.1002/polb.23394.

[48] J. A. Baird and L. S. Taylor, "Evaluation of amorphous solid dispersion properties using thermal analysis techniques," *Adv. Drug Deliv. Rev.*, vol. 64, no. 5, pp. 396–421, 2012, doi: 10.1016/j.addr.2011.07.009.

[49] E. Meaurio, N. Hernandez-Montero, E. Zuza, and J. R. Sarasua, "Miscible Blends Based on Biodegradable Polymers," in *Characterization of Polymer Blends: Miscibility, Morphology and Interfaces*, vol. 9783527331, Wiley Blackwell, 2015, pp. 7–92.

[50] R. S. Khupse and P. W. Erhardt, "Total synthesis of xanthohumol," *J. Nat. Prod.*, vol. 70, no. 9, pp. 1507–1509, Sep. 2007, doi: 10.1021/np070158y.

[51] R. Hänsel and J. Schulz, "Desmethylxanthohumol: Isolierung aus Hopfen und Cyclisierung zu Flavanonen," *Arch. Pharm. (Weinheim).*, vol. 321, no. 1, pp. 37–40, Jan. 1988, doi: 10.1002/ardp.19883210112.

[52] S. Song-San, S. Watanabe, and T. Saito, "Chalcones from Humulus lupulus," *Phytochemistry*, vol. 28, no. 6, pp. 1776–1777, Jan. 1989, doi: 10.1016/S0031-9422(00)97849-X.

[53] F. Govaert, M. Verzele, M. Anteunis, F. Fontyn, and J. Stockx, "Xanthohumol," *Experientia*, vol. 13, no. 3, pp. 105–106, 1957, doi: 10.1007/BF02157558.

[54] J. W. Lee, L. C. Thomas, and S. J. Schmidt, "Can the thermodynamic melting temperature of sucrose, glucose, and fructose be measured using rapid-scanning differential scanning calorimetry (DSC)?," *J. Agric. Food Chem.*, vol. 59, no. 7, pp. 3306–3310, Apr. 2011, doi: 10.1021/jf104852u.

[55] A. Magoń *et al.*, "Heat capacity and transition behavior of sucrose by standard, fast scanning and temperature-modulated calorimetry," *Thermochim. Acta*, vol. 589, pp. 183–196, Aug. 2014, doi: 10.1016/j.tca.2014.05.029.

[56] P. J. Marsac, T. Li, and L. S. Taylor, "Estimation of drug-polymer miscibility and solubility in amorphous solid dispersions using experimentally determined interaction parameters," *Pharm. Res.*, vol. 26, no. 1, pp. 139–151, Jan. 2009, doi: 10.1007/s11095-008-9721-1.

[57] M. M. Knopp *et al.*, "Comparative Study of Different Methods for the Prediction of Drug-Polymer Solubility," *Mol. Pharm.*, vol. 12, no. 9, pp. 3408–3419, Sep. 2015, doi: 10.1021/acs.molpharmaceut.5b00423.

[58] M. A. Altamimi and S. H. Neau, "A study to identify the contribution of Soluplus® component homopolymers to the solubilization of nifedipine and sulfamethoxazole using the melting point depression method," *Powder Technol.*, vol. 338, pp. 576–585, 2018, doi: 10.1016/j.powtec.2018.07.027.

[59] E. G. Lezcano, C. Salom Coll, and M. G. Prolongo, "Melting behaviour and miscibility of poly(ϵ-caprolactone) + poly(4-hydroxystyrene) blends," *Polymer (Guildf).*, vol. 37, no. 16, pp. 3603–3609, 1996, doi: https://doi.org/10.1016/0032-3861(96)00170-X.

[60] E. Meaurio, E. Sanchez-Rexach, A. Butron, and J.-R. Sarasua, "The conformation of chloramphenicol in the ordered and disordered phases," *Spectrochim. Acta - Part A Mol. Biomol. Spectrosc.*, vol. 211, 2019, doi: 10.1016/j.saa.2018.12.021.

[61] M. Arczewska *et al.*, "The molecular organization of prenylated flavonoid xanthohumol in DPPC multibilayers: X-ray diffraction and FTIR spectroscopic studies," *Biochim. Biophys. Acta - Biomembr.*, vol. 1828, no. 2, pp. 213–222, 2013, doi: https://doi.org/10.1016/j.bbamem.2012.10.009.

[62] I. Budziak, M. Arczewska, and D. M. Kamiński, "Formation of Prenylated Chalcone Xanthohumol Cocrystals: Single Crystal X-ray Diffraction, Vibrational Spectroscopic Study Coupled with Multivariate Analysis," *Molecules* , vol. 24, no. 23. 2019, doi: 10.3390/molecules24234245.

[63] L. R. Chadwick *et al.*, "Estrogens and Congeners from Spent Hops (Humulus lupulus)," *J. Nat. Prod.*, vol. 67, no. 12, pp. 2024–2032, Dec. 2004, doi: 10.1021/np049783i.

[64] A. Lejardi, E. Meaurio, J. Fernández, and J.-R. Sarasua, "Miscibility of poly(vinyl alcohol)-graft-hydroxy ester/ poly(vinylpyrrolidone) blends," *Macromolecules*, vol. 44, no. 18, pp. 7351–7363, 2011, doi: 10.1021/ma2012305.

[65] C. Hou, T. Yang, X. Sun, Z. Ren, H. Li, and S. Yan, "Branched Crystalline Patterns of Poly(ε-caprolactone) and Poly(4-hydroxystyrene) Blends Thin Films," *J. Phys. Chem. B*, vol. 120, no. 1, pp. 222–230, Jan. 2016, doi: 10.1021/acs.jpcb.5b09960.

[66] R. Abreu-Villela, M. Schönenberger, I. Caraballo, and M. Kuentz, "Early stages of

drug crystallization from amorphous solid dispersion via fractal analysis based on chemical imaging," *Eur. J. Pharm. Biopharm.*, vol. 133, pp. 122–130, Dec. 2018, doi: 10.1016/j.ejpb.2018.10.007.

[67] L. Jiang and J. Zhang, "6 - Biodegradable Polymers and Polymer Blends," in *Plastics Design Library*, S. B. T.-H. of B. and B. P. Ebnesajjad, Ed. Boston: William Andrew Publishing, 2013, pp. 109–128.

[68] C. C. Neikirk, J. W. Chung, and R. D. Priestley, "Thermomechanical behavior of hydrogen-bond based supramolecular poly(ε-caprolactone)-silica nanocomposites," *RSC Adv.*, vol. 3, no. 37, pp. 16686–16696, 2013, doi: 10.1039/C3RA42031K.

[69] I. Manavitehrani, A. Fathi, H. Badr, S. Daly, A. Negahi Shirazi, and F. Dehghani, "Biomedical Applications of Biodegradable Polyesters," *Polymers (Basel).*, vol. 8, no. 1, p. 20, Jan. 2016, doi: 10.3390/polym8010020.

[70] J. F. Stevens, A. W. Taylor, J. E. Clawson, and M. L. Deinzer, "Fate of xanthohumol and related prenylflavonoids from hops to beer," *J. Agric. Food Chem.*, vol. 47, no. 6, pp. 2421–2428, Jun. 1999, doi: 10.1021/jf990101k.

3c. MISCIBILITY, INTERACTIONS AND POSSIBLE ANTI-CANCER ACTIVITY OF POLY(ε-CAPROLACTONE)/MYCOPHENOLIC ACID BLENDS

ABSTRACT

The obtention of amorphous solid dispersions (ASDs) of mycophenolic acid (MPA) in poly(ε-caprolactone) (PCL) is reported in this paper. The improvement of the bioavailability of the drug is possible thanks to the favorable specific interactions occurring in this system. Differential scanning calorimetry (DSC) was used to investigate the miscibility of PCL/MPA blends, measuring their glass transition temperature ($T_{g)}$ and analyzing melting point depression to obtain a negative interaction parameter which indicates the development of favorable interassociation interactions. Fourier transform infrared spectroscopy (FTIR) was used to analyze the specific interaction occurring in the blends. Drug release measurements showed that at least 70% of the drug was released by the third day *in vitro* in all compositions. Finally, preliminary *in vitro* cell culture experiments showed a decreased number of cancerous cells over the scaffolds containing MPA, which might be attributed to the possible anti-cancer activity of the MPA to be further addressed in future experiments.

3c.1. INTRODUCTION

As new treatments and drugs appear for all kind of diseases, we are also faced with great challenges to achieve a satisfactory application of these remedies. Although they may be effective in theory, most of the drugs that are being approved are not feasible in terms of their biopharmacological properties. The main causes are low permeability, poor solubility or rapid elimination from the body. In fact, 90% of the drugs being developed are molecules with low solubility, in addition to almost 40% of drugs already approved [1]. The dimensions of this problem can be seen as an example in the case of oral administration of doses. In order to reach the systemic circulation, the drug must be dissolved in the intestinal fluids of the gastrointestinal tract, which is difficult in the case of low solubility [2]. The cause of this low bioavailability is due to the different molecular arrangements, being the crystalline compounds the ones that present the greatest problem [3]. In order to solve it, one of the established strategies is amorphization, which transforms low-energy crystalline substances into high-energy amorphous compounds, giving them greater solubility and bioavailability [4]. However, these amorphous solids are not thermodynamically stable due to their excess enthalpy,

entropy and free energies, which causes them to tend to form crystals [1], [5]. For this reason, achieving the stability of these compounds is a great challenge.

One of the strategies used for this purpose is developing amorphous solid dispersions (ASDs). In the 1970s, Chiou and Riegelman defined the term solid dispersions as the dispersion of an active pharmaceutical ingredient (API) in an amorphous carrier in solid state prepared by solvent, melting or solvent-melting methods [5]. In these systems, there is a mixture at the molecular level between a polymer and the drug in an amorphous state, increasing its bioavailability [6]–[10]. It is known that the low thermodynamic stability due to the high energy of the amorphous state causes relaxation, nucleation and recrystallization under different variables [11]. Thus, the role of the polymeric matrix is to inhibit this process and maintain the mixture in a single homogeneous phase [12], [13]. To avoid this crystallization and maintain the mixture in the metastable region of the binary phase diagram, miscibility between API and polymer is essential [14], [15]. The kinetic stability provided by storage below glass transition temperature (T_g) must also be taken into account. In fact, according to Hancock et al., the stability of the mixture could be ensured for years by storing it at least 50 K below T_g [16], [17]. The biggest complication this system presents is the lack of predictability of polymer-drug interactions, which is why obtaining them is based on trial-and-error effort [18].

One interesting drug to test this system is mycophenolic acid (MPA – $C_{17}H_{20}O_6$, 320 g/mol; aqueous solubility: 35.5 mg/L). Mycophenolic acid (Figure 3c.2) is an antibiotic produced by *Penicillium* family, best known for its use as an immunosuppressive agent to prevent rejection in organ transplants [19], [20]. In addition, this drug has more biological properties, such as antifungal of antiviral properties [21]. It also has potential to prevent and perhaps treat chronic allograft vasculopathy, as it can inhibit the proliferation of vascular smooth muscle cells (VSMCs), mesangial cells, and myofibroblasts [22]. However, one of the most striking properties is its ability to act against tumor cells of various types such as leukemia or lymphoma, among others [23]. This is because MPA is an inhibitor of inosine monophosphate dehydrogenase (IMPDH), which leads to the reduction of xanthine monophosphate (XMP), guanosine-5'-triphosphate (GTP) and deoxyguanosine triphosphate (dGTP), thus inhibiting the

proliferation of lympholeukocytes and cancer cells [20], [24]. Despite having so many favorable properties, the bioavailability of MPA *in vivo* is relatively poor due to the high clearance inside a living organism, which limits its possibility of clinical application [19]. This, added to its low aqueous solubility, makes it a perfect candidate to form amorphous solid dispersions.

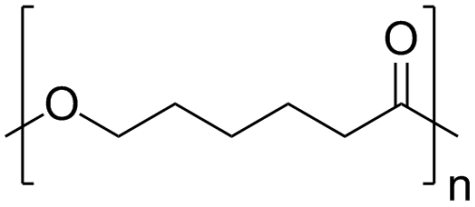

Figure 3c. 1. Poly(ε-caprolactone)

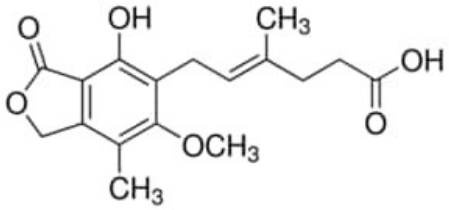

Figure 3c. 2. Mycophenolic acid

In this work, the polymer selected as matrix to disperse MPA in amorphous form has been poly(ε-caprolactone) (PCL) (Figure 3c.1), a biodegradable semicrystalline polyester. Its glass transition temperature is around -60°C, and its melting point at around 60°C. This polymer is suitable for long-term biomedical application, as the degradation can last from several months to years [25], [26]. In this work, miscibility and interactions between PCL and MPA have been studied to verify the suitability of this mixture for the formation of an amorphous solid dispersion. In addition, it has been tested separately the interaction of the blends containing increasing concentrations of MPA with both a non-cancerous fibroblast cell line (MRC5) approved by the ISO 10993 for cytotoxicity studies [27] and a widely used immortalized HeLa cell line derived from a cervical cancer [28].

3c.2. EXPERIMENTAL SECTION

3c.2.1. Starting Materials

Poly(ε-caprolactone) (PURASORB® PC12 trade name) with an average molecular weight (M_w) of 1.3 x 10^5 g/mol and M_w/M_n = 1.76 was purchased from Purac Biochem (The Netherlands). Mycophenolic acid ($C_{17}H_{20}O_6$, M = 320.34 g/mol) was obtained from Fluorochem Ltd (United Kingdom) and Dichloromethane (DCM) was supplied by Labkem.

3c.2.2. Blend Preparation

Films were prepared by solvent casting from dichloromethane (DCM) solutions containing 2.5 wt% of PCL/MPA blend at room temperature.

3c.2.3. Differential Scanning Calorimetry (DSC)

A Modulated DSC Q200 from TA Instruments was used for thermal analyses. All the scans were performed in hermetic aluminum pans under nitrogen atmosphere with sample weights between 5 and 10 mg. Two scans from -80°C to 160°C with a scan rate of 20°C/min were performed, in order to measure glass transition temperatures (T_g) in the second one.

3c.2.4. Melting Point Depression Analysis.

The melting point depression of MPA was observed in MPA-rich blends containing 0-20 wt% PCL. To obtain the melting temperature of MPA crystals, samples were heated in the DSC with a scan rate of 1°C/min.

The samples were weighed again after the DSC scans, and no weight loss was observed during the thermal treatments.

3c.2.5. Fourier Transform Infrared Spectroscopy (FTIR).

A Nicolet AVATAR 370 Fourier transform infrared spectrophotometer was used to record FTIR spectra of the blends, with a resolution of 2 cm^{-1} and averaged over 64 scans in the range of 400-4000 cm^{-1}. Dichloromethane solutions containing 2 wt% of blends were cast on KBr pellets by evaporation of the solvent at room temperature. The absorbance of the samples was within the range where Lambert-Beer law is obeyed.

3c.2.6. *In vitro* drug release.

In vitro drug release experiments were performed for PCL/MPA 99.95/0.05, 99.9/0.1, 99.8/0.2, 99.5/0.5, 99/1 and 98/2 blends. Round samples of PCL/MPA of Ø10 mm obtained by solvent casting were immersed in 1 mL of 0.1M PBS buffer (pH 7.4) at 37°C. At fixed intervals, samples of 200 µL were taken and replaced with fresh PBS at 37°C. Drug concentration in solution was determined using a BioTech Sinergy H1M MicroPlate Reader using a calibration curve that was previously obtained measuring the absorbance at a wavelength of 305 nm for solutions of MPA in 0.1 M PBS.

The release kinetics of mycophenolic acid were examined considering four mathematical models:

$$\text{Zero order: } C_t/C_\infty = k_0 t \tag{3c.1}$$

$$\text{First order: } \ln(1 - C_t/C_\infty) = -k_1 t \tag{3c.2}$$

$$\text{Higuchi: } C_t/C_\infty = k_h t^{1/2} \tag{3c.3}$$

$$\text{Korsmeyer – Peppas: } C_t/C_\infty = k t^n \tag{3c.4}$$

C_t is the cumulative amount of drug released at time *t,* C_∞ is the starting amount of drug, *n* is the release exponent, and k_0, k_1, k_h and *k* are the kinetic constants. Zero order kinetics (Eq. (3c.1)) represents a release process that is controlled by relaxation of polymeric chains, independent of its concentration and with a constant release rate. First order kinetics model (Eq. (3c.2)) represents a drug release rate that depends on its concentration [26]. Higuchi (Eq. (3c.3)) describes drug release as a diffusion process based in Fick´s law, square root time dependent. If the release mechanism is not well known or when more than one type of release phenomena could be involved, Korsmeyer-Peppas model (Eq. (3c.4)) is applied. It is possible to define whether if the release happens by Fickian diffusion, anomalous transport, Case-II transport or Super Case-II transport depending on the values obtained for the release exponent, *n* [29], [30].

3c.2.7. *In vitro* cell culture experiments.

In vitro cell culture experiments were performed on PCL/MPA 99.5/0.5, 99/1 and 98/2 blends. Circular samples of PCL/MPA of Ø6 mm were obtained and each side sterilized for 30 min under UV light. Either the immortalized HeLa cell line (ATCC, United States) derived from a cervical cancer or the non-cancerous fibroblasts MRC5 (CCL-171, ATCC, United States) derived from lung tissue were drop seeded over the materials at a concentration of 25000 cells per scaffold. After 1 h, 480 ml of DMEM (Fisher Scientific, Spain) supplemented with 10% fetal bovine serum (FBS) (Fisher Scientific, Spain), 1% L-glutamine (Fisher Scientific, Spain) and penicillin/streptomycin (Fisher Scientific, Spain) were added. PCL was used as negative control and for the positive control MPA at a concentration of 300 ppm was dissolved on the culture media and filtrated (0.2 μm). Cells were incubated at 37°C and 5% CO_2.

3c.2.8. Immunostaining.

After 1 or 3 days *in vitro* (DIV), samples were fixed with 4% paraformaldehyde (PFA) (Fisher Scientific, Spain) and permeabilized with 0.3% triton-X100 (Fisher Scientific, Spain) in 1% PBS-Bovine Serum Albumin (BSA) (Sigma Aldrich, Spain). For the staining, rhodamine/phalloidin (Fisher Scientific, Spain) and DAPI, 4',6-diamidino-2-fenilindol, dihydrochloride (Fisher Scientific, Spain) were diluted in PBS (Fisher Scientific, Spain) containing 1% BSA and incubated for 1.5 h. After washing each sample 2 times in PBS containing 0.1% Tween-20 (Fisher Scientific, Spain) and 1 time in PBS, samples were mounted using mounting medium (Abcam, USA). The samples were analyzed in an inverted fluorescence microscope (Nikon Eclipse Ts2).

3c.2.9. Statistical Analysis.

Data were subjected to one-way analysis of variant (ANOVA) using Kruskal-Wallis followed by Dunn´s post hoc test. Level of significance was set at $p<0.05$. Results were presented as mean ± SD or SEM.

3c.3. RESULTS AND DISCUSSION

3c.3.1. Miscibility analysis by Differential Scanning Calorimetry (DSC).

When two components are miscible, a single glass transition temperature (T_g) between the T_g of each material which changes progressively with the composition is expected

[31], [32]. On the contrary, the detection of more than one single value would indicate a separation into individual amorphous phases within the system. Different methods have been employed to predict the glass transition temperature of amorphous binary systems, such as Gordon-Taylor (GT), Couchman-Karasz (CK) or Fox equations (Eq (3c.5). Considering that Fox equation was developed to analyze systems formed by components of equal densities, it is appropriate to use it in order to estimate this intermediate T_g, as the densities of PCL and MPA are 1.14 g/cm^3 and 1.3 g/cm^3, respectively [33]:

$$\frac{1}{T_{gb}} = \frac{w_1}{T_{g1}} + \frac{w_2}{T_{g2}} \qquad \text{(3c.5)}$$

where w_1 and w_2 are the weight fractions of components 1 and 2 respectively, T_{g1} and T_{g2} are the glass transition temperatures of the pure components, and T_{gb} is the glass transition temperature of the blend.

Pure PCL is a semicrystalline polymer displaying a glass transition temperature located at about -60°C and a melting endotherm at about 60°C. In turn, MPA displays a glass transition at 11°C and a melting point at 145°C.

Figure 3c.3. shows first DSC traces obtained for the pure components and for different PCL/MPA blends.

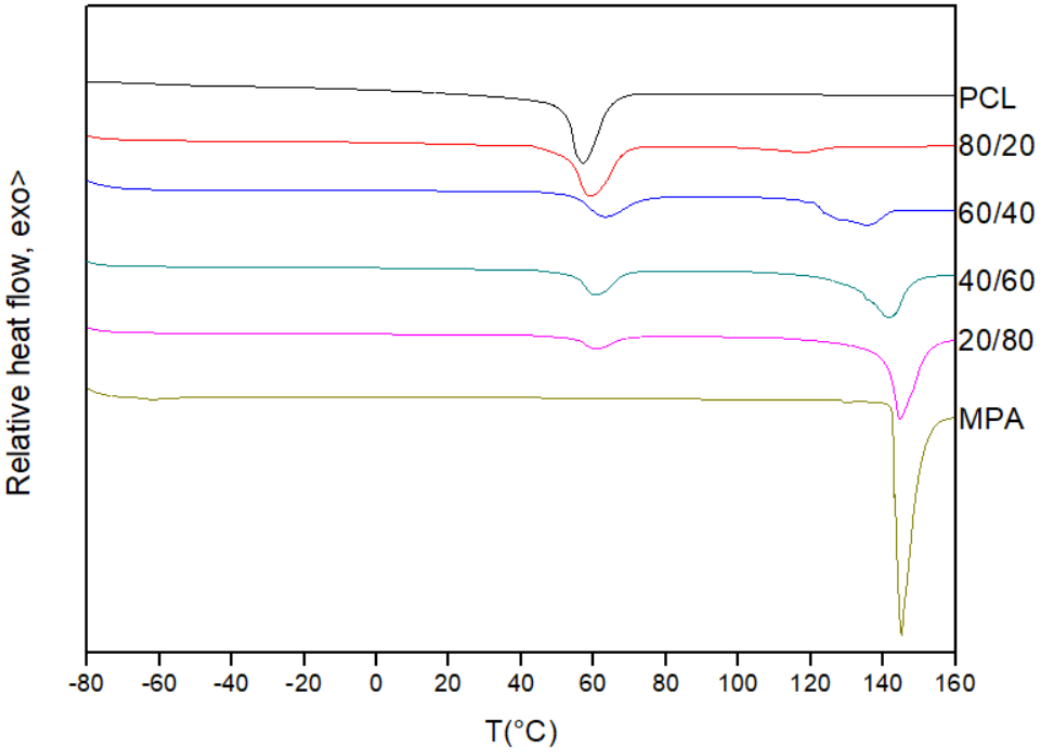

Figure 3c. 3. First scan DSC traces for PCL, MPA and PCL/MPA blends.

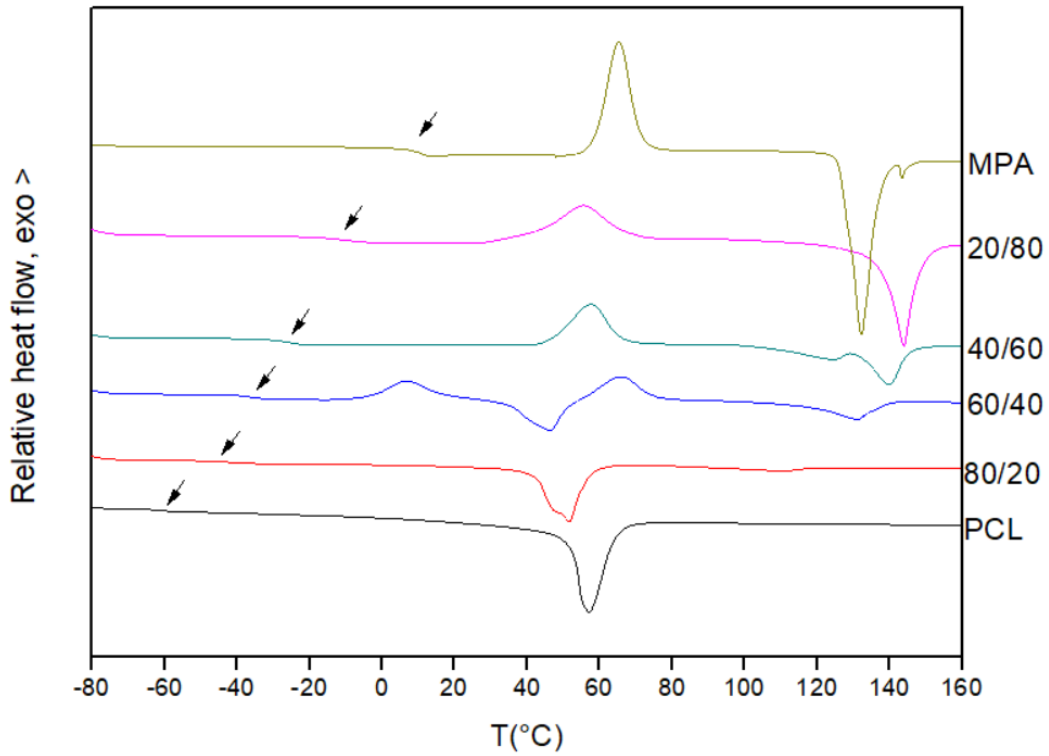

Figure 3c. 4. Second scan DSC traces for PCL, MPA and PCL/MPA blends.

The traces taken after cooling from the melt showed miscibility in the blends. The T_g of pure PCL is -60°C and pure MPA displays a T_g at 11°C. As it can be seen in Figure 3c.4., PCL/MPA blends show a single T_g intermediate between pure components for all compositions and close to those predicted using the Fox equation (table 3c.1), as Figure 3c.5. shows. Consequently, it can be inferred that the two components are fully miscible in the amorphous phase. Furthermore, melting endotherm and T_m of PCL are lowered as the content of MPA becomes higher, until crystallization is totally suppressed when there is more than 50 wt% of drug in the blend.

Table 3c. 1. Thermal properties of PCL/MPA blends.

PCL/MPA	T_g Experimental (°C)	T_g Theoretical (Fox) (°C)	T_m PCL (°C)	ΔH_f PCL (J/g)
PCL	-60	-	57.2	66.4
80/20	-44.1	-48.8	51.7	49.8
60/40	-36.3	-36.3	46.4	25.9
40/60	-25.7	-22.4	-	-
20/80	-10.2	-6.8	-	-
MPA	11.1	-	-	-

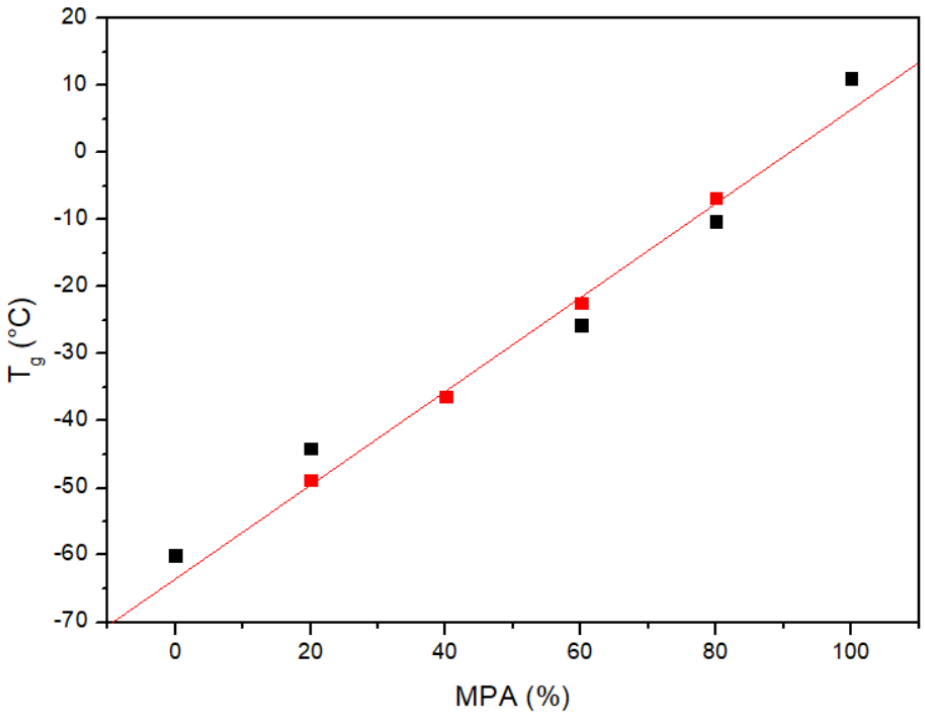

Figure 3c. 5. Glass transition temperature *versus* composition for the PCL/MPA system: (■) experimental values, (■) Fox equation.

3c.3.2. Melting point depression analysis.

If the free energy of mixing of the two components (ΔG_{mix}) is negative, a system can be considered thermodynamically miscible.

$$\Delta G_{mix} = \Delta H_{mix} - T\Delta S_{mix} \quad \text{(3c.6)}$$

where ΔH_{mix} and ΔS_{mix} are the enthalpy and entropy of mixing, respectively. $T\Delta S_{mix}$ is always positive, since the entropy of mixing is added to the entropy of melting, making the entropy change in a miscible blend larger than in the pure component. Consequently, the sign of ΔG_{mix} depends on the value of ΔH_{mix}. In order to avoid phase separation, the cohesive interactions need to be lower than the sum of adhesive interactions, generating a favorable enthalpy of mixing. The miscibility between two components in terms of the change of the Gibbs free energy can be described using melting point depression method, based on Flory-Huggins theory. According to this method, the melting point temperature of the drug will decrease as the polymer content in the mixture increases if the cohesive forces in the pure components are weaker than the adhesive forces between the drug and the polymer [26], [34]. Flory's relationship can be used to analyze the depression of the equilibrium melting point:

$$\frac{1}{T_m} - \frac{1}{T_m^0} = \frac{-R}{\Delta H_{2u}} \frac{V_{2u}}{V_{1u}} \left(\frac{\ln \phi_2}{m_2} + \left(\frac{1}{m_2} - \frac{1}{m_1} \right) \phi_1 + \chi_{12} \phi_1^2 \right) \quad \text{(3c.7)}$$

where T_m^0 is the equilibrium melting point of the pure crystallizable component and T_m is the equilibrium melting point of its blends, the subscripts 1 and 2 refer to the amorphous and crystallizable components respectively. R is the universal gas constant, while ΔH_{2u} is the heat of fusion per mole of crystalline repeat units. V_u is the molar volume of the repeating unit, m is the degree of polymerization, ϕ is the volumen fraction, and χ_{12} is the interaction parameter.

In order to apply (Eq (3c.7)), the molar volume of MPA ($V_2 = 246.3$ cm^3/mol) can be considered as the molar volume of the lattice sites, resulting in $m_2 = 1$. The same

volume can be taken as the molar volume of the polymeric repeat unit $V_2 = V_{1u}$. Since $m_1 = V_{pol}/V_{1u}$ is large, $1/m_1 \approx 0$. As a result, (Eq (3c.7)) simplifies to:

$$\frac{1}{T_m} - \frac{1}{T_m^0} = \frac{-R}{\Delta H_2}(\ln \phi_2 + \phi_1 + \chi \phi_1^2) \quad (3c.8)$$

Melting points of pure components and different PCL/MPA blends were measured at low heating rate (1°C/min). The average melting point of pure MPA is $T_m^0 = 140.3$°C, and this temperature is decreased by nearly 5°C when 20 wt% PCL is added to the blend. The data obtained for each blend can be seen in Table 3c.2. These results, with the average melting enthalpy of pure MPA ($\Delta H_{MPA} = 114.7$ J/g) were used to plot (Eq (3c.8)) as a function of the square of the volume fraction of the polymer, ϕ_1^2. The slope of this plot, which can be seen in Figure 3c.6., gives an approximation of the interaction parameter of $\chi = -1.18$. The negative values for the interaction parameter indicate an exothermic reaction, confirming a thermodynamically miscible blend. It is also possible to calculate the interaction energy density, B, at the melting temperature of MPA according to (Eq (3c.9)):

$$\chi = \frac{BV_r}{RT} \quad (3c.9)$$

where V_r is a reference volumen ($V_r = V_2 = 246.3$ cm^3/mol), yielding $B = -16.5$ J/cm^3.

Table 3c. 2. Melting temperatures of MPA obtained from 1 °C min-1 scan rates.

MPA wt%	T_m (°C)		
	Sample 1	Sample 2	Sample 3
100	139.2	140.5	140.9
95	139.6	139.9	138.3
90	138.4	138.1	137.4
85	137.4	138.9	136.8
80	135.8	135.7	135.9

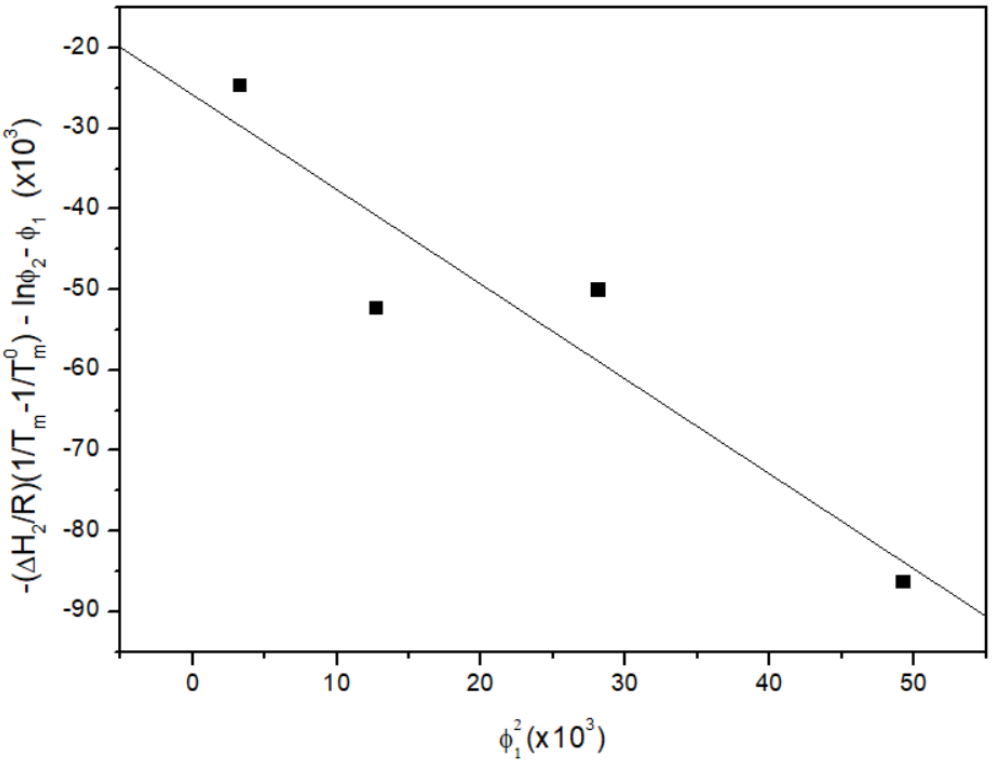

Figure 3c. 6. Analysis of the melting temperature of MPA according to (Eq (3c.8)) for the PCL/MPA system. The slope of the plot gives the interaction parameter χ = -1.18.

3c.3.3. Fourier Transform Infrared Spectroscopy (FTIR).

The analysis of the changes observed in the infrared spectrum upon blending provides information about the changes in specific interactions, and can eventually aid to explain the energetic contributions driving the miscibility of the system. In the PCL/MPA system both the carbonyl and the hydroxyl stretching regions are of main interest because hydrogen bonding interactions can be expected for those groups. Figure 3c.7. shows the carbonyl stretching region for PCL, MPA and their blends. The spectrum of pure PCL shows a peak at 1725 cm^{-1} attributable to crystalline PCL and a shoulder at 1735 cm^{-1} arising from the amorphous phase [26], [34]. On the other hand, pure MPA shows two different peaks located at 1744 and 1708 cm^{-1} attributable respectively to the lactone carbonyl and the carboxylic acid carbonyl. Both locations are in the lower end of the spectral ranges corresponding to those functional groups [35] because of the hydrogen bonding interactions occurring in pure MPA. Figure 3c.8. sketches these interactions as derived from XRD studies [36]–[38]. As it can be seen, in pure MPA molecules are joined

in the crystal by carboxylic acid groups forming dimers, along with bifurcated hydrogen bonds between the hydroxyl group and the carboxylic acid carbonyl (absorption band at 1708 cm^{-1}). In addition, an intramolecular bifurcated hydrogen bond red shifts the absorption of the lactone carbonyl to the reported wavenumber (1744 cm^{-1}).

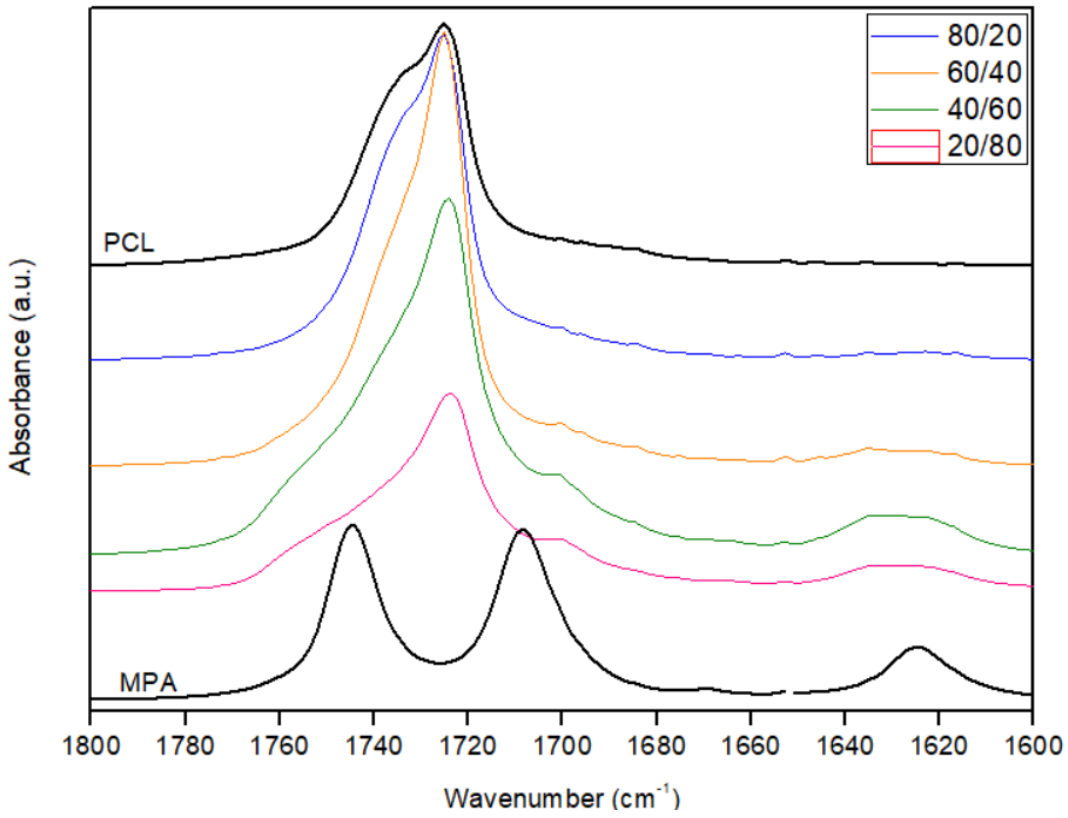

Figure 3c. 7. Carbonyl stretching region for pure PCL and MPA and PCL/MPA blends of different compositions.

The PCL/MPA 20/80 and 40/60 blends show a major peak located at about 1724 cm^{-1}, accompanied by two shoulders at higher wavenumbers located at about 1735 cm^{-1} and 1750 cm^{-1}. At these compositions, PCL is almost in amorphous form according to the DSC results (hence the contribution corresponding to crystalline PCL should be negligible) and the absorption bands corresponding to MPA are expected to prevail over those of PCL; hence, the band at 1724 cm^{-1} is most likely attributable carboxylic acid carbonyls forming dimers in the amorphous phase. Probably, this band is strongly overlapped with PCL carbonyls hydrogen bonded with hydroxyl groups present in MPA, but unfortunately, these two components are not distinguishable. The shoulder at about 1735 cm^{-1} can be attributed to free C=O groups in PCL, and the one at about 1750 cm^{-1} to lactone carbonyls in the amorphous phase.

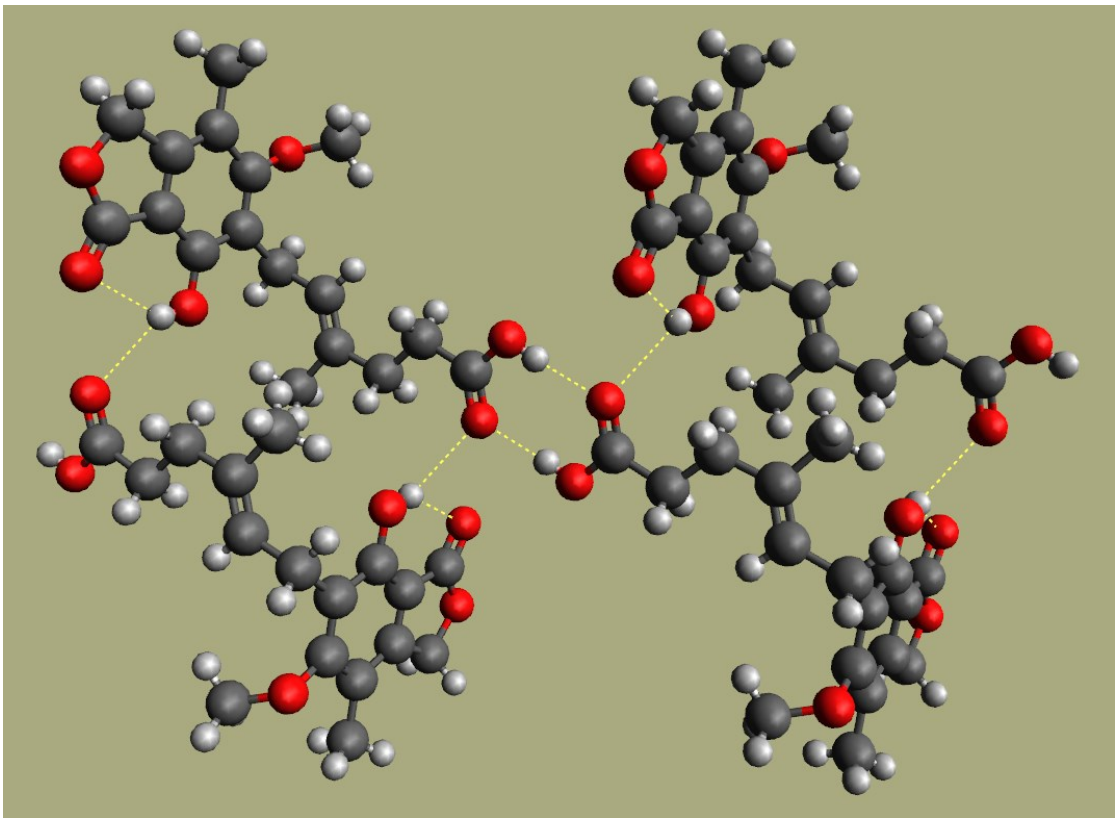

Figure 3c. 8. Hydrogen bonding in crystalline MPA (see text).

Finally, Figure 3c.9. shows the hydroxyl stretching region for MPA and its blends with PCL. As it can be seen, the OH stretching band in pure MPA is located at about 3416 cm^{-1}, and blending broadens the band and shifts it to higher wavenumbers. Band broadening is a consequence of the presence of amorphous MPA, while shifting to higher wavenumbers can be attributed to weaker hydrogen bonding interactions in the blends compared to pure MPA. In spite of the weaker nature of the interactions, the energetic balance will still render favorable to miscibility as long as the blend achieves a larger number of interactions, arising from the introduction of additional interacting groups (the PCL carbonyls).

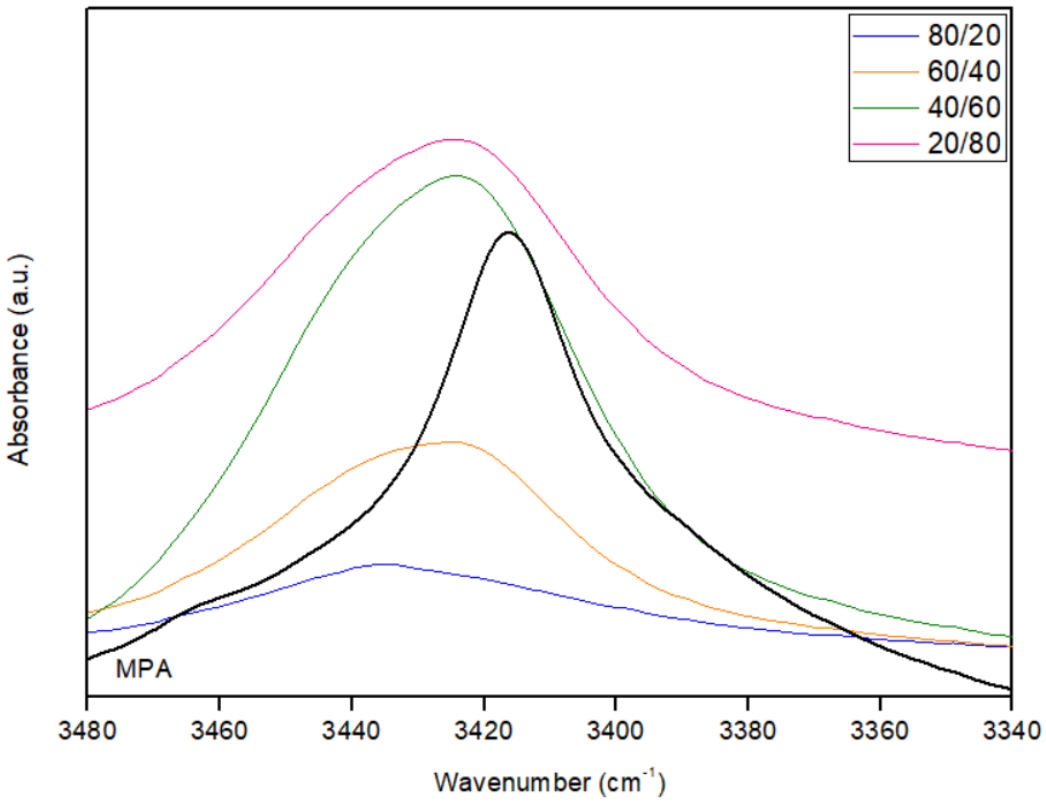

Figure 3c. 9. Hydroxyl stretching region for pure MPA and PCL/MPA blends of different compositions.

3c.3.4. *In vitro* drug release.

Figure 3c.10. shows the *in vitro* release profiles of MPA from different PCL/MPA blend (0.05, 0.1, 0.2, 0.5, 1 and 2 wt% MPA) samples for 3 days (72 hours). From the first moment, the release of MPA starts, being faster in the samples with the lowest drug content. By the third day, samples of 0.05 and 0.1 wt% MPA had released all the drug, while the rest of the samples had released between 69 and 79 wt% of the total amount. Figure 3c.11. shows that the release rate slowed down after the third day following an asymptotic tendency, thus, it is thought that the remaining drug will be fully released when bulk erosion begins.

The amorphous MPA dissolved in the matrix can easily travel across the polymer matrix reaching the outer solution, as the solution temperature (37°C) is higher than the glass transition temperature of PCL (-60°C), allowing the chains to have enough mobility.

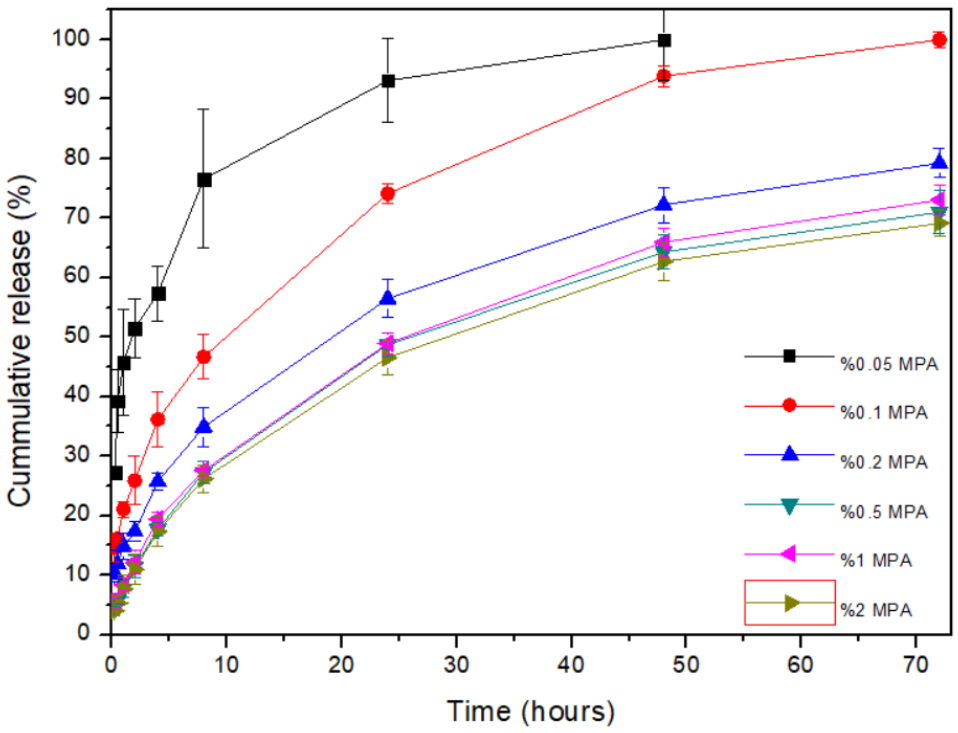

Figure 3c. 10. Drug release profiles of PCL/MPA films containing different drug concentrations immersed into 0.1 PBS buffer at 37 °C, shown in %.

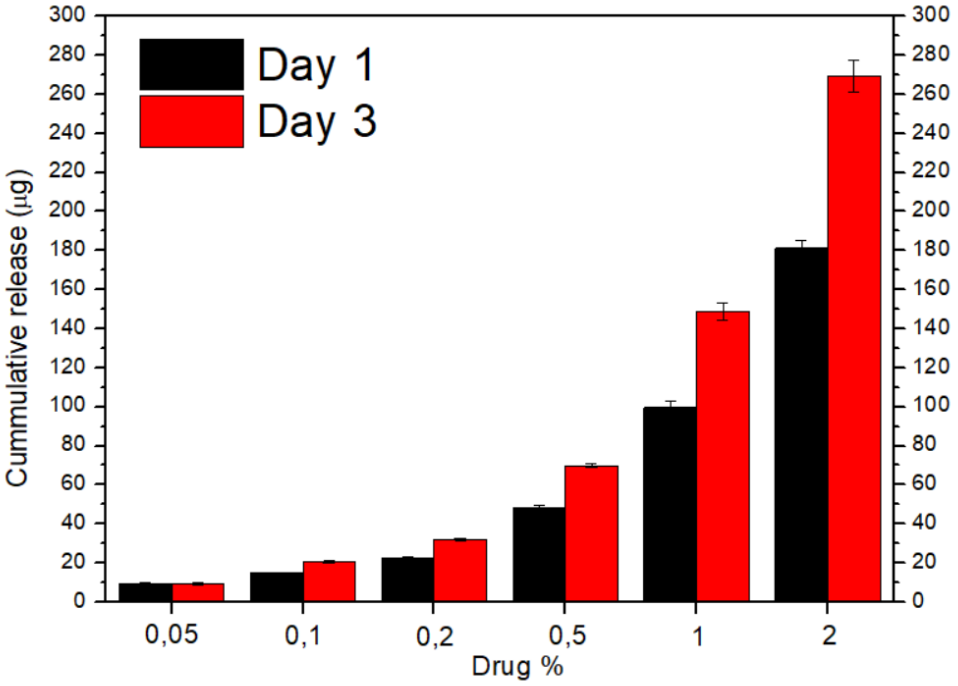

Figure 3c. 11. Drug release profiles of PCL/MPA films containing different drug concentrations immersed into 0.1 PBS buffer at 37 °C, shown in µg.

According to the results observed in table 3c.3., the release mechanisms vary depending on the concentration of MPA. For those with the lowest concentration (0.05 and 0.1 wt% MPA) the model that fits the results is First order [39], while for the rest of the concentrations the trend towards Higuchi model is seen [40]. Therefore, at very low concentrations, the release kinetics depends on the concentration, while as the amount of MPA increases, the drug is released by a diffusion process based in Fick's law, square root time dependent.

Table 3c. 3. Fitting of the release data to the mathematical models for drug release kinetics. R2 is the correlation coefficient, and n is the release exponent.

MPA %	Zero order	First order	Higuchi	Korsmeyer-Peppas	
	R^2	R^2	R^2	R^2	n
0.05	0.64	0.94	0.87	0.81	0.58
0.1	0.86	0.99	0.98	0.92	0.5
0.2	0.74	0.88	0.94	0.95	0.46
0.5	0.75	0.85	0.94	0.99	0.5
1	0.77	0.89	0.95	0.99	0.5
2	0.77	0.87	0.95	0.99	0.5

3c.3.5. Cell viability with HeLa immortalized cancer cells.

In the last decade, some groups have reported the suppression of proliferation and the enhancement of apoptosis mediated by MPA in cancerous cells [20], [41], [42]. These properties are attributed to several interactions of the MPA with molecules involved in cell cycle, cell death, cell proliferation and movement [43]. Here, the combination of the PCC with MPA as a possible anticancer therapy was studied. For this purpose, HeLa cells, a widely used immortalized cell line derived from cervical cancer were chosen. Remarkably, HeLa cells are also the oldest and more used cell line worldwide [44]. First, attachment and proliferation capabilities of HeLa cells were analyzed on PCL scaffolds containing increasing concentrations of MPA after 1 and 3 days post-seeding (DIV1 and DIV3 respectively) by immunofluorescence assays against DAPI and rhodamine/Phalloidin (Rh/Ph). Results at DIV1 suggested that the PCL/MPA substrates affected the number of attached HeLa cells in a dose-dependent manner achieving even the same impairment on cell viability as the MPA in solution (PCL/MPA 0.5 71.5±6.1%;

PCL/MPA 1 64.6±5.3%; PCL/MPA 2 40.1±7.6%; Dis 53.6±5%; PCL 100±9.2%; $p < 0.0001$, One-way ANOVA). Results were further demonstrated at DIV3, when again the number of the HeLa cells over the scaffolds containing MPA was reduced with respect to the PCL control (PCL/MPA 0.5 32.6±3.1%; PCL/MPA 1 39.1±5.3%; PCL/MPA 2 28.2±2.4%; Dis 30.0±1.4%; PCL 100±7.6 %; $p < 0.0001$, One-way ANOVA) (Figure 3c.12.). The results are in accordance with other studies were MPA caused the impairment on HeLa cell viability [43], [47]. But it may also be taken in consideration the clearance effect of the tissues *in vivo* [48], where the slow release of the MPA by the scaffolds may be an advantage compared to the drug administration [49]. Moreover, in future experiments, these scaffolds could be further engineered to adequate the release of the MPA to the kinetics of the drug by just modifying the degradation ratio of the scaffolds, or the anchoring mechanism of the drug [49] being a promising tool for anticancer drug delivery.

3c.3.6. Cell viability with fibroblasts.

One big hallmark of anticancer therapies is the possibility of treating cancer cells without affecting non-cancerous cells [50]. In this regard, the adhesion and proliferation of the normal fibroblasts cell line MRC5 or CCL-171 were tested. This cell line is not immortalized and according to ISO 10993-5:2009 it is considered a good control for cytotoxic experiments [27]. Results suggested that the number of MRC5 cells able to attach and proliferate on the PCL scaffolds containing increasing amounts of MPA at DIV1 (PCL/MPA 0.5 113.7±17.2%; PCL/MPA 1 128.7±13.7%; PCL/MPA 2 110.7±11.6%; PCL 100±7.1%) and DIV3 (PCL/MPA 0.5 109.1±4.8%; PCL/MPA 1 113.3±8.4%; PCL/MPA 2 91.6±7.3%; PCL 100±3%) were similar to the pristine PCL scaffolds (Figure 3c.13.). Surprisingly, both at DIV1 (Dis 32.2±3.5%; $p < 0.05$, One-way ANOVA) and DIV3 (Dis 69.4±4.9%; $p < 0.05$, One-way ANOVA), the MRC5 cells seeded on the PCL scaffolds together with MPA in solution appeared to have an impaired proliferation. These results are in accordance with other studies where several tumorigenic and non-tumorigenic cell lines showed to be resistant to MPA treatment, by converting MPA into its inactive form 7-*O*-glucuronide [51]–[53]. However, further research is needed to study the anticancer capabilities of the MPA blended in PCL films with other cancerous and non-cancerous cells lines and the advantages and disadvantages compared with MPA in solution.

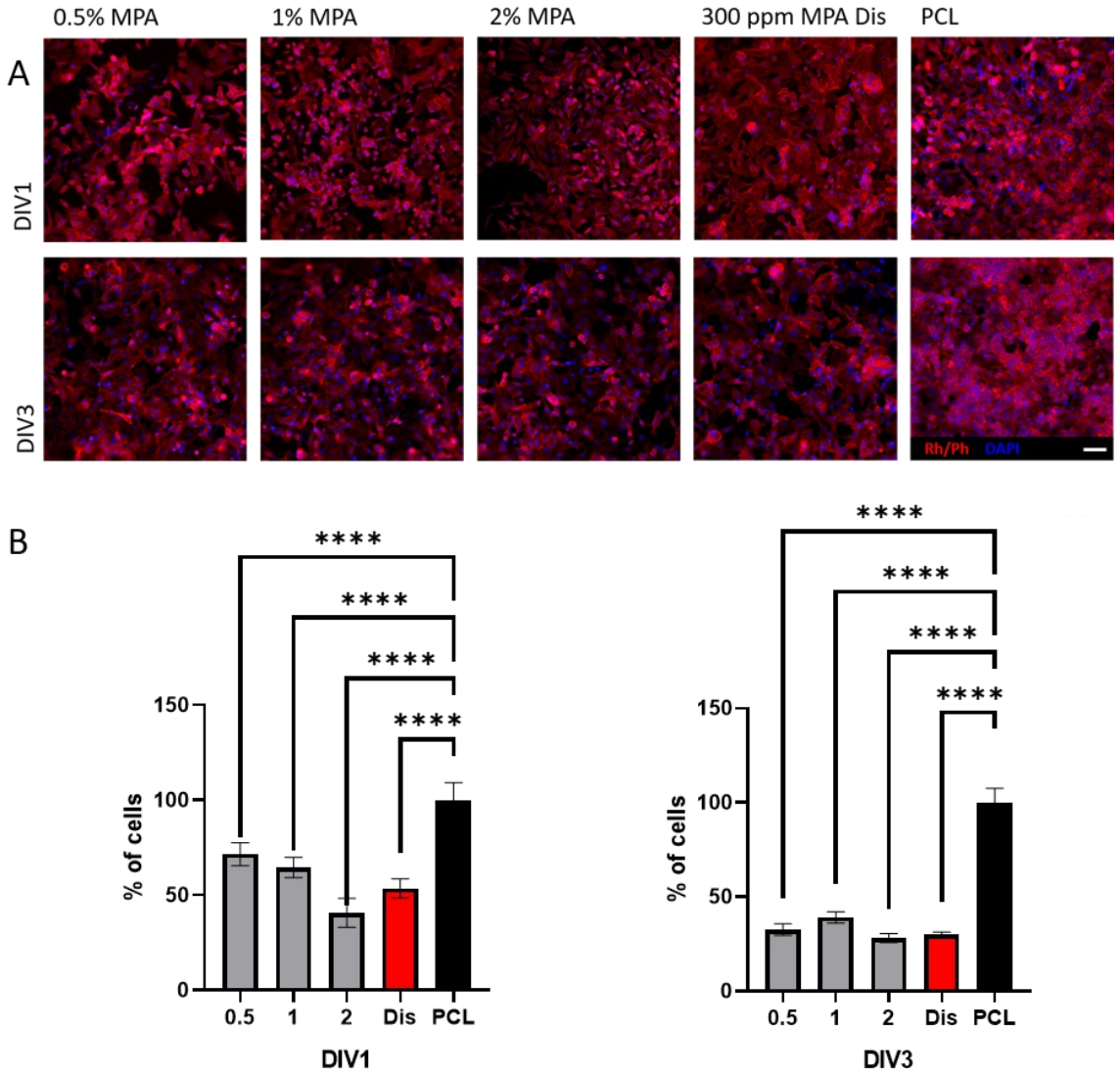

Figure 3c. 12. Immunofluorescence assays against rhodamine/phalloidin (Rh/Ph) in red and DAPI in blue of HeLa cells cultured over the PCL/MPA scaffolds containing increasing amount of MPA. As negative control HeLa cells were cultured over the PCL scaffolds and as positive control HeLa cells cultured over PCL scaffolds were incubated with 300 ppm MPA in dissolution. (B) Quantification of the percentage of cells over the scaffolds at DIV1 and DIV3. (*p<0.0001 compared to the PCL scaffold at the same time-points. Dunn´s or Holm-Sidak method One-way Anova Analysis of Variance on Ranks). Scale bar 50 µm.

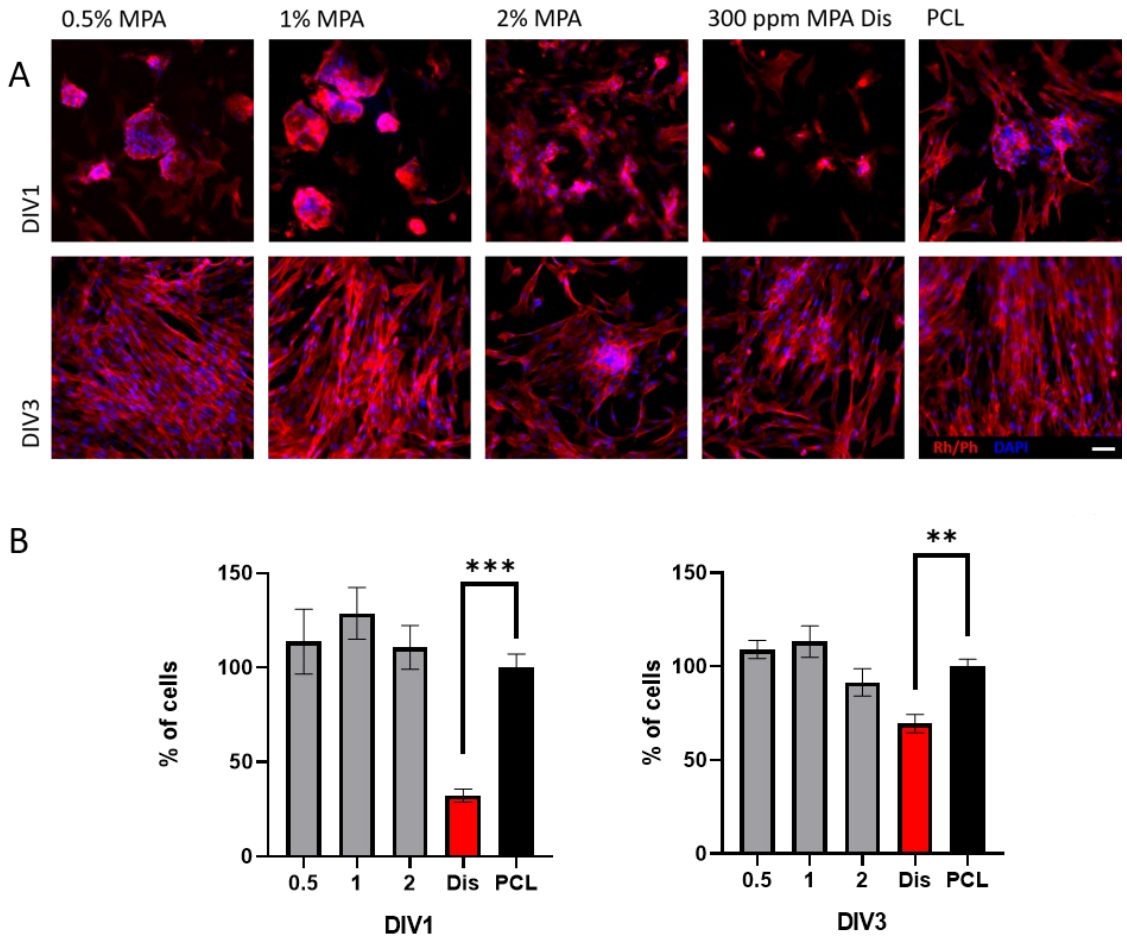

Figure 3c. 13. (A) Immunofluorescence assays against rhodamine/phalloidin (Rh/Ph) in red and DAPI in blue of MRC5 cells cultured over the PCL/MPA scaffolds containing increasing amount of MPA. As negative control MRC5 cells were cultured over the PCL scaffolds and as positive control MRC5 cells cultured over PCL scaffolds were incubated with 300 ppm MPA in dissolution. (B) Quantification of the percentage of cells over the scaffolds at DIV1 and DIV3. (*p<0.05 compared to the PCL scaffold at the same time-points. Dunn´s or Holm-Sidak method One-way Anova Analysis of Variance on Ranks). Scale bar 50 μm.

3c.4. CONCLUSIONS

In the present work the possibility to form an amorphous solid dispersion of mycophenolic acid using poly(ε-caprolactone) as matrix was confirmed. Miscibility between the two compounds was observed in thermal properties. On the one hand, the intermediate glass transition temperature criterion was confirmed for all the compositions. On the other hand, the analysis of the melting point depression of the MPA crystals resulted in a negative interaction parameter, $\chi = -1.18$, indicating favorable interactions between the polymer and the bioactive molecule.

The analysis by FTIR spectroscopy for the PCL/MPA blends does not allow to clearly confirm the occurrence of hydrogen bonding interactions between the hydroxyl groups present in MPA and the C=O groups of PCL due to the complex nature of the C=O stretching region. Nevertheless, the overall results observed in both the C=O and O-H stretching regions follow the typical trends observed in other polymer blends with miscibility driven by hydrogen bonding interactions.

The potential application of this PCL/MPA amorphous solid dispersion as drug delivery matrices was proven, as at least 70% of the drug was delivered by the third day *in vitro* in all compositions. In addition, *in vitro* cell culture experiments with HeLa and MRC5 cells showed that it is possible to maintain the active form of MPA for cancer treatment, as there is a decreased viability of cancerous cells when cultured over PCL materials containing MPA. Here the possible beneficiary outcome of dissolving MPA in PCL matrices for anticancer treatment was observed, although further research is needed to study the anticancer capabilities with other cell lines and the advantages and disadvantages these amorphous solid dispersions offer compared to crystalline MPA.

3c.5. REFERENCES

[1] S. Kalepu and V. Nekkanti, “Insoluble drug delivery strategies: review of recent advances and business prospects,” *Acta Pharmaceutica Sinica B*, vol. 5, no. 5, pp. 442–453, Sep. 2015, doi: 10.1016/J.APSB.2015.07.003.

[2] D. M. Mudie, G. L. Amidon, and G. E. Amidon, “Physiological Parameters for Oral Delivery and in Vitro Testing,” *Molecular Pharmaceutics*, vol. 7, no. 5, pp. 1388–1405, Sep. 2010, doi: 10.1021/mp100149j.

[3] Q. Shi, F. Li, S. Yeh, Y. Wang, and J. Xin, “Physical stability of amorphous pharmaceutical solids: Nucleation, crystal growth, phase separation and effects of the polymers,” *International Journal of Pharmaceutics*, vol. 590, p. 119925, Nov. 2020, doi: 10.1016/J.IJPHARM.2020.119925.

[4] Q. Shi, Y. Wang, S. M. Moinuddin, X. Feng, and F. Ahsan, “Co-amorphous Drug Delivery Systems: a Review of Physical Stability, In Vitro and In Vivo

Performance," *AAPS PharmSciTech*, vol. 23, no. 7, 2022, doi: 10.1208/s12249-022-02421-7.

[5] W. L. Chiou and S. Riegelman, "Pharmaceutical Applications of Solid Dispersion Systems," *Journal of Pharmaceutical Sciences*, vol. 60, no. 9, pp. 1281–1302, Sep. 1971, doi: 10.1002/JPS.2600600902.

[6] C. Parulski *et al.*, "Fused deposition modeling 3D printing of solid oral dosage forms containing amorphous solid dispersions: How to elucidate drug dissolution mechanisms through surface spectral analysis techniques?," *International Journal of Pharmaceutics*, vol. 626, p. 122157, Oct. 2022, doi: 10.1016/J.IJPHARM.2022.122157.

[7] J. S. Bhanushali, S. Dhiman, U. Nandi, and S. S. Bharate, "Molecular interactions of niclosamide with hydroxyethyl cellulose in binary and ternary amorphous solid dispersions for synergistic enhancement of water solubility and oral pharmacokinetics in rats," *International Journal of Pharmaceutics*, vol. 626, p. 122144, Oct. 2022, doi: 10.1016/J.IJPHARM.2022.122144.

[8] J. Becelaere *et al.*, "Stable amorphous solid dispersion of flubendazole with high loading via electrospinning," *Journal of Controlled Release*, vol. 351, pp. 123–136, Nov. 2022, doi: 10.1016/J.JCONREL.2022.09.028.

[9] A. G. Nambiar *et al.*, "Continuous Manufacturing and Molecular Modeling of Pharmaceutical Amorphous Solid Dispersions," *AAPS PharmSciTech*, vol. 23, no. 7, 2022, doi: 10.1208/s12249-022-02408-4.

[10] T. Vasconcelos, B. Sarmento, and P. Costa, "Solid dispersions as strategy to improve oral bioavailability of poor water soluble drugs," *Drug Discovery Today*, vol. 12, no. 23–24, pp. 1068–1075, Dec. 2007, doi: 10.1016/J.DRUDIS.2007.09.005.

[11] T. P. Holm, M. M. Knopp, R. Berthelsen, and K. Löbmann, "Supersaturated amorphous solid dispersions of celecoxib prepared in situ by microwave irradiation," *International Journal of Pharmaceutics*, vol. 626, p. 122115, Oct. 2022, doi: 10.1016/J.IJPHARM.2022.122115.

[12] G. Van Den Mooter, "The use of amorphous solid dispersions: A formulation strategy to overcome poor solubility and dissolution rate," *Drug Discovery Today: Technologies*, vol. 9, no. 2, pp. e79–e85, Jun. 2012, doi: 10.1016/J.DDTEC.2011.10.002.

[13] P. Pandi, R. Bulusu, N. Kommineni, W. Khan, and M. Singh, "Amorphous solid dispersions: An update for preparation, characterization, mechanism on bioavailability, stability, regulatory considerations and marketed products," *International Journal of Pharmaceutics*, vol. 586, p. 119560, Aug. 2020, doi: 10.1016/J.IJPHARM.2020.119560.

[14] P.-Y. Qian, Y. Xu, and N. Fusetani, "Natural products as antifouling compounds: recent progress and future perspectives," *Biofouling*, vol. 26, no. 2, pp. 223–234, 2009, doi: 10.1080/08927010903470815.

[15] M. M. Knopp, N. E. Olesen, Y. Huang, R. Holm, and T. Rades, "Statistical Analysis of a Method to Predict Drug-Polymer Miscibility," *Journal of Pharmaceutical Sciences*, vol. 105, no. 1, pp. 362–367, Jan. 2016, doi: 10.1002/jps.24704.

[16] B. C. Hancock, S. L. Shamblin, and G. Zografi, "Molecular Mobility of Amorphous Pharmaceutical Solids Below Their Glass Transition Temperatures," *Pharmaceutical Research*, vol. 12, no. 6, pp. 799–806, 1995, doi: 10.1023/A:1016292416526.

[17] A. Newman, G. Knipp, and G. Zografi, "Assessing the performance of amorphous solid dispersions," *Journal of Pharmaceutical Sciences*, vol. 101, no. 4, pp. 1355–1377, Apr. 2012, doi: https://doi.org/10.1002/jps.23031.

[18] K. DeBoyace and P. L. D. Wildfong, "The Application of Modeling and Prediction to the Formation and Stability of Amorphous Solid Dispersions," *Journal of Pharmaceutical Sciences*, vol. 107, no. 1, pp. 57–74, Jan. 2018, doi: 10.1016/J.XPHS.2017.03.029.

[19] D. Han, M. Sasaki, H. Yoshino, S. Kofuji, A. T. Sasaki, and A. J. Steckl, "In-vitro evaluation of MPA-loaded electrospun coaxial fiber membranes for local

treatment of glioblastoma tumor cells," *Journal of Drug Delivery Science and Technology*, vol. 40, pp. 45–50, Aug. 2017, doi: 10.1016/J.JDDST.2017.05.017.

[20] Z. H. Zheng *et al.*, "Mycophenolic acid induces adipocyte-like differentiation and reversal of malignancy of breast cancer cells partly through PPARγ," *European Journal of Pharmacology*, vol. 658, no. 1, pp. 1–8, May 2011, doi: 10.1016/J.EJPHAR.2011.01.068.

[21] R. Bentley, "Mycophenolic Acid: A One Hundred Year Odyssey from Antibiotic to Immunosuppressant," *Chemical Reviews*, vol. 100, no. 10, pp. 3801–3826, Sep. 2000, doi: 10.1021/cr990097b.

[22] J. Park *et al.*, "Mycophenolic Acid Inhibits Platelet-Derived Growth Factor-Induced Reactive Oxygen Species and Mitogen-Activated Protein Kinase Activation in Rat Vascular Smooth Muscle Cells," *American Journal of Transplantation*, vol. 4, no. 12, pp. 1982–1990, Dec. 2004, doi: https://doi.org/10.1111/j.1600-6143.2004.00610.x.

[23] D. Floryk and E. Huberman, "Mycophenolic acid-induced replication arrest, differentiation markers and cell death of androgen-independent prostate cancer cells DU145," *Cancer Letters*, vol. 231, no. 1, pp. 20–29, Jan. 2006, doi: 10.1016/J.CANLET.2005.01.006.

[24] A. Hackl, R. Ehren, and L. T. Weber, "Effect of mycophenolic acid in experimental, nontransplant glomerular diseases: new mechanisms beyond immune cells," *Pediatric Nephrology*, vol. 32, no. 8, pp. 1315–1322, 2017, doi: 10.1007/s00467-016-3437-y.

[25] E. Sanchez-Rexach *et al.*, "Miscibility, interactions and antimicrobial activity of poly(ε-caprolactone)/chloramphenicol blends," *European Polymer Journal*, vol. 102, pp. 30–37, May 2018, doi: 10.1016/J.EURPOLYMJ.2018.03.011.

[26] E. Sanchez-Rexach, I. Martínez de Arenaza, J. R. Sarasua, and E. Meaurio, "Antimicrobial poly(ε-caprolactone)/thymol blends: Phase behavior, interactions and drug release kinetics," *European Polymer Journal*, vol. 83, pp. 288–299, Oct. 2016, doi: 10.1016/J.EURPOLYMJ.2016.08.029.

[27] "ISO 10993-5:2009 Biological evaluation of medical devices — Part 5: Tests for in vitro cytotoxicity." ISO standards, 2009.

[28] F. Rashid, A. Saeed, and J. Iqbal, "In Vitro Anticancer Effects of Stilbene Derivatives: Mechanistic Studies on HeLa and MCF-7 Cells," *Anti-Cancer Agents in Medicinal Chemistry (Formerly Current Medicinal Chemistry-Anti-Cancer Agents)*, vol. 21, no. 6, pp. 793–802, 2021, doi: 10.2174/1871520620666200811123230.

[29] P. Costa and J. M. Sousa Lobo, "Modeling and comparison of dissolution profiles," *European Journal of Pharmaceutical Sciences*, vol. 13, no. 2, pp. 123–133, May 2001, doi: 10.1016/S0928-0987(01)00095-1.

[30] O. Sánchez-Aguinagalde, A. Lejardi, E. Meaurio, R. Hernández, C. Mijangos, and J.-R. Sarasua, "Novel Hydrogels of Chitosan and Poly(vinyl alcohol) Reinforced with Inorganic Particles of Bioactive Glass," *Polymers*, vol. 13, no. 5. 2021. doi: 10.3390/polym13050691.

[31] R. Pezzoli, J. G. Lyons, N. Gately, and C. L. Higginbotham, "Investigation of miscibility estimation methods between indomethacin and poly(vinylpyrrolidone-co-vinyl acetate)," *International Journal of Pharmaceutics*, vol. 549, no. 1–2, pp. 50–57, Oct. 2018, doi: 10.1016/J.IJPHARM.2018.07.039.

[32] N. Hernandez-Montero, J. M. Ugartemendia, H. Amestoy, and J. R. Sarasua, "Complex phase behavior and state of miscibility in Poly(ethylene glycol)/Poly(l-lactide-co-ε-caprolactone) Blends," *Journal of Polymer Science Part B: Polymer Physics*, vol. 52, no. 2, pp. 111–121, Jan. 2014, doi: 10.1002/polb.23394.

[33] J. A. Baird and L. S. Taylor, "Evaluation of amorphous solid dispersion properties using thermal analysis techniques," *Advanced Drug Delivery Reviews*, vol. 64, no. 5, pp. 396–421, Apr. 2012, doi: 10.1016/J.ADDR.2011.07.009.

[34] O. Sánchez-Aguinagalde, E. Meaurio, A. Lejardi, and J.-R. Sarasua, "Amorphous solid dispersions in poly(ε-caprolactone)/xanthohumol bioactive blends: physicochemical and mechanical characterization," *Journal of Materials Chemistry B*, vol. 9, no. 20, pp. 4219–4229, 2021, doi: 10.1039/D0TB02964E.

[35] N. B. Colthup, L. H. Daly, and S. E. Wiberley, "CHAPTER 9 - CARBONYL COMPOUNDS," N. B. Colthup, L. H. Daly, and S. E. B. T.-I. to I. and R. S. (Third E. Wiberley, Eds. San Diego: Academic Press, 1990, pp. 289–325. doi: https://doi.org/10.1016/B978-0-08-091740-5.50012-0.

[36] W. Harrison, H. M. M. Shearer, and J. Trotter, "Crystal structure of mycophenolic acid," *Journal of the Chemical Society, Perkin Transactions 2*, no. 11, pp. 1542–1544, 1972, doi: 10.1039/P29720001542.

[37] A. Covarrubias, N. Zúñiga-Villarreal, A. González-Lucas, J. Díaz-Domínguez, and G. Espinosa-Pérez, "Crystal Structure of Mycophenolic Acid: 6-(4-Hydroxy-6-methoxy-7-methyl-3-oxo-1,3-dihydroisobenzofuran-5-yl)-4-methyl-hex-4-enoic Acid," *Analytical Sciences*, vol. 16, no. 7, pp. 783–784, 2000, doi: 10.2116/analsci.16.783.

[38] Q. Z. Zeng, J. Ouyang, S. Zhang, and L. Zhang, "Structural characterization and dissolution profile of mycophenolic acid cocrystals," *European Journal of Pharmaceutical Sciences*, vol. 102, pp. 140–146, 2017, doi: 10.1016/j.ejps.2017.02.035.

[39] J. Li and D. J. Mooney, "Designing hydrogels for controlled drug delivery," *Nature Reviews Materials*, vol. 1, no. 12, p. 16071, 2016, doi: 10.1038/natrevmats.2016.71.

[40] H. Baishya, "Application of Mathematical Models in Drug Release Kinetics of Carbidopa and Levodopa ER Tablets," *Journal of Developing Drugs*, vol. 06, no. 02, pp. 1–8, 2017, doi: 10.4172/2329-6631.1000171.

[41] J. Klangjorhor *et al.*, "Mycophenolic acid is a drug with the potential to be repurposed for suppressing tumor growth and metastasis in osteosarcoma treatment," *International Journal of Cancer*, vol. 146, no. 12, pp. 3397–3409, 2020, doi: 10.1002/ijc.32735.

[42] B. Dun *et al.*, "Mycophenolic acid inhibits migration and invasion of gastric cancer cells via multiple molecular pathways," *PLoS ONE*, vol. 8, no. 11, pp. 1–12, 2013, doi: 10.1371/journal.pone.0081702.

[43] B. Dun *et al.*, "Transcriptomic changes induced by mycophenolic acid in gastric cancer cells," *American Journal of Translational Research*, vol. 6, no. 1, pp. 28–42, 2014, doi: 10.1371/journal.pone.0081702.

[44] F. Rashid, A. Saeed, and J. Iqbal, "In Vitro Anticancer Effects of Stilbene Derivatives: Mechanistic Studies on HeLa and MCF-7 Cells," *Anticancer Agents Med Chem*, vol. 21, no. 6, pp. 793–802, Aug. 2020, doi: 10.2174/1871520620666200811123230.

[45] S. Kwon, W. Yang, D. Moon, and K. S. Kim, "Comparison of cancer cell elasticity by cell type," *Journal of Cancer*, vol. 11, no. 18, pp. 5403–5412, 2020, doi: 10.7150/jca.45897.

[46] S. Saboormaleki, H. Sadeghian, A. R. Bahrami, A. Orafaie, and M. M. Matin, "7-farnesyloxycoumarin exerts anti-cancer effects on a prostate cancer cell line by 15-LOX-1 inhibition," *Archives of Iranian Medicine*, vol. 21, no. 6, pp. 251–259, 2018.

[47] B. Dun *et al.*, "Delineation of biological and molecular mechanisms underlying the diverse anticancer activities of mycophenolic acid," *International Journal of Clinical and Experimental Pathology*, vol. 6, no. 12, pp. 2880–2886, 2013.

[48] E. M. Howgate, K. Rowland Yeo, N. J. Proctor, G. T. Tucker, and A. Rostami-Hodjegan, "Prediction of in vivo drug clearance from in vitro data. I: Impact of inter-individual variability," *Xenobiotica*, vol. 36, no. 6, pp. 473–497, 2006, doi: 10.1080/00498250600683197.

[49] K. J. Rambhia and P. X. Ma, "Controlled drug release for tissue engineering," *Journal of Controlled Release*, vol. 219, pp. 119–128, Dec. 2015, doi: 10.1016/J.JCONREL.2015.08.049.

[50] D. Hanahan and R. A. Weinberg, "The Hallmarks of Cancer," *Cell*, vol. 100, no. 1, pp. 57–70, Jan. 2000, doi: 10.1016/S0092-8674(00)81683-9.

[51] C. Morath *et al.*, "Effects of mycophenolic acid on human fibroblast proliferation, migration and adhesion in vitro and in vivo," *American Journal of Transplantation*, vol. 8, no. 9, pp. 1786–1797, 2008, doi: 10.1111/j.1600-6143.2008.02322.x.

[52] K. Chen *et al.*, "Differential sensitivities of fast-and slow-cycling cancer cells to inosine monophosphate dehydrogenase 2 inhibition by mycophenolic acid," *Molecular Medicine*, vol. 21, pp. 792–802, 2015, doi: 10.2119/molmed.2015.00126.

[53] T. J. Franklin, V. Jacobs, P. Bruneau, and P. Ple, "Glucuronidation by human colorectal adenocarcinoma cells as a mechanism of resistance to mycophenolic acid," *Advances in Enzyme Regulation*, vol. 35, no. C, pp. 91–100, Jan. 1995, doi: https://doi.org/10.1016/0065-2571(94)00010-Z.

GENERAL CONCLUSIONS

GENERAL CONCLUSIONS

Chapter 2. Novel hydrogels of chitosan and poly (vinyl alcohol) reinforced with inorganic particles of bioactive glass.

- Initial chitosan/poly (vinyl alcohol) hydrogels with 2% chitosan are useful in terms of drug release, but lack sufficient mechanical properties to withstand the mechanical loads they may receive in the human body.

- The addition of bioactive glass particles and the increase of chitosan to 4% are effective in increasing the mechanical properties of hydrogels.

- The addition of bioactive glass particles in 2% CS hydrogels does not influence the drug release kinetics. However, increasing chitosan to 4% slows it down.

- Scanning electron microscopy (SEM) and X-ray diffraction (XRD) confirmed the formation of apatite crystals on the surface of hydrogels reinforced with bioactive glass particles after immersion in simulated body fluid (SBF) for 28 days at physiological temperature (37°C).

- The increase in chitosan to 4% complicates the manufacture of hydrogels due to its high viscosity, as well as its injectability.

- It is necessary to optimize the dispersion process of the bioactive glass particles, in order to achieve a more homogeneous hydrogel with fewer agglomerates.

Chapter 3. Poly (ε-caprolactone) based polymer/drug amorphous solid dispersions.

3a. Introduction and miscibility prediction

- Experimentally, analysis of the glass transition temperature of a polymer/drug system provides information about the miscibility of the mixture.

- In order to confirm miscibility, the melting point depression must be studied in order to obtain the interaction parameter, χ, applying the Flory-Huggins theory.

- It is possible to predict the miscibility of a polymer/drug system using its solubility parameters, but only in an approximate way, since at the moment it has not been possible to find a connection between the theoretical and the experimental prediction.

- It is more difficult to find drugs that are miscible with PDLLA than with PCL.

3b. Amorphous solid dispersion in poly (ε-caprolactone)/xanthohumol bioactive blends: physicochemical and mechanical characterization.

- Initially, the intermediate glass transition temperature criterion indicates miscibility in the PCL/XH system.

- Miscibility is confirmed by obtaining a negative interaction parameter, χ=-1.3.

- Up to 50% XH content, solid amorphous dispersions of PCL/XH can be obtained as observed in DSC, XRD and AFM imaging results.

- The analysis by FTIR spectroscopy shows the existence of new interassociative interactions between drug and polymer, reducing the autoassociative interactions.

- The mechanical resistance of PCL is reduced by the addition of XH, but the mixtures maintain a high ductility until reaching 50% XH.

3c. Miscibility, interactions and anti-cancer activity of poly (ε-caprolactone)/mycophenolic acid blends.

- Initially, the intermediate glass transition temperature criterion indicates miscibility in the PCL/MPA system.

- The miscibility is confirmed by obtaining a negative interaction parameter, χ=-1.18.

- Using FTIR spectroscopy, the overall results observed follow typical trends seen in other polymer blends with miscibility driven by hydrogen bonding interactions.

- All compositions showed the ability to release at least 70% drug in the first three days in vitro.

- In vitro cell assays with HeLa and MRC5 cells showed the ability of these mixtures to fight cancer cells without affecting healthy cells.

CONCLUSIONES GENERALES

Capítulo 2. Nuevos hidrogeles de quitosano y poli (vinil alcohol) reforzados con partículas de vidrio bioactivas.

- Los hidrogeles iniciales de quitosano/poli (vinil alcohol) con quitosano de 2% resultan útiles en cuanto a la liberación del fármaco, pero carecen de propiedades mecánicas suficientes para hacer frente a cargas mecánicas que pueden recibir en el cuerpo humano.

- La adición de partículas de vidrio bioactivas y el aumento del quitosano al 4% resultan efectivas a la hora de aumentar las propiedades mecánicas de los hidrogeles.

- La adición de partículas de vidrio bioactivas en hidrogeles de 2%CS no influye en la cinética de liberación de fármaco. No obstante, el aumento del quitosano al 4% la ralentiza.

- Mediante microscopía electrónica de barrido (SEM) y difracción de rayos-X (XRD) se confirma la formación de cristales de apatita en la superficie de los hidrogeles reforzados con partículas de vidrio bioactivas tras su inmersión en fluido corporal simulado (SBF) durante 28 días a temperatura fisiológica (37°C).

- El aumento del quitosano al 4% complica la fabricación de los hidrogeles debido a su alta viscosidad, al igual que su inyectabilidad.

- Resulta necesario optimizar el proceso de dispersión de las partículas de vidrio bioactivas, para poder conseguir un hidrogel más homogéneo y con menos aglomerados.

Capítulo 3. Dispersiones sólidas amorfas polímero/fármaco basadas en poli (ε-caprolactona)

3a. Introducción y predicción de la miscibilidad.

- Experimentalmente, el análisis de la temperatura de transición vítrea de un sistema polímero/fármaco proporciona información acerca de la miscibilidad de la mezcla.

- Para poder confirmar la miscibilidad, se debe estudiar la depresión del punto de fusión para poder así obtener el parámetro de interacción, χ, mediante la teoría de Flory-Huggins.

- Cabe la posibilidad de predecir la miscibilidad de un sistema polímero/fármaco utilizando sus parámetros de solubilidad, pero solamente de una forma aproximada, ya que de momento no ha sido posible encontrar una conexión entre la predicción teórica y la experimental.

- Resulta más complicado encontrar fármacos miscibles con PDLLA que con PCL.

3b. Dispersiones sólidas amorfas en mezclas bioactivas poli (ε-caprolactona/xanthohumol) : caracterización fisicoquímica y mecánica.

- Inicialmente, el criterio de temperatura de transición vítrea intermedia indica miscibilidad en el sistema PCL/XH.

- La miscibilidad se confirma mediante la obtención de un parámetro de interacción negativo, $\chi = -1.3$.

- Hasta un 50% de contenido de XH, se pueden obtener dispersiones sólidas amorfas de PCL/XH, según se aprecia en los resultados de DSC, XRD y las imágenes obtenidas mediante AFM.

- El análisis por espectroscopía FTIR muestra la existencia de nuevas interacciones interasociativas entre fármaco y polímero, reduciendo las interacciones autoasociativas.

- La resistencia mecánica del PCL se ve reducida ante la adición de XH, pero las mezclas mantienen una alta ductilidad hasta alcanzar un 50% XH.

3c. Miscibilidad, interacciones y actividad anticáncer de mezclas poli (ε-caprolactona)/ácido micofenólico.

- Inicialmente, el criterio de temperatura de transición vítrea intermedia indica miscibilidad en el sistema PCL/MPA.

- La miscibilidad se confirma mediante la obtención de un parámetro de interacción negativo, $\chi = -1.18$.

- Mediante espectroscopía FTIR, los resultados generales observados siguen las tendencias típicas observadas en otras mezclas de polímeros con miscibilidad impulsada por interacciones de enlaces de hidrógeno.

- Todas las composiciones mostraron la capacidad de liberar como mínimo un 70% de fármaco en los tres primeros días in *vitro.*

- Los ensayos celulares *in vitro* con células HeLa y MRC5 mostraron la capacidad de estas mezclas para hacer frente a las células cancerígenas sin afectar a las células sanas.

ONDORIO OROKORRAK

2. kapitulua. Beira bioaktibo partikulekin sendotutako kitosano/poli (binil alkohol) hidrogel berriak.

- Lehen kitosano/poli (binil alkohol) hidrogelak %2 kitosanoarekin erabilgarriak dira farmakoen liberaziorako, baina bere propietate mekanikoak ez dira nahikoak giza gorputzean jaso ditzakeen kargei aurre egiteko.

- Beira bioaktibozko partikulen gehitzea eta kitosanoaren kontzentrazioa %4ra igotzea eraginkorrak dira hidrogelen propietate mekanikoak hobetzeko.

- %2 kitosano hidrogelei beira bioaktibozko partikulak gehitzeak ez du eraginik farmakoen liberazioan, baina kitosanoaren kontzentrazioa %4ra igotzeak liberazioa moteltzen du.

- Ekorketa elektronikoko mikroskopia (SEM) eta X-izpien difrakzioaren (XRD) bidez beira bioaktibozko partikulaz kargatutako hidrogelen gainazalean apatita kristalen formazioa baieztatu da, gorputz-fluido simulatuan (SBF) 28 egunez murgilduta egon ondoren, tenperatura fisiologikoan (37°C).

- Kitosanoaren kontzentrazioa %4ra igotzeak hidrogelen fabrikazioa eta injektagarritasuna zailagoa egiten du, biskositate altuaren ondorioz.

- Beira bioaktibo partikulen dispertsio prozesua hobetu beharra dago, hidrogel homogeneoago bat lortu ahal izateko, aglomeratu gutxiagorekin.

3. kapitulua. Poli (ε-kaprolaktona)n oinarritutako polímero/farmako dispertsio solido amorfoak

3a. Sarrera eta nahasgarritasunaren predikzioa

- Esperimentalki, polimero/farmako sistema baten beira trantsizio tenperaturaren analisiak sistemaren nahasgarritasunari buruzko informazioa ematen du.

- Nahasgarritasuna baieztatu ahal izateko, urtze puntuaren depresioa aztertu behar da, interakzio-parametroa, χ, kalkulatu ahal izateko Flory-Huggins teoriaren bidez.

- Polimero/farmako sistema baten nahasgarritasuna aurreikusi daiteke bere disolbagarritasun-parametroak erabiliz, baina hurbilpen bat soilik, oraingoz ezin izan baita predikzio teorikoaren eta esperimentalaren arteko loturarik aurkitu.

- PDLLArekin nahasgarriak diren farmakoak aurkitzea zailagoa da PCLrekin nahasgarriak direnak aurkitzea baino.

3b. Poli (ε-kaprolaktona)/xanthohumol nahaste bioaktibozko dispertsio solido amorfoak: karakterizazio fisikokimiko eta mekanikoa.

- Hasiera batean, erdiko beira trantsizio tenperaturaren irizpideak PCL/XH sistemaren nahasgarritasuna adierazten du.

- Nahasgarritasuna interakzio-parametro negatiboaren (χ=-1,3) lorpenarekin baieztatu daiteke.

- %50 XH arte, PCL/XH dispertsio solido amorfoak ikusi daitezke, DSC eta XRD emaitzek eta AFM bidez lortutako irudiek erakusten dutenaren arabera.

- FTIR espektroskopia bidezko analisiak polímero eta farmakoaren arteko interakzio interasoziatio berriak erakusten ditu, interakzio autoasoziatiboak murriztuz.

- XHen gehitzearen ondorioz PCLaren erresistentzia mekanikoa jaisten da, baina %50 XH arte nahasketek harikortasun altua mantentzen dute.

3c. Poli (ε-kaprolaktona)/azido mikofenoliko nahasketen nahasgarritasun, elkarrekintza eta minbiziaren aurkako aktibitatea.

- Hasiera batean, erdiko beira trantsizio tenperaturaren irizpideak PCL/MPA sistemaren nahasgarritasuna adierazten du.

- **N**ahasgarritasuna interakzio-parametro negatiboaren (χ=-1,18) lorpenarekin baieztatu daiteke.

- FTIR espektroskopia bidez lortutako emaitza orokorrek nahasgarritasuna duten beste poljmero nahaste batzuetan ikusten den hidrogeno-loturen elkarrekintzek bultzatutako joera tipikoak jarraitzen dituzte.

- *In vitro*, konposizio guztiek lehen hiru egunetan gutxienez farmakoaren %70a askatzeko gaitasuna erakutsi dute.

- HeLa eta MRC5 zelulekin *in vitro* egindako saiakuntza zelularrek nahasketa hauek zelula kantzerigenoei aurre egiteko gai direla erakutsi dute, zelula osasuntsuei kalterik eragin gabe.

APPENDIX

A1. LIST OF FIGURES

Chapter 1

Chapter 2

Chapter 3b

Chapter 3c

A2. LIST OF TABLES

Chapter 1

Chapter 2

Chapter 3a

Chapter 3b

Chapter 3c

A3. ABBREVIATIONS AND SYMBOLS

AFM	Atomic Force Microscopy
AIDS	Acquired Immunodeficiency Syndrome
AMR	Antimicrobial Resistance
ANOVA	Analysis of Variance
API	Active Pharmaceutical Ingredient
ASD	Amorphous Solid Dispersion
ATP	Adenosine Triphosphate
BG	Bioactive Glass
BSA	Bovine Serum Albumin
BVDV	Bovine Viral Diarrhea Virus
CA	L-arginine Conjugated Chitosan
CED	Cohesive Energy Density
Cip	Ciprofloxacin
CLARI	Clarithromycin
CMV	Cytomegalovirus
CNM	Carbon Nanomaterials
CS	Chitosan
DAPI	4’,6-diamidino-2-phenyndole
DCM	Dichloromethane
dGTP	Deoxyguanosine Triphosphate
DIV	Days in Vitro
DMEM	Dulbecco’s Modified Eagle Medium
DMSO	Dimethyl sulfoxide

DNA	Deoxyribonucleic acid
DOX	Doxycycline
DSC	Differential Scanning Calorimetry
EPM	Extracellular Polymeric Matrix
ESKAPE	*Enterococcus faecium, Staphylococcus aureus, Klebsiella pneumoniae, Acinetobacter baumanii, Pseudomonas aeruginosa* and *Enterobacter species*
EWC	Equilibrium Water Content
FBS	Fetal Bovine Serum
FDA	Food and Drug Administration
FLX	Fluoxetine
FTIR	Fourier-Transform Infrared Spectroscopy
GC	Group contribution method
GTP	Guanosine-5'-triphosphate
HA	Hydroxyapatite
h-EGF	Human Epidermal Growth Factor
HeLa	Henrietta Lacks cancer cells
HIV	Human Immunodeficiency Virus
HSV	Herpes Simplex Virus
HVK	Hoftyzer-Van Krevelen
IC_{50}	Half maximal inhibitory contentration
IMPDH	Inosine Monophosphate Dehydrogenase
LbL	Layer by Layer technique
MIC	Minimal Inhibitory Concentration

MPA	Mycophenolic Acid
MRC5	Medical Reasearch Council cell strain 5
NC	Nanocapsules
NIR	Near-infrared Light
NM	Not miscible
NP	Nanoparticles
PBS	Phosphate Buffered Saline
PCL	Poly (ε-caprolactone)
PDA	Polydopamine
PDLLA	Poly (D,L-lactide)
PEG	Poly (ethilene glicol)
PFA	Paraformaldehyde
PLA	Poly (lactic acid)
PLGA	Poly (lactide-co-glycolide)
PM	Partially miscible
PPT	Photothermal therapy
PSD	Position Sensitive Detector
PU	Polyurethane
PVA	Poly (vinyl alcohol)
QS	Quorum Sensing
Rh/Ph	Rhodamine-Phalloidin Staining
RNA	Ribonucleic Acid
ROS	Reactive Oxygen Species
SBF	Simulated Body Fluid

SEM	Scanning Electron Microscopy
SI	Swelling Index
THF	Tetrahydrofuran
TTO	Tea Tree Oil
UV-Vis	Ultraviolet-Visible
VSMC	Vascular Smooth Muscle Cell
WHO	World Health Organization
XH	Xanthohumol
XMP	Xanthine Monophosphate
XRD	X-Ray Diffraction

ΔG	Free energy
ΔH	Enthalpy
ΔS	Entropy
δ	Solubility parameter
ε_b	Strain at break
σ_y	Yield stress
ϕ	Volume fraction
χ	Interaction parameter
B	Interaction energy density
C_t	Cumulative amount
C_∞	Starting amount
E	Young's modulus
G'	Elastic modulus

G''	Viscous modulus
k	Boltzmann constant
m	Degree of polymerization
M_n	Number average molecular weight
M_w	Weight average molecular weight
R	Universal gas constant
t	Time
T	Temperature
T_g	Glass transition temperature
T_m	Melting temperature
V	Volume
w	Weight fraction

A4. LIST OF PUBLICATIONS AND CONGRESSES

Publications related to this thesis

- O. Sánchez-Aguinagalde, A. Lejardi, E. Meaurio, R. Hernández, C. Mijangos and J.R. Sarasua, *Novel hydrogels of chitosan and poly(vinyl alcohol) reinforced with inorganic particles of bioactive glass*, Polymers, vol. 13, no. 5, pp. 1-15, Feb. 2021, doi: 10.3390/polym13050691
- O. Sánchez-Aguinagalde, E. Meaurio, A. Lejardi and J.R. Sarasua, *Amorphous solid dispersions in poly(ε-caprolactone)/xanthohumol bioactive blends: physicochemical and mechanical characterization,* J Mater Chem B, vol. 9, no. 20, pp. 4219-4229, Apr. 2021, doi: 10.1039/d0tb02964e

Participation in congresses

- O. Sánchez, C. Bello, N. Arranz, A. Larrañaga, A. Lejardi, J.R. Sarasua, *Hidrogeles termosensibles basados en quitosano para liberación dual de fármacos.* CASEIB 2017 XXXV Congreso Anual de la Sociedad Española de Ingeniería Biomédica. Oral presentation. Bilbao, Spain, November 2017.
- O. Sánchez, A. Lejardi, R. Hernández, C. Mijangos, J.R. Sarasua, *Estudio de nuevos hidrogeles basados en mezclas de poli(vinil alcohol) (PVA) y quitosano (CS) reforzados con partículas inorgánicas de vidrio bioactivo.* CASEIB 2018 XXXVI Congreso Anual de la Sociedad Española de Ingeniería Biomédica. Oral presentation. Ciudad Real, Spain, November 2018.
- O. Sánchez, A. Lejardi, E. Meaurio, J.R. Sarasua, *Miscibility and interactions between poly(ε-caprolactone)/xanthohumol blends.* JIP2019 X Congreso de Jóvenes Investigadores en Polímeros 2019. Oral presentation. Burgos, Spain, May 2019.
- O. Sánchez, E. Sánchez-Rexach, Y. Polo, A. Lejardi, E. Meaurio, J.R. Sarasua, *Development of a new biomedical material with immunosuppressive properties for stent application.* WBC2020 virtual 11th World Biomaterials Congress. Oral presentation. Glasgow, United Kingdom, December 2020.
- O. Sánchez-Aguinagalde, E. Sánchez-Rexach, A. Lejardi, E. Meaurio, J.R. Sarasua, *Poli(ε-kaprolaktona)/azido mikofenoliko dispertsio solido amorfoak:*

nahasgarritasuna eta farmako liberazioa. MZT Materialen Zientzia eta Teknologia V. kongresua. Oral presentation. Bilbao, Spain, November 2021.